

Aus der Medizinischen Klinik und Poliklinik II  
Klinik der Ludwig-Maximilians-Universität München

Vorstand: Prof. Dr. med. Julia Mayerle

***Epigenetic reprogramming of pancreatic cancer cells as a new  
therapeutic option***

Dissertation

zum Erwerb des Doktorgrades der Medizin  
an der Medizinischen Fakultät der  
Ludwig-Maximilians-Universität zu München

vorgelegt von

Svenja Pichlmeier

aus

München

Jahr

2023

Mit Genehmigung der Medizinischen Fakultät  
der Universität München

Berichterstatter:	Prof. Dr. med. Julia Mayerle
Mitberichterstatter:	Prof. Dr. med. Stefan Böck, MHBA Prof. Dr. med. Sebastian Kobold
Mitbetreuung durch den promovierten Mitarbeiter:	PD Dr. rer. biol. hum. Ivonne Regel Prof. Dr. rer. nat. Roland Kappler
Dekan:	Prof. Dr. med. Thomas Gudermann
Tag der mündlichen Prüfung:	12.01.2023

## Zusammenfassung

Genexpressionsstudien haben gezeigt, dass das duktales Pankreasadenokarzinom (PDAC) in zwei unterschiedliche, klinisch relevante molekulare Subtypen eingeteilt werden kann (Collisson et al., 2011, Moffitt et al., 2016, Bailey et al., 2016). In der Vergangenheit konnten bereits verschiedene Faktoren identifiziert werden, die für die Tumorerheterogenität in Pankreaskarzinomen eine Rolle spielen. Da epigenetische Regulatoren neben den vier wichtigsten Mutationen *KRAS*, *p16*, *p53* und *SMAD4* zu den am häufigsten mutierten Genen in Pankreaskarzinomen zählen, wurde die Bedeutung von epigenetischen Aberrationen in zwei molekularen PDAC Subtypen, dem klassischen und dem basalen Phänotyp, sowie ihr therapeutisches Potenzial in humanen Pankreaskarzinom-Zelllinien untersucht (Bailey et al., 2016).

Die Ergebnisse zeigen, dass die Subtyp-spezifische Genexpression wichtiger Differenzierungsmarker, wie *EpCAM* oder *GATA6*, epigenetisch reguliert wird. Chromatin-Immunopräzipitation-Assays konnten nachweisen, dass die Expression dieser epithelialen Differenzierungsmarker im klassischen Subtyp durch Histonacetylierung aktiviert wird. Im Gegensatz dazu wird die Expression in Zelllinien des basalen/quasimesenchymalen Subtyps durch eine erhöhte Konzentration an Histonubiquitinierung, sowie einem Verlust von Histonacetylierungen im Promoterbereich der Gene unterdrückt. DNA-Methylierung spielt in der Regulation der Subtyp-spezifischen Genexpression von *EpCAM* und *GATA6* hingegen nur eine untergeordnete Rolle.

Trotz unterschiedlicher Histonacetylierungsniveaus im klassischen und basalen PDAC Subtyp, zeigte die Behandlung mit Histonacetylierungs- oder Histondeacetylierungs-Inhibitoren nur begrenzte Erfolge. Sowohl klassische, als auch basale Zelllinien zeigten eine beinahe vollständige Resistenz gegen die Behandlung mit dem Histonacetylierungs-Inhibitor A485. Das Zellüberleben konnte nur in einer der basalen Zelllinien, MIAPaca-2, durch die maximale Inhibitordosis von 10 µM A485 auf 50 % im Vergleich zu unbehandelten Zellen reduziert werden. Unter hochdosierter Behandlung mit dem Histondeacetylierungs-Inhibitor Vorinostat wurde zwar eine trendmäßige Reduktion des Zellüberlebens beobachtet, ein Zusammenhang zwischen Therapieansprechen und dem molekularen PDAC Subtyp konnte hier jedoch nicht gezeigt werden. Ursächlich für den fehlenden therapeutischen Effekt könnte die kompensatorische Hochregulation anderer epigenetischer Regulatoren sein. Aus diesem Grund wurde ein Multiplex-CRISPR/Cas9 Plasmid zum simultanen genetischen Knockout von drei epigenetischen Regulatoren (*HDAC2*, *DNMT3A*, *RING1B*) etabliert. Allerdings brachte die Transfektion einer humanen PDAC Zelllinie des basalen Subtyps keine erfolgreiche Knockout-Zelllinie hervor. Höchstwahrscheinlich behindert der zeitgleiche Knockout mehrerer epigenetischer Regulatoren wesentliche zelluläre Funktionen so entscheidend, dass es zum Zelltod kommt. Um diese

Einschränkungen des Multiplex-CRISPR/Cas9 Knockouts zu umgehen und die Auswirkungen eines kombinatorischen Knockouts verschiedener epigenetischer Regulatoren untersuchen zu können, könnte ein schrittweiser Knockout der drei Zielgene nacheinander durchgeführt werden. Darüber hinaus sollte ein Selektionsmarker in das Plasmid integriert werden, um eine erfolgreiche Transfektion sicherstellen zu können.

Um mit den präklinischen Ergebnissen aus epigenetischen Arzneimitteltests erfolgreiche klinische Studien initiieren zu können, sind weitere Experimente über die Auswirkungen epigenetischer Inhibitoren auf unterschiedliche molekulare PDAC Subtypen nötig. Unpublizierte Daten der Arbeitsgruppe zeigen beispielsweise, dass die Behandlung mit einem Histonacetylierungs-Inhibitor in Zelllinien des klassischen PDAC Subtyps die Expression von *GATA6* stark herunterreguliert, sowie die Sensitivität für das Chemotherapeutikum Gemcitabin vermindert, was wiederum mit einer schlechteren Prognose assoziiert ist. Diese Ergebnisse unterstreichen die Bedeutung von Patientenstratifizierung, um den Therapieerfolg zu maximieren.

Insgesamt zeigt diese Dissertation, dass die Transkriptionsprofile der molekularen PDAC Subtypen zum Teil epigenetisch reguliert werden. Obwohl die Monotherapie mit epigenetischen Inhibitoren begrenzte Erfolge in der Tumorzell-Reprogrammierung zeigt, bleibt der Therapieerfolg epigenetischer Arzneimittel limitiert. Daher sind weitere Studien über die genauen Effekte einer Kombinationstherapie mit verschiedenen epigenetischen Inhibitoren nötig.

# Table of contents

<b>Zusammenfassung</b> .....	<b>I</b>
<b>Table of contents</b> .....	<b>III</b>
<b>List of abbreviations</b> .....	<b>VI</b>
<b>1. Introduction</b> .....	<b>1</b>
1.1. Pancreatic ductal adenocarcinoma (PDAC).....	1
1.1.1. Risk factors .....	2
1.1.2. Precursor lesions .....	4
1.1.3. Driver mutations in PDAC.....	5
1.1.3.1. Tumor oncogenes.....	6
1.1.3.2. Tumor suppressor genes .....	6
1.1.4. Molecular subtypes .....	8
1.1.5. Therapeutic strategies for PDAC .....	10
1.2. Epigenetic modifications .....	12
1.2.1. DNA methylation .....	13
1.2.2. Histone modifications.....	13
1.2.2.1. Activating histone modifications.....	14
1.2.2.2. Repressive histone modifications.....	15
1.3. Pancreatic tumor model systems.....	17
1.3.1. Pancreatic cancer cell lines.....	17
1.3.2. Genome editing .....	18
<b>2. Aim of the study</b> .....	<b>20</b>
<b>3. Materials and Methods</b> .....	<b>21</b>
3.1. Specific chemicals and reagents.....	21
3.2. Kits .....	23
3.3. Antibodies .....	23
3.3.1. Primary antibodies .....	23
3.3.2. Secondary antibodies .....	24
3.4. Enzymes.....	25
3.5. Inhibitors .....	26
3.6. Oligonucleotides.....	26
3.6.1. Gene expression primer (for qRT-PCR).....	26
3.6.2. ChIP primer (for qRT-PCR) .....	27
3.6.3. Methylation-specific PCR (MSP) primer (for PCR).....	28

3.6.4.	sgRNAs (single guide RNAs).....	28
3.6.5.	Sequencing primer .....	28
3.7.	Plasmids.....	29
3.8.	Cell lines.....	29
3.9.	Consumption materials .....	29
3.10.	Equipment .....	30
3.11.	Computer applications .....	31
<b>4.</b>	<b>Methods.....</b>	<b>33</b>
4.1.	Cell biological methods .....	33
4.1.1.	Cell culture conditions.....	33
4.1.2.	Passaging of cells .....	33
4.1.3.	Cryopreservation of cells.....	34
4.1.4.	Revitalization of cells.....	34
4.1.5.	Treatment of cells with inhibitors .....	34
4.1.6.	MTT cell proliferation .....	35
4.1.7.	MTT cell survival .....	35
4.1.8.	Gene editing with the CRISPR/Cas9 system .....	35
4.2.	Molecular biological methods.....	37
4.2.1.	DNA isolation from cells .....	37
4.2.2.	Determination of DNA concentration .....	37
4.2.3.	RNA isolation from cells .....	37
4.2.4.	Determination of RNA concentration .....	37
4.2.5.	cDNA synthesis .....	37
4.2.6.	Polymerase chain reaction (PCR) .....	38
4.2.7.	Quantitative RT-PCR (qRT-PCR) .....	38
4.2.8.	Agarose gel electrophoresis .....	40
4.3.	Biochemical methods.....	40
4.3.1.	Protein extraction.....	40
4.3.2.	Determination of protein concentration.....	40
4.3.3.	SDS polyacrylamide gel electrophoresis (SDS-PAGE) .....	41
4.3.4.	Western blot.....	42
4.3.5.	Immunofluorescence staining .....	42
4.3.6.	In-cell western .....	43
4.4.	Epigenetic methods.....	44
4.4.1.	Chromatin immunoprecipitation (ChIP) .....	44
4.4.2.	DNA methylation analysis .....	46

<b>5. Results.....</b>	<b>47</b>
5.1. Characterizing pancreatic cancer cell lines representing the classical and basal subtype .	47
5.1.1. Classical and basal PDAC cell lines show a subtype-specific expression profile .....	47
5.1.2. Important epithelial and mesenchymal differentiation markers are epigenetically regulated	49
5.1.3. Epigenetic modifiers are differentially expressed in the two subtypes .....	51
5.2. The transcription of subtype-specific markers is regulated through epigenetic modifications.....	52
5.2.1. Transcription of <i>EpCAM</i> and <i>GATA6</i> is activated in the classical subtype and repressed in the basal subtype through histone modifications.....	53
5.2.2. <i>EpCAM</i> is epigenetically silenced through DNA methylation in the basal subtype .....	54
5.3. Cell survival response to single-drug histone acetylase or histone deacetylase inhibitor treatment is independent of the molecular subtype.....	56
5.4. Genetic reprogramming of pancreatic cancer cells through knockout of a combination of epigenetic modifiers.....	57
5.4.1. Generating a multiplex CRISPR-Cas9 plasmid .....	58
5.4.2. Establishing a multiplex knockout cell line.....	59
<b>6. Discussion.....</b>	<b>62</b>
6.1. Transcriptional profiles define PDAC subtypes .....	63
6.2. The role of epigenetic modifications in molecular subtypes .....	64
6.3. Therapeutic targeting of epigenetic modifiers.....	66
6.4. Unsuccessful triple-knockout of epigenetic modifiers in pancreatic cancer cells .....	67
<b>7. Summary and outlook.....</b>	<b>69</b>
<b>8. References.....</b>	<b>71</b>
<b>9. Appendix.....</b>	<b>84</b>
9.1. List of tables .....	84
9.2. List of figures .....	85
<b>Acknowledgements.....</b>	<b>86</b>
<b>Affidavit.....</b>	<b>87</b>
<b>Curriculum vitae.....</b>	Fehler! Textmarke nicht definiert.

## List of abbreviations

% v/v	Percent volume concentration
% w/v	Percent mass concentration
°C	Degree celsius
µg	Microgram
µl	Microliter
µM	Micromolar
ADEX	Aberrantly differentiated exocrine
ADM	Acinar-to-ductal metaplasia
AGR2	Anterior gradient 2
AIM	Absent in melanoma 2
AMY 1	Alpha-amylase 1
APS	Ammoniumperoxodisulfat
ARID1A	AT-rich interaction domain 1
ATM	ATM serine/threonine kinase
BHLHA15	Basic helix-loop-helix family member A15
BMI	Body mass index
BP	Base pair
BRCA	Breast cancer gene
BSA	Bovine serum albumin
Cas9	CRISPR associated protein 9
CDK	Cyclin-dependent kinase
CDKN2A	Cyclin-dependent kinase inhibitor 2A
cDNA	Complementary DNA
ChIP	Chromatin immunoprecipitation
co-SMAD	SMAD4
CpG island	5'-C-phosphate-G-3' island
CREBBP	CREB binding protein
CRISPR	Clustered regularly interspaced short palindromic repeats
C <sub>T</sub>	Threshold value
CUX1	Cut like homeobox 1
DABCO	1,4-diAzabicyclo[2.2.2]octane
DAPI	4',6-diamidino-2-phenylindole dihydrochloride
Decitabine	5-Aza-2'-deoxycytidine
DMEM	Dulbecco's modified eagle's medium
DMSO	Dimethyl sulfoxid
DNA	Deoxyribonucleic acid
DNMT	DNA methyltransferase
dNTP	Deosynucleotide
DPC4	Deleted in pancreatic carcinoma locus 4
DSB	Double-strand break
DTT	Dithiothreitol
E2F1	E2F transcription factor 1

EDTA	Ethylenediaminetetraacetic acid disodium salt dihydrate
EED	Embryonic ectoderm development
EGFR	Epidermal growth factor receptor
EHMT2	Euchromatic histone lysine methyltransferase 2
ELF	E74 like ETS transcription factor
EMT	Epithelial-to-mesenchymal transition
EP300	E1A binding protein P300
EpCAM	Epithelial cell adhesion molecule
ERBB	Erb-B2 receptor tyrosine kinase
EZH2	Enhancer of zeste homolog2
FAM150A	ALK and LTK ligand 1
FAMMM	Familial atypical multiple mole and melanoma syndrome
FBS	Fetal bovine serum
FGFBP1	Fibroblast growth factor binding protein 1
FITC	Fluorescein-5-isothiocyanate
FOS	Fos proto-oncogene, AP-1 transcription factor subunit
FOXA2	Forkhead box A2
FOXP	Forkhead box
g	Gravitational force
GAP	GTPase-activating protein
GAPDH	Glyceraldehyde-3-phosphate dehydrogenase
GATA6	GATA binding protein 6
GDP	Guanosine-5'-diphosphate
GEF	Guanine nucleotide exchange factor
GFP	Green fluorescent protein
GPM6B	Glycoprotein M6B
gRNA	Guide RNA
GTP	Guanosine-5'-triphosphate
GTPase	Guanine nucleotide-binding regulatory protein
Gy	Gray
h	Hour
H2AK119ub	Mono-ubiquitination of lysine 119 of histone 2A
H3K27ac	Acetylation of lysine 27 on histone 3
H3K27me	Methylation of lysine 27 on histone 3
H3K27me3	Trimethylation of lysine 27 of histone 3
H3K36me	Methylation of lysine 36 on histone 3
H3K4me3	Trimethylation of lysine 4 on histone 3
H3K79me	Methylation of lysine 79 on histone 3
H3K9me	Methylation of lysine 9 on histone 3
H4K20me	Methylation of lysine 29 on histone 4
HAT	Histone acetyl transferase
HDAC	Histone deacetylase
HDR	Homology-directed repair
HMT	Histone methyltransferase
HNF	Hepatocyte nuclear factor
HOX	Homeobox

HPRT	Hypoxanthine phosphoribosyltransferase 1
HRP	Horseradish peroxidase
IC <sub>50</sub>	Half maximal inhibitory concentration
ICW	In-cell western
IF	Immunofluorescence
IgG	Immunoglobulin G
Indel	Insertion/deletion
IPMN	Intraductal papillary mucinous neoplasm
JARID2	Jumonji and AT-rich interaction domain containing 2
KAT2B	Lysine acetyltransferase 2B
KDM6A	Lysine demethylase 6A
KLF	Kruppel like factor
KMT	Lysine methyltransferase
KO	Knockout
KRAS	Kirsten rat sarcoma viral oncogene homolog
KRT	Keratin
LHX1	LIM homeobox 1
M	Methylated
M. Sssl	CpG methyltransferase
mA	Milliampere
MBD	Methyl-CpG-binding domain protein
MCN	Mucinous cystic neoplasms
MDM2	Mouse double minute 2 homolog
MeCP2	Methyl CpG binding protein 2
mFOLFIRINOX	Modified Folfirinox
min	Minute
MIST1/BHLHA15	Basic helix-loop-helix family, member A1 5
Mnase	Micrococcal nuclease
MNX1	Motor neuron and pancreas homeobox 1
mRNA	Messenger RNA
MSP	Methylation-specific PCR
MTT	3-(4,5-dimethylthiazol-2-yl)-2,5-diphenyl
MYBL1	MYB proto-oncogene like 1
n	Number
NEUROD1	Neurogenic differentiation factor 1
NFIX	Nuclear factor I X
NHEJ	Non-homologous end joining
NKX2	NK2-homeobox
nm	Nanometer
NP-40	Nonident P-40
NPC1L1	NPC1 like intracellular cholesterol transporter 1
NPTX2	Neuronal pentraxin 2
NR5A2	Nuclear receptor subfamily 5 group A member 2
Ns	Not significant
PAM	Protospacer-adjacent motif
PanIN	Pancreatic intraepithelial neoplasia

PARPi	Poly (ADP-ribose) polymerase inhibitor
PBS	Phosphate buffered saline
PcG	Polycomb group
PCR	Polymerase chain reaction
PD-1	Programmed cell death protein 1
PDAC	Pancreatic ductal adenocarcinoma
PDX1	Pancreatic and duodenal homeobox 1
PIPES	1,4-piperazinediethanesulfonic acid
PJS	Peutz-Jeghers syndrome
PRBM1	Polybromo 1
PRC	Polycomb repressive complex
pre-crRNA	Pre-CRISPR RNA
PRSS1	Protease, serine 1
P/S	Penicillin/Streptomycin
PTF1a	Pancreas-associated transcription factor 1a
PTHLH	Parathyroid hormone like hormone
qRT-PCR	Quantitative RT-PCR
RASSF10	Ras association domain family member 10
RB	Retinoblastoma protein
RBPJL	Recombination signal binding protein for immunoglobulin kappa J region-like
RING1A	Ring finger protein 1
RING1B	Ring finger protein 2
rpm	Revolutions per minute
RPMI Medium	Roswell park memorial institute medium
RPRM	Reprimo, TP53 dependent G2 arrest mediator homolog
r-SMAD	Receptor-regulated SMADs
RT	Room temperature
S100A2	S100 calcium binding protein A2
SAHA	Vorinostat
SARP2	Secreted frizzled related protein 2
SDS	Sodium dodecyl sulfate
SDS-PAGE	SDS polyacrylamide gel electrophoresis
sec	Second
SEM	Standard error of the mean
SETD2	SET domain containing 2, histone lysine methyltransferase
sgRNA	Single guide RNA
SIRT	Sirtuin
SMAD	Sma- and mad-related protein
SMARCA4	SWI/SNF related, matrix associated, actin dependent regulator of chromatin, subfamily A, member 4
SNAI2	Snail family transcriptional repressor 2
SOX9	Sex-determining region y-box 9
SpCas9	Streptococcus pyogenes derived Cas9
SSBP3	Single stranded DNA binding protein 3

STK11	Serine/threonine kinase 11
TALEN	Transcription activator-like effector nucleases
TBP	TATA-box binding protein
TEMED	Tetramethylethylenediamine
TF	Transcription factor
TGF- $\beta$	Transforming growth factor-beta
TP	Tumor protein
tracrRNA	Trans-activating crRNA
TRIS	Tris(hydroxymethyl)aminomethane
U	Unit
U	Unmethylated
UV	Ultraviolet
V	Volt
WB	Western blot
ZFN	Zinc finger nuclease

# 1. Introduction

## 1.1. Pancreatic ductal adenocarcinoma (PDAC)

The vast majority of primary pancreatic malignancies constitutes of pancreatic ductal adenocarcinoma (PDAC) (Becker, Hernandez, Frucht & Lucas, 2014). In 2020 PDAC represented the 12<sup>th</sup> most frequent form of cancer and the seventh leading cause of cancer mortality worldwide (Figure 1) (Sung et al., 2021). Although the five-year survival rate rose from six to nine percent during the last years, it is still a devastating prognosis (Rawla, Sunkara & Gaduputi, 2019).

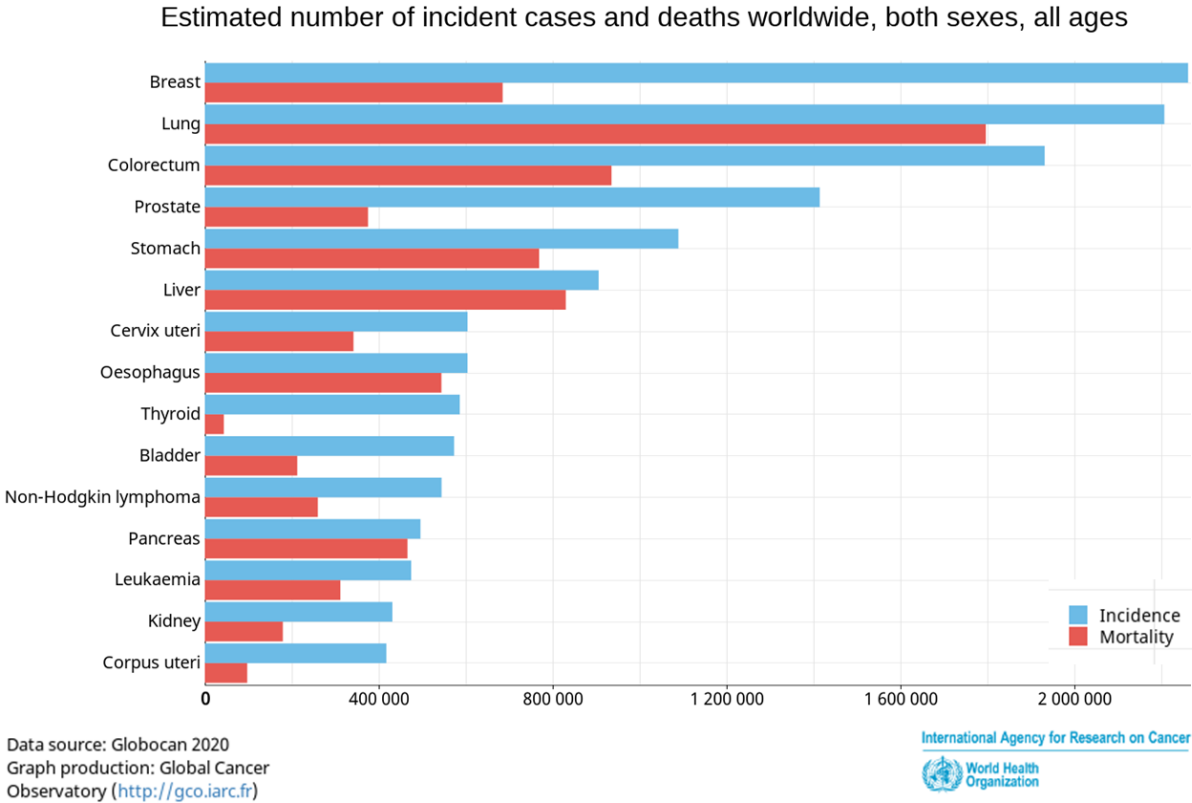


**Figure 1: Cancer incidence and mortality.** Graph showing total number of newly diagnosed cancer cases per year (incidence: blue bars) as well as total number of cancer-related deaths (mortality: red bars) worldwide for the year 2020. Graph includes 15 most common types of cancer. Pancreatic cancer is ranked as the 12th most common form of cancer and exhibits the seventh highest mortality of all cancers. Graph adapted from <http://gco.iarc.fr> (Ferlay et al., 2020).

The poor prognosis is due to the aggressive tumor growth, late detection in absence of early symptoms or specific biomarkers, and high levels of resistance to current treatment strategies. Ultimately, over 80 % of patients with clinical symptoms present with unresectable tumor stages at the time of diagnosis and can therefore not be considered for curative surgical treatment (Adamska, Domenichini & Falasca, 2017). The only curative approach to date is complete surgical resection. However, the five-year survival rate of patients who underwent surgical resection and received

adjuvant chemotherapy (Gemcitabine plus Capecitabine) only increased to 30 % due to local recurrence or metastatic spread of the disease (Neoptolemos et al., 2018).

Hence, there is a great need to improve the diagnostic tools available in order to diagnose patients at a treatable stage, as well as to identify new treatment strategies to avoid treatment resistance and significant side effects of current treatment regimens.

### 1.1.1. Risk factors

The poor survival rates and limited success of current treatment strategies highlight the need to identify PDAC-related risk factors. This would allow the screening of high-risk populations and the application of new therapeutic approaches. Risk factors can be divided into modifiable and non-modifiable factors.

**Cigarette smoking** represents the most significant life-style risk factor for PDAC with a population attributable risk of 25 – 35 % (Maisonneuve & Lowenfels, 2010). Indirect exposure of the pancreas to tobacco-metabolites can cause mutations in the important tumor oncogene KRAS (Kirsten rat sarcoma viral oncogene homolog) and the tumor protein P53 (TP53) (Schuller, 2020, Sonoyama et al., 2011). It has also been shown to promote a pro-tumorigenic environment by inducing inflammation in a dose-dependent manner (Duell, 2012). Interestingly, passive smoking has been shown to significantly increase the risk of pancreatic cancer as well (Chuang et al., 2011). However, after 15 – 20 years of tobacco abstinence, the risk for pancreatic cancer is renormalized (Lynch et al., 2009).

Another identified risk factor is heavy **alcohol** use. Consumption of three or more drinks per day increments the risk of developing pancreatic cancer by 1.22 in a dose-dependent manner (Tramacere et al., 2010). While alcohol is a known risk factor for pancreatitis, toxic metabolites like acetaldehyde also have direct effects on pancreatic inflammation and fibrosis (Midha, Chawla & Garg, 2016).

Notably, increased **body mass index** (BMI) also has a positive correlation to PDAC development. A meta-analysis of 21 prospective studies from 2007 showed a mean relative risk of 1.12 per 5 kg/m<sup>2</sup> increase in BMI (Larsson, Orsini & Wolk, 2007). This could be related to hyperglycemia and insulin resistance. 25 – 50 % of patients with PDAC develop diabetes mellitus type 1 – 3 prior to their PDAC diagnosis (Becker et al., 2014). Furthermore, a study has shown a positive correlation between the number of pancreatic intraepithelial neoplasia (PanIN) lesions and the percentage of intravisceral fat. Hence, pro-carcinogenic mediators secreted by adipocytes, such as adiponectin, could influence pancreatic carcinogenesis (Rebours et al., 2015).

Acute or chronic inflammation of the pancreas is associated with pancreatic tissue damage through premature activation of digestive enzymes. Hence, **chronic pancreatitis** represents an independent risk factor for the development of pancreatic cancer. Besides shared risk factors like smoking, alcohol abuse, and diabetes mellitus, chronic inflammation also induces fibrotic remodeling of the stroma. Chronic inflammation and exocrine damage provoke further scarring as well as exocrine insufficiency (Ramsey, Conwell & Hart, 2017). In a former multicenter cohort study, the cumulative risk of pancreatic cancer in patients with chronic pancreatitis was calculated at 4 % within 20 years (Lowenfels et al., 1993). Epidemiological studies suggest that chronic pancreatitis may be the result of recurrent episodes of acute pancreatitis in some patients (Uomo & Rabitti, 2000). **Acute pancreatitis** occurs in roughly 13 to 45 per 100 000 people per year. The main causes for acute pancreatitis are biliary obstruction, most frequently caused by gallstones in the distal part of the common bile duct, or alcohol abuse (Lankisch, Apte & Banks, 2015). Pancreatic duct obstruction results in retention of zymogen granules in acinar cells. Upon fusion with intracellular lysosomes, the lysosomal enzyme cathepsin B activates the zymogen trypsinogen to its active metabolite trypsin (Halangk et al., 2000). The resulting autodigestive processes induce an inflammatory response.

Besides modifiable lifestyle factors, some patients suffer from genetic risk factors predisposing them to the development of pancreatic cancer. Approximately 10 % of patients with pancreatic cancer have a positive family health history (Brand et al., 2007). There are a few hereditary syndromes recognized to promote PDAC formation. Germline mutations in the *PRSS1* (protease, serine 1) gene can promote **hereditary pancreatitis**, an autosomal dominant disorder with high penetrance. The *PRSS1* gene encodes the cationic trypsinogen protein, which activates zymogen through proteolytic cleavage. Point mutations in the protein's active site inhibit a negative feedback loop of trypsin activation. This promotes uncontrolled trypsin activation within the pancreas, which leads to chronic pancreatitis with early manifestation (Whitcomb et al., 1996). Patients with hereditary pancreatitis have a cumulative risk of pancreatic cancer of approximately 40 % at the age of 70 (Lowenfels et al., 1997). Several inherited cancer susceptibility syndromes are also associated with an increased risk for pancreatic cancer. **Peutz-Jeghers syndrome** (PJS) is characterized by germline mutations in the *STK11* (Serine/threonine kinase 11) gene. Patients typically develop hamartomatous polyps of the intestinal tract and pigmented macules of the digits, lips, and buccal mucosa. Patients with PJS have a significantly increased risk for a variety of solid tumors with a cumulative risk for all cancers of 93 % and a cumulative risk for pancreatic cancer of 36 % (Giardiello et al., 2000). **Familial atypical multiple mole and melanoma syndrome** (FAMMM) results from a germline mutation in the *CDKN2A* (cyclin-dependent kinase inhibitor 2A) gene. In a subset of patients with the specific *p16* Leiden mutation, the risk for developing pancreatic cancer is significantly increased (Vasen, Gruis, Frants, van Der Velden, Hille & Bergmann, 2000).

### 1.1.2. Precursor lesions

The mean five-year overall survival rate of only 9 % with current chemotherapeutic treatments highlights the need for early tumor detection to improve survival (Rawla, Sunkara & Gaduputi, 2019). Therefore, diagnostic screening tools need to consider pancreatic precursor lesions and determine their potential for malignant progression based on size, growth rate, radiological and histological characteristics (European Study Group on Cystic Tumours of the Pancreas, 2018).

**Pancreatic intraepithelial neoplasia (PanIN)** lesions represent histologically characterized precursor lesions of less than 5 mm in size with a ductal morphology. Based on the highest degree of cytological and structural atypia, they are graded into low-grade or high-grade lesions. Low-grade PanINs (previously PanIN-1 or PanIN-2) have a papillary or flat morphology with columnar epithelial cells, mostly basally oriented nuclei, and only mild to moderate cytological atypia, like nuclear pleomorphism, hyperchromasia, or nuclear crowding (Hruban, Maitra & Goggins, 2008). High-grade PanINs (previously PanIN-3) are characterized by architectural dysplasia, such as the formation of papillary or cribriform structures as well as major cytological atypia, aberrant mitoses, and loss of polarity (Kim & Hong, 2018). Low- and high-grade PanIN lesions have also been associated with specific mutational profiles. Mutations in the *KRAS* proto-oncogene and the tumor suppressor gene *CDKN2A* as well as telomere shortening are early mutational events and already present in low-grade PanINs. Mutations in the tumor suppressor genes *TP53* and *SMAD4* (sma- and mad-related protein 4) however, have been reported to occur in later stages of PDAC carcinogenesis (Hruban et al., 2008).

Besides PanINs, several other PDAC precursor lesions have been characterized. **IPMNs (intraductal papillary mucinous neoplasms)** originate from the main pancreatic duct or its branches and are characterized by papillary epithelial structures and mucin production (Kim & Hong, 2018). **MCNs (mucinous cystic neoplasms)** are also mucin-producing neoplasms, which originate from epithelial cells in the pancreatic body or tail. These precursor lesions show no connection to the ductal system and are surrounded by so-called ovarian-like stroma (Yonezawa, Higashi, Yamada & Goto, 2008).

The cell of origin for precancerous lesions and PDAC is still under debate. However, mouse model studies have shown that pancreatic acinar cells are vulnerable to oncogenic Kras-driven carcinogenesis under specific conditions. Besides Kras-mediated acinar cell transformation, pancreatic acinar cells display extensive plasticity in regeneration processes. Upon organ damage, pancreatic acinar cells are capable of transdifferentiating into cells with a duct-like phenotype and progenitor cell-like characteristics. This process is termed **acinar-to-ductal metaplasia (ADM)** (Figure 2) (Strobel et al., 2007, Guerra et al., 2007). Transient ADM formation restores the organ's integrity. Interestingly, the expression of oncogenic Kras in pancreatic progenitor cells is able to induce a spontaneous and irreversible formation of ADMs and PanINs, which eventually develop into invasive

PDAC (Hingorani 2003). Notably, adult mice are refractory to *Kras*-induced carcinogenesis, until the effect is abolished through tissue injury and inflammation-induced ADM formation (Guerra et al., 2007).

Acinar cell transdifferentiation is marked by characteristic gene expression changes. In ADMs the expression of transcription factors (TFs) associated with undifferentiated pancreatic progenitor cells, such as *Pdx1* (pancreatic and duodenal homeobox 1), *Hnf6* (hepatocyte nuclear factor 6), and *Sox9* (sex-determining region y-box 9), is increased. In contrast, acinar-differentiation genes like *AMY 1* (Alpha-Amylase 1), *Ptf1a* (Pancreas-Associated Transcription Factor 1a), or *Mist1/Bhlha15* (basic helix-loop-helix family member a15) are downregulated (Jensen et al., 2005, Prévot et al., 2012, Reichert & Rustgi, 2011).

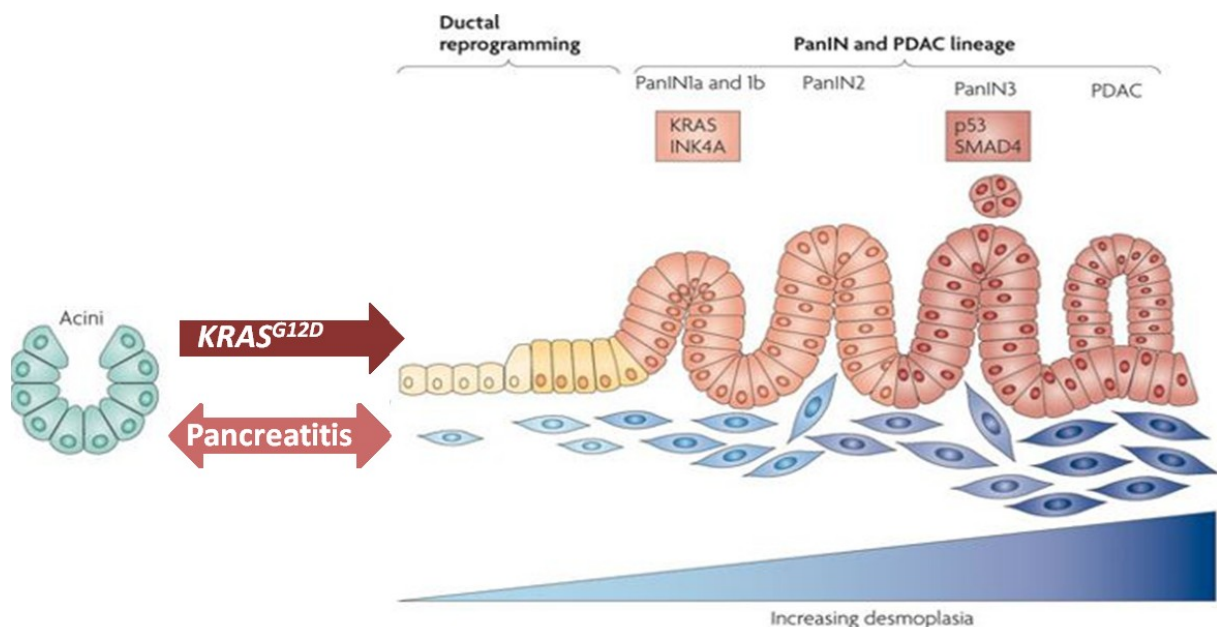


**Figure 2: Acinar-to-ductal metaplasia mediates PDAC development.** Pancreatitis can induce a reversible transformation of acinar cells towards a ductal-like phenotype in the context of tissue regeneration. However, the simultaneous presence of oncogenic *KRAS* mutations in ADM cells initiates the formation of precursor lesions like PanINs and further progression to PDAC. Graph adapted and modified from Morris, Wang & Hebrok, 2010.

### 1.1.3. Driver mutations in PDAC

For PDAC, crucial genetic changes occur in tumor suppressor genes and oncogenes. Oncogenes are highly conserved genes controlling important cell proliferation pathways. The conversion of a proto-oncogene into an oncogene through a gain-of-function mutation in one of the two alleles results in uncontrollable mitosis, cell growth, and division (Croce, 2008). Tumor suppressor genes mostly encode proteins with inhibitory effects on cell proliferation. Due to their recessive mode of inheritance, mutations in both alleles are required to induce a loss-of-function mutation (Velez &

Howard, 2015). According to the two-hit hypothesis by Knudson, the first allele is usually mutated through an inherited germline or a sporadic mutation. In the course of a lifetime, mitotic recombination can result in the crucial mutation of the second allele, giving rise to the development of cancer (Knudson, 1971). In PDAC, some common important driver mutations in oncogenes and tumor suppressor genes have been identified and extensively studied.

#### **1.1.3.1. Tumor oncogenes**

Essentially, all cases of PDAC in humans show activating **KRAS** mutations (Rozenblum et al., 1997). The frequency of **KRAS** mutations also correlates with the grade of PanIN lesions, accounting for 36 %, 44 %, and 87 % in PanIN-1a, 1b and 2-3 lesions, respectively (Löhr, Klöppel, Maisonneuve, Lowenfels & Lüttges, 2005). Furthermore, the expression of physiological levels of oncogenic Kras<sup>G12D</sup> has the potential to induce PDAC precursor lesions in mice (Hingorani et al., 2003). These data demonstrate the essential role of **KRAS** mutations in the development, progression, and maintenance of pancreatic cancer. The **KRAS** proto-oncogene encodes a GTPase protein (guanine nucleotide-binding regulatory protein) of the RAS family, which transmits signals from growth factor receptors like EGFR (epidermal growth factor receptor). In order to promote an active state, RAS requires the help of guanine nucleotide exchange factors (GEFs) to exchange GDP (guanosine-5'-diphosphate) for GTP (guanosine-5'-triphosphate) and activate further downstream signaling. Inactivation of **KRAS** is mediated by GTPase-activating proteins (GAPs) through hydrolytic cleavage of GTP to GDP (Eser, Schnieke, Schneider & Saur, 2014). In human PDAC, point mutations at codon 12 resulting in a single change of an amino acid impair intrinsic GTPase activity so that **KRAS** is constitutively activated (Scheffzek et al., 1997). This leads to continuous stimulation of downstream signaling pathways like PI3K/PDK1/AKT and RAF/MEK/ERK promoting cell proliferation, migration, and metastasis as well as changes in the metabolism and tumor microenvironment (Eser et al., 2014).

#### **1.1.3.2. Tumor suppressor genes**

The tumor suppressor **TP53** has been widely recognized as “the guardian of the genome” (Lane, 1992). It is mutated in the majority of human cancers and germline mutations of one **TP53** allele can lead to the Li-Fraumeni syndrome, which is characterized by the premature development of various types of solid cancers (Oliver, Hollstein & Hainaut, 2010). P53 protein levels are regulated through post-translational processes. In healthy cells, p53 is continuously subjected to proteosomal degradation following Mdm2-mediated (mouse double minute 2 homolog) ubiquitination. Cellular stress, like DNA (deoxyribonucleic acid) damage, abnormal mitosis, hypoxia, or oncogene activation,

represses the inhibitory effect of Mdm2. P53 is further stabilized through N-terminal phosphorylation (Aylon & Oren, 2011). Activated p53 acts as a transcription factor for various DNA repair and cell cycle arrest genes and induces the expression of genes promoting apoptosis of damaged cells (Levine & Oren, 2009). Consequently, p53 loss is a critical event in ensuring cancer cell survival. In most cases, the *TP53* gene shows missense mutations in exons 4-9 of the DNA-binding domain (Rivlin, Brosh, Oren & Rotter, 2011). P53 mutations do not only cause impaired tumor suppressor function but also promote additional oncogenic functions (Oren & Rotter, 2010). In pancreatic cancer, models of carcinogenesis suggest a late loss of *TP53*, following *KRAS*-mutations (Rivlin et al., 2011).

In approximately 55 % of PDAC, the tumor suppressor **SMAD4**, encoded by the gene **DPC4** (deleted in pancreatic carcinoma locus 4) is inactivated, which is associated with a significantly shorter time of survival (Liu, 2001). SMAD4 is a member of the TGF- $\beta$  (transforming growth factor-beta) signaling pathway. The binding of TGF- $\beta$  to the TGF- $\beta$  receptors activates their intrinsic intracellular serine/threonine kinase domains, which phosphorylate intracellular molecules, such as members of the SMAD family. Then, the common partner SMAD4 (co-SMAD) forms heteromeric complexes with the phosphorylated receptor-regulated SMADs (r-SMADs) SMAD2 and SMAD3 (Samanta & Datta, 2012). These complexes migrate into the nucleus and regulate gene expression. Notably, cell cycle inhibitors, such as p15 or p21, are activated, while proto-oncogenes, like MYC, are down-regulated to inhibit cell proliferation and induce cell cycle arrest (Massagué, Blain & Lo, 2000).

The tumor suppressor gene **CDKN2A** is ubiquitously expressed and encodes the p16<sup>INK4A</sup>, as well as the p14<sup>arf</sup> protein. The expression of p16<sup>INK4A</sup> is significantly reduced in several human cancers. Specifically, the loss of p16 signaling in approximately 67 % of PDAC patients is associated with lymphatic invasion and the occurrence of postoperative widespread metastases (Oshima et al., 2013). P16 binds to CDK4 and CDK6 (cyclin-dependent kinase 4 and 6) and inhibits their kinase activity. As a result, the retinoblastoma protein (RB) remains unphosphorylated and prevents the transcription of E2F target genes. The lowered expression levels of DNA replication genes cause an irreversible cell cycle arrest in the G1 phase, putting the cells into senescence (Ohtani, Yamakoshi, Takahashi & Hara, 2004). The loss of p16<sup>INK4A</sup> through intragenic mutations and homozygous deletion allows pancreatic cancer cells to escape senescence and remain in an active, proliferative state. Nevertheless, some patients harbored wild-type p16 but had lost p16 expression. Interestingly, in these cases, the p16 locus was epigenetically silenced through DNA methylation at 5'-CpG islands (Schutte et al., 1997). These results indicate that tumorigenesis and progression can also be mediated by epigenetic alterations of key regulatory molecules and pathways.

#### 1.1.4. Molecular subtypes

The majority of pancreatic tumors share a similar mutational profile affecting predominantly four driver genes: the oncogene *KRAS* and the tumor suppressor genes *CDKN2A* (p16), *TP53*, and *SMAD4* (see 1.1.3). However, the heterogenic response of unselected PDAC populations to conventional treatment suggests the presence of additional, differentially altered genes and signaling pathways. Whole-genome sequencing and expression analysis of advanced pancreatic adenocarcinomas identified a large number of passenger genes, besides the main driver mutations, which were genetically altered in PDAC samples, albeit at a lower prevalence (Jones et al., 2008, Bailey et al., 2016). These mutated genes can be further divided into 12 different groups characterized by specific tumor-related core signaling pathways and processes. 67 to 100 % of the analyzed samples showed alterations in these core molecular pathways including cell cycle regulation, cell differentiation, invasion, DNA damage repair, apoptosis, and TGF- $\beta$ -signaling (Jones et al., 2008, Bailey et al., 2016). Nonetheless, the use of the core signaling pathways as treatment targets is impeded by the great variety of genetically altered genes from patient to patient (Jones et al., 2008).

To overcome molecular heterogeneity as a limiting factor in the treatment of PDAC, tumor gene expression profiles have been thoroughly investigated in order to identify clinically relevant molecular pancreatic cancer subtypes. The stratification of molecular tumor subtypes has been shown to improve treatment outcomes in other solid tumor entities, for example, lung and breast cancer (Lynch et al., 2004, Slamon et al., 2001). Global gene expression analysis of whole tissue and microdissected PDAC samples revealed three different subtypes with specific gene signatures: the **classical**, **quasimesenchymal**, and **exocrine-like subtypes** (Collisson et al., 2011). In the classical subtype, epithelial differentiation genes, such as the transcription factor *GATA6* (GATA Binding Protein 6) were highly expressed. Contrary, in the quasimesenchymal subtype the expression of epithelial genes was downregulated while mesenchymal genes were enriched. The exocrine-like subtype was characterized by high expression of genes involved in enzymatic digestion. Importantly, these subtypes correlated with overall survival and drug response. While patients with tumors of the quasimesenchymal subtype had a significantly shorter time of survival, their tumors were more sensitive to Gemcitabine treatment than tumors of the classical subtype. The EGFR-inhibitor Erlotinib showed to be more effective in classical cell lines indicating the presence of EGFR wildtype (Collisson et al., 2011). The study of Moffitt et al. in 2015 has confirmed the existence of a **classical** and a **quasimesenchymal/basal PDAC subtype** using microarray data. Identified genes that were upregulated in the basal PDAC subtype, for example, keratins *KRT5*, *KRT6A*, and *KRT15* also corresponded to previously described gene signatures in basal subtypes of bladder and breast cancer. Epithelial differentiation genes in PDAC samples like *GATA3* or *ERBB2* (Erb-B2 Receptor

Tyrosine Kinase 2) were also upregulated in luminal breast cancer subtypes (Moffitt et al., 2016, Damrauer et al., 2014). In 2016, Bailey et al. also defined four PDAC subtypes that correlated with patient survival. The gene expression profiles of the **squamous** and **ADEX** (aberrantly differentiated exocrine) subtype directly overlapped with those of the quasimesenchymal and exocrine-like subtype defined by Collisson et al., while the classical subtype was further separated into the **pancreatic progenitor** and **immunogenic subtype** based on specific gene expression patterns (Bailey et al., 2016). The transcriptome profile of the squamous subtype was characterized by an upregulation of squamous differentiation genes such as *TP63* and its target genes as well as *TP53* and *KDM6A* (lysine demethylase 6A) mutations. Additionally, the squamous subtype was associated with hypermethylation and thereby downregulation of endodermal cell-fate determination genes like *GATA6*, *HNF1B*, or *PDX1*. The ADEX subtype expresses markers for both endocrine and exocrine cell lineages, for example, *MIST1* or *RBPJL* (Recombination signal binding protein for immunoglobulin kappa J region-like) and *NEUROD1* (Neurogenic differentiation factor 1) or *NKX2-2* (NK2-homeobox) respectively. The pancreatic progenitor class was defined by transcription factors regulating early pancreatic cell differentiation (*PDX1*, *MNX1* (motor neuron and pancreas homeobox 1), *HNF1B*, *HNF1A*, *FOXA2* (Forkhead box A2)) and the immunogenic subtype included upregulated immune cell programs (Bailey et al., 2016). Overall, these results highlight the distinctive genetic and transcriptomic separation into two main PDAC subtypes with prognostic significance: the **classical/pancreatic progenitor** as well as the **quasimesenchymal/basal-like/squamous subtype** (Regel, Mayerle & Mahajan, 2020).

To further investigate the mechanisms underlying the separation into these two PDAC subtypes, large-scale genomic sequencing of PDAC samples and cell lines has been conducted. A study showed that approximately 35 % of PDAC patients harbor mutations in genes coding for epigenetic remodeling enzymes (Bailey et al., 2016). The altered genes include histone modifications (*KDM6A*, *SETD2* (SET domain containing 2, histone lysine methyltransferase), *HDAC1* (histone deacetylase 1), *CREBBP* (CREB binding protein), *EP300* (E1A binding protein P300), *JARID2* (Jumonji and AT-rich interaction domain containing 2)), DNA methylation (*KMT2A*, *DNMT3B* (DNA methyltransferase 3B), *DNMT1*), and transcription regulators (*ARID1A* (AT-rich interaction domain 1), *SMARCA4* (SWI/SNF related, matrix associated, actin dependent regulator of chromatin, subfamily A, member 4), *PRBM1* (polybromo 1)) (Regel, Mayerle & Mahajan, 2020) and define specific epigenetic profiles (see 1.2). Importantly, these gene expression profiles revealed a correlation to pancreatic cancer phenotypes and their differentiation status. Diaferia et al. were able to show that low-grade and high-grade PDAC cell lines display a distinct histone acetylation pattern regulating the expression and binding of subtype-specific transcription factors. For instance, in low-grade PDAC cell lines, the transcription of endodermal genes was activated through histone acetylation of enhancers. Conversely, the loss of

acetylation in high-grade PDAC cells was associated with a loss of cellular differentiation (Diaferia et al., 2016). Furthermore, some transcription factors exert a subtype-specific function. In the classical subtype, super-enhancers like GATA6, FOS (Fos proto-oncogene, AP-1 transcription factor subunit), FOXP1 (forkhead box 1), FOXP4, KLF4 (kruppel-like factor 4), ELF3 (E74 like ETS transcription factor), NFIX (nuclear factor I X), CUX1 (cut like homeobox 1), or SSBP3 (single-stranded DNA binding protein 3) further regulate other upregulated TFs, thereby amplifying their regulatory function. Transcription factors associated with the basal subtype include KLF5, MET, MYC, MYBL1 (MYV proto oncogene like 1), E2F1 (E2 transcription factor 1), SNAI2 (snail family transcriptional repressor 2), and TP63 (Lomberk et al., 2018, Bailey et al., 2016). Knockdown of MET proto-oncogene in vivo enabled an overall shift towards the classical phenotype with upregulation of GATA6 and inhibition of cell cycle-related pathways (Lomberk et al., 2018). Lately, single-cell RNA-sequencing of human PDAC samples also showed that basal-like and classical-like gene signatures can coexist within the same tumor, thereby explaining clinical heterogeneity (Chan-Sen-Yue et al., 2020).

These results show that epigenetic profiles could potentially play a part in defining molecular PDAC subtypes. Since the reversible nature of epigenetic modifications makes them an attractive therapeutic target, several clinical studies are currently investigating the effect of epigenetic drugs, such as Vorinostat in pancreatic cancer patients (see 1.1.5).

### **1.1.5. Therapeutic strategies for PDAC**

Although the incidence of pancreatic cancer represents only 2.5 % of all new cancer cases per year (Bray et al., 2018), its mortality is estimated to become the second highest of all types of cancer in the US by 2030 (Rahib et al., 2014). This demonstrates the need for more efficient therapeutic strategies.

The only curative therapeutic option for pancreatic cancer available at the moment is complete surgical removal. However, only 20 % of patients present with locally restricted tumors where surgical resection is feasible (Kleeff et al., 2016). To reduce the risk of locoregional tumor recurrence after surgical resection, adjuvant chemotherapy is recommended (Lambert et al., 2019). Currently, the recommended adjuvant chemotherapy regimen is modified FOLFIRINOX (mFOLFIRINOX: Folinic acid, Fluorouracil, Irinotecan, and Oxaliplatin) in fit patients or Gemcitabine/Gemcitabine-Capecitabine in patients with low performance status (Leitlinienprogramm Onkologie, 2021). These treatment recommendations are based on results of the PRODIGE 24 randomized controlled trial, which demonstrated an increase in median disease-free survival from 12.8 months under Gemcitabine monotherapy to 21.6 months with the mFOLFIRINOX regimen at the expense of higher

toxicity (Conroy et al., 2018). Gemcitabine showed comparable survival rates but higher tolerability than Fluorouracil-folinic acid in patients with R0 resections in the ESPAC-3 study (Neoptolemos et al., 2010). Furthermore, the ESPAC-4 study demonstrated increased survival rates from 25.5 months to 28 months with the Gemcitabine-Capecitabine combination therapy compared to the Gemcitabine monotherapy (Neoptolemos et al., 2017). The role of neoadjuvant treatment in patients with resectable disease is currently under debate.

Patients with locally advanced or metastatic disease should receive multimodal systemic therapies as well as palliative care. Standard of care neoadjuvant chemotherapy regimens for patients with borderline resectable or locally advanced PDAC include FOLFIRINOX or nab-Paclitaxel-Gemcitabine combination therapies. If restaging CT shows stable disease, exploratory surgery is recommended to assess secondary resectability. In the palliative setting, different systemic therapies are available depending on the patient's performance status, comorbidity, and personal preference (Leitlinienprogramm Onkologie, 2021). In the absence of response to first-line and second-line therapies, patients should be included in clinical trials investigating new chemotherapy regimens.

Although increasing knowledge about inter- and intratumoral molecular heterogeneity (see 1.3.4) may explain the low efficacy of conventional chemotherapy, it also provides opportunities for personalized targeted therapies. For example, PD-1 (programmed cell death protein 1) immune checkpoint inhibitors like Pembrolizumab showed high response rates in patients with deficient mismatch repair or high microsatellite instability tumors, though only 1 % of pancreatic cancers exhibit this specific genetic alteration (Le et al., 2017). 8.4 % of PDAC samples show defects in the DNA-damage response pathway, most often *ATM* (ATM serine/threonine kinase) and *BRCA2* (breast cancer gene 2) mutations, which makes them more susceptible to DNA double-strand break-induced cell death (Pishvaian et al., 2018). Hence, these tumors respond well to poly (ADP-ribose) polymerase inhibitors (PARPi) and platinum-based chemotherapies by inducing DNA double-strand breaks (Farmer et al., 2005). The randomized phase 3 trial POLO showed significantly longer progression-free survival of PDAC patients with a germline *BRCA1* or *BRCA2* mutation under treatment with the PARPi Olaparib compared to the placebo group (Golan et al., 2019). Despite encouraging studies for several small molecule inhibitors, these drugs remain limited to a very small percentage of patients harboring specific genotypes. Further research is needed to explore frequently altered genetic targets and their effectiveness in treating pancreatic cancer.

Furthermore, several epigenetic drugs are being investigated in clinical studies. Vorinostat, which is an inhibitor of class I and II histone deacetylases (HDACs), has been a part of the FDA-approved treatment regimen for cutaneous T cell lymphoma since 2006. Several clinical studies are now investigating the effects of Vorinostat on solid tumors since it showed broad antiproliferative and

antiangiogenic effects in vitro (Pichlmeier & Regel, 2020). A phase I study including patients with different solid cancers, including pancreatic cancer, showed stable disease in 61 % of patients (Millward et al., 2012). Another small phase I clinical trial with solely PDAC patients showed auspicious results of a combination therapy with Vorinostat and Capecitabine as radiosensitizers (Chan et al., 2016). These data show promising results for combination therapies of epigenetic drugs with conventional chemotherapeutic agents or radiation therapy.

## 1.2. Epigenetic modifications

Epigenetics describe heritable structural modifications of nucleosomes that affect gene expression levels without changing the underlying nucleic acid sequence (Bird, 2007). Two important pillars of epigenetic regulation are DNA methylation and post-translational histone modifications. Through open or closed chromatin conformations, they promote transcriptional activation or repression respectively (Figure 3). Importantly, the epigenetic profile is highly changed in cancer cells representing a promising new therapeutic target (Flavahan, Gaskell & Bernstein, 2017).

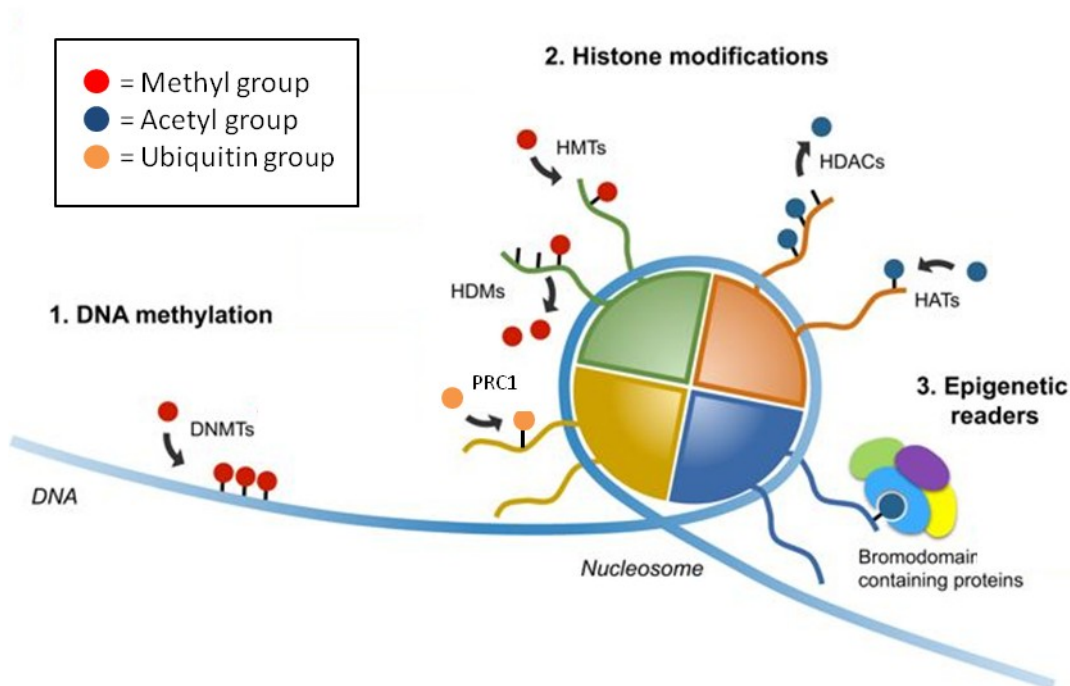


**Figure 3: Epigenetic mechanisms.** DNA methylation, histone modifications, and epigenetic readers represent the three main pillars of epigenetic regulation. The most frequent posttranslational histone modifications consist of histone methylation by histone methyltransferases (HMTs), histone ubiquitination by the Polycomb repressor complex 1 (PRC1), and histone acetylation regulated by histone acetyltransferases (HATs) and histone deacetylases (HDACs). Graph adapted and modified from Jubierre et al., 2018. (Jubierre et al., 2018)

### 1.2.1. DNA methylation

DNA methylation serves as an important epigenetic tool to regulate gene expression and occurs most frequently at the cytosine residue of CpG (5'-Cytosine-phosphate-Guanine-3') islands, which are CG dinucleotide clusters within the genome. In humans, a total of 70 – 80 % of all CpG dinucleotides are methylated, taking into account the highly dynamic processes (Bird, 2002). While CpG islands at promoter regions are mostly unmethylated, CpG regions in heterochromatin and repetitive elements are heavily methylated (Bernstein, Meissner & Lander, 2007).

In embryonic development, de-novo methylation by the DNA methyltransferases 3A and 3B (DNMT3A and DNMT3B) is involved in genomic imprinting and X chromosome inactivation, resulting in stable gene silencing. This is thought to produce a stable genomic methylation pattern during embryogenesis (Bird, 2002). On the contrary, DNMT1 catalyzes the methylation of the newly synthesized DNA strand during replication in order to maintain the methylation status through multiple cell generations (Lomberk, Iovanna & Urrutia, 2016). DNA methylation not only represses the binding of transcription factors through chromatin compaction, but it also enables the binding of methyl-CpG-binding domain proteins (MBDs) as epigenetic readers. MBD proteins like MeCP2 (methyl CpG binding protein 2) recruit epigenetic repressor complexes, for example, histone deacetylases (Nan et al., 1998) or histone methyltransferases (Fuks et al., 2003), in order to intensify chromatin compaction.

In cancer cells, DNA methylation is a common driver of tumor development and progression. On one hand, tumor suppressor genes like *p16<sup>INK4A</sup>* are epigenetically silenced through promoter hypermethylation (Schutte et al., 1997). On the other hand, malignant cells exhibit a global hypomethylation fostering chromosomal instability and oncogenicity (Flavahan et al., 2017). Furthermore, pancreatic precursor lesions like PanINs show elevated expression levels of *DNMT1*, *DNMT3A*, and *DNMT3B* as well as hypermethylation of *p16<sup>INK4A</sup>* and other transcription factors. Notably, increased methylation frequency for several genes (*NPTX2* (neuronal pentraxin 2), *SARP2* (secreted frizzled related protein 2), *RPRM* (reprimin, TP53 dependent G2 arrest media or homolog), *LHX1* (LIM homeobox 1)) correlates with increased staging degree of PanIN lesions (Sato, Fukushima, Hruban & Goggins, 2008).

### 1.2.2. Histone modifications

To reach a level of compaction that allows the DNA to fit into the nucleus with a diameter of only a few micrometres, the majority of DNA is subjected to chromatin compaction processes. Nucleosomes are the structural correlative of DNA packaging and result from the binding of

negatively charged DNA to a core of positively charged histone proteins. Exactly 146 bp (base pairs) of DNA wrap around one histone octamer (formed by two H2A-H2B heterodimers and one H3-H4 tetramer) to form a nucleosome (D'Addario, Di Francesco, Pucci, Finazzi Agrò & Maccarrone, 2013). The following 20 bp connect and further stabilize the adjacent nucleosomes by binding to the so-called H1 linker histone (Bednar et al., 1998). The chromatin undergoes further coiling until it reaches the highest compaction level as chromosomes.

Histones demonstrate post-translational modifications of their N-terminal tails or core domains. Common histone modifications include phosphorylation, methylation, acetylation, or ubiquitination at different positions. The addition of these functional groups affects the level of chromatin compaction. Hence, histone modifications control the accessibility of promoters to the transcriptional machinery and thereby regulate gene expression (Jubierre et al., 2018). Importantly, changes in the histone profile play a crucial role in pancreatic carcinogenesis. The dynamic nature of these processes makes them an attractive target for new therapeutic options (Träger & Dhayat, 2017).

#### **1.2.2.1. Activating histone modifications**

Histone acetylation and deacetylation through histone acetyl transferases (HATs) and histone deacetylases (HDACs) represent a leading mechanism for regulating gene transcription. The addition of acetyl groups to lysine residues on histone tails through HATs, such as CREBBP, p300, and KAT2B (lysine acetyltransferase 2B), activates gene expression. On the contrary, loss of acetyl groups through class I HDAC, or class III sirtuin (SIRT) enzymes promotes genetic silencing (Legoube & Trouche, 2003). HAT-mediated lysine acetylation can activate gene expression in a few different ways. First, the addition of acetyl groups neutralizes positive charges of lysine residues, thereby promoting an open chromatin conformation, which can be easily accessed by the transcriptional machinery (Clayton, Hazzalin & Mahadevan, 2006). Second, histone acetylation marks further enable the binding of other regulatory proteins. Bromodomains recognize and bind to acetylated histone tails to form large complexes with histone acetyltransferases and other cofactors. These complexes activate further histone acetylation along with the binding of transcription factors (Josling, Selvarajah, Petter & Duffy, 2012). For example, the human protein p300 has a bromodomain and a HAT domain. Upon binding of the bromodomain of p300 to acetylated lysine residues, the intrinsic HAT function is activated and results in further acetylation of histone and non-histone substrates like specific transcription factors (Chen, GhAzawi & Li, 2010). In healthy cells, the balance of histone acetylation and deacetylation is tightly regulated to ensure dynamic yet controlled gene transcription. In PDAC, low-grade tumors were characterized by high levels of the acetylation of

histone H3 on lysine 27 (H3K27ac), which activated epithelial gene signatures (Diaferia et al., 2016). Likewise, overexpression of HDACs correlated with increased tumor grade, high proliferative activity, epithelial-to-mesenchymal transition (EMT), and ultimately poor patient survival (Schneider, Krämer, Schmid & Saur, 2011).

Besides activating histone acetylation, histone methylation can have activating or repressive properties on gene expression. Activating histone methylation marks include the methylation of lysine 4 (H3K4me), lysine 36 (H3K36me), and lysine 79 (H3K79me) on histone H3, while methylation of lysine 9 (H3K9me) and lysine 27 on histone H3 (H3K27me) as well as lysine 20 on histone H4 (H4K20me) promote a closed chromatin conformation associated with genetic silencing (Bernstein et al., 2007) (Figure 4).

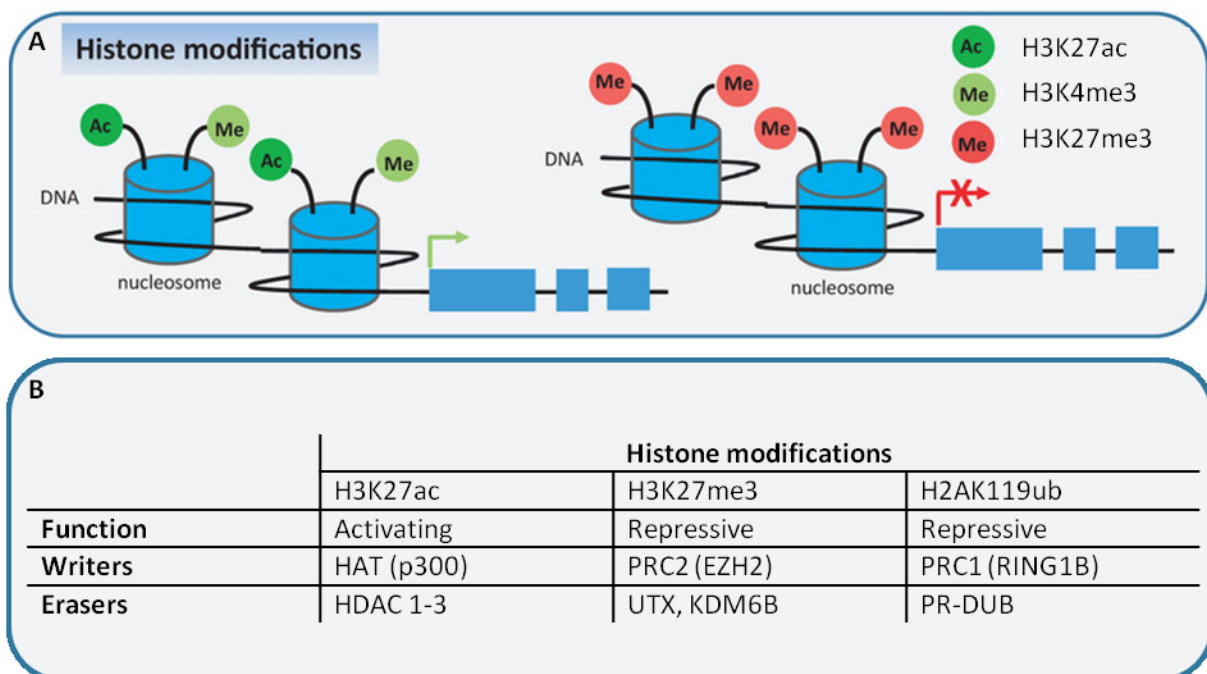


**Figure 4: Overview of active and repressive histone modifications.** (A) Activating histone modifications like histone acetylation (H3K27ac) or methylation (H3K4me3) promote an open chromatin state, thereby activating transcription. In contrast, repressive DNA methylation (H3K27me3) or histone ubiquitination (H2AK119ub) further a closed chromatin conformation, which correlates with transcriptional repression. (B) Overview of relevant histone modifications with their specific writers and erasers (Calo & Wysocka, 2014, Hyun, Jeon, Park & Kim, 2017, Decourcelle, Leprince & Dehennaut, 2019). Graph adapted and modified from D'Addario et al., 2013.

#### 1.2.2.2. Repressive histone modifications

Repressive histone modifications are mostly catalyzed by the so-called Polycomb group (PcG) proteins, which form the two major polycomb repressive complexes 1 and 2 (PRC1 and PRC2). First, the histone methyltransferase-domain EZH2 (enhancer of zeste homolog2) of PRC2 catalyzes the trimethylation of H3K27 (H3K27me3). This promotes the recruitment and binding of the PRC1

complex whose E3 ubiquitin ligases, RING1A (ring finger protein 1) and RING1B (ring finger protein 2), catalyze the mono-ubiquitination of lysine 119 of histone H2A (H2AK119ub) (Cao et al., 2002). Histone ubiquitination can repress transcriptional initiation by blocking RNA polymerase II-dependent transcriptional elongation (Zhou et al., 2008) or by keeping RNA polymerase II in an inactive state through C-terminal phosphorylation at serine 5 (Stock et al., 2007). Furthermore, PcG proteins also interact with other epigenetic modifiers to stabilize the epigenetic status. For instance, the PRC2 subunits EED (embryonic ectoderm development) and EZH2 interact with HDAC proteins and DNMTs, respectively, to promote transcriptional silencing (van der Vlag & Otte, 1999, Viré et al., 2007).

Members of the PRC1 and PRC2 are upregulated in a variety of solid tumors and correlate with a poor prognosis (Martínez-Romero et al., 2009). In 68 % of human pancreatic cancer samples, EZH2 was overexpressed, particularly in poorly differentiated areas (Ougolkov, Bilim & Billadeau, 2009). In vivo, suppression of EZH2 resulted in re-expression of the cell cycle inhibitor p27<sup>Kip1</sup> causing decreased proliferation and increased doxorubicin sensitivity (Ougolkov et al., 2009). Besides deregulation of members of the PRC2 complex, RING1B was also found to be overexpressed in 56 % of PDAC samples and correlated with poorer differentiation, lymph node metastasis, larger tumor size, and shorter time of survival (Chen, Chen et al., 2014). Consequently, *Ring1b* knockdown decreased cell proliferation and tumor volume in nude mice. Furthermore, simultaneous knockdown of *RING1B* and *EZH2* in pancreatic cancer cell lines led to transcriptional repression of *HOX* (homeobox) genes, which significantly impaired cell proliferation and promoted apoptosis in vitro and in vivo (Chen et al., 2014).

In a recent study, the authors have demonstrated that acinar cell transcription factors, such as *Ptf1a*, *Rbpjl*, *Bhlha15* (basic helix-loop-helix family member A15), *Nr5a2* (nuclear receptor subfamily 5 group A member 2), and *Klf15* were epigenetically silenced in PDAC development (Benitz et al., 2019). More precisely, in adult acinar cells, acinar differentiation genes were marked with the activating H3K4me3 modification. Embryonic acinar cells and ADMs showed a bivalent epigenetic profile, harboring both activating (H3K4me3) and repressive histone modifications (H3K27me3, H2AK119ub) suggesting a progenitor-like cell program. Finally, in pancreatic tumor cells, the activating influence of H3K4me3 was lost on acinar differentiation genes in favor of repressive histone marks (Benitz et al., 2019). Consequently, changes in the transcriptional profile in pancreatic carcinogenesis are tightly controlled by epigenetic mechanisms.

### **1.3. Pancreatic tumor model systems**

Basic molecular analysis as well as translational research of PDAC heavily relies on pancreatic tumor models to reflect common pathobiology. In vivo models include tumor cell lines or three-dimensional culture systems like organoid culture, while xenografts and genetically engineered mouse models are important in vitro tumor models.

#### **1.3.1. Pancreatic cancer cell lines**

Human cancer cell lines have been one of the most widely used scientific tumor model systems to study the biology of cancer and the molecular basis and efficacy of new drug treatments since the development of the first immortalized cell line HeLa in 1951 (Scherer, Syverton & Gey, 1953). This is mostly due to their easy handling and reliable high proliferation at a relatively low cost. In addition, cancer cell lines can be genetically modified with the help of the CRISPR/Cas9 system (clustered regularly interspaced short palindromic repeats/CRISPR associated protein 9) to specifically knock out the genes of interest (see 1.3.2). This method is commonly used to study the function of specific genes in pathologic processes as well as to test the therapeutic potential of a genetic loss-of-function.

However, several important limitations of human cancer cell lines have to be taken into consideration. Although cancer cell lines share many genomic aspects with the primary tumor, aberrant mutations specific to each cell line can occur during cell culture processes (Goodspeed, Heiser, Gray & Costello, 2016). Similarly, while DNA methylation profiles of cancer cell lines mostly represent the tumor-specific methylome, changes in the epigenome can occur in immortalized cell lines (Varley et al., 2013). Moreover, traditional cancer cell lines are monoclonal populations and therefore do not depict intratumoral heterogeneity (Goodspeed et al., 2016). Lastly, conventional cell culture methods do not take into account the influence of other cell types, like inflammatory cells, on the tumor cells (Weinstein, 2012).

Human cancer-derived cell lines are a useful tool to mimic main tumor cell characteristics. Nonetheless, the limitations mentioned above need to be considered, especially when translating in vivo findings to in vitro models.

### 1.3.2. Genome editing

Genetic engineering is an important method to study the function and regulation of individual genes in-vitro and in-vivo.

Over the years, there have been different approaches to induce genetic modifications through double-strand breaks (DSBs). Natural repair mechanisms of double-strand breaks include the highly efficient but rare homology-directed repair (HDR) and the more frequent but less effective non-homologous end joining (NHEJ). NHEJ results in insertion/deletion (indel) mutations which can cause frameshift mutations at the target gene locus resulting in premature chain termination and loss of or impaired protein function (Ma, Zhang, and Huang 2014). In the presence of a DNA repair template, specific mutations can be generated at the target sequence through HDR (Ran et al., 2013). For many years, zinc finger nucleases (ZFNs) and transcription activator-like effector nucleases (TALENs) have been used to induce DSBs at specific genomic loci through DNA-protein interactions. However, the use of these methods is limited by the need to design a complex new ZFN or TALEN protein for each target sequence (Miller et al., 2011).

The CRISPR/Cas9 (Clustered regularly short palindromic repeats/CRISPR-associated protein 9) system overcomes this problem by using Watson-Crick base pairing of its guide RNA to direct the endonuclease to the target sequence (Hsu, Lander & Zhang, 2014). CRISPR/Cas9 originated from the acquired immune system of bacteria as a defense mechanism against bacteriophages. In response to phage infection, some bacteria are capable to integrate short sequences of the bacteriophage genome, commonly referred to as spacers, into their own genome. Upon reinfection, the bacterial endonuclease is directed to its target through complementary binding of the spacer to the phage genome (Sorek, Kunin & Hugenholtz, 2008). CRISPR loci consist of a Cas9 gene cassette followed by the variable DNA fragments (spacers) interspaced by repeat sequences (direct repeats) (Figure 5) (Mojica et al., 2005). Spacers and direct repeats are transcribed and converted into pre-crRNAs (CRISPR RNAs). In the course of crRNA maturation, they form complexes with tracrRNAs (trans-activating crRNA). This dual crRNA-tracrRNA-structure directs the Cas9 protein to its target DNA locus through sequence homology (Jinek et al., 2012). The Cas9 endonuclease then induces a DNA double-strand break at the target site. To facilitate its use in genetic engineering, the crRNA-tracrRNA-complex was chemically engineered into one RNA chimera, the so-called sgRNA (single guide RNA) (Jinek et al., 2012).

The only prerequisite for sgRNA construction is the so-called protospacer-adjacent motif (PAM). This short sequence is species-specific and located directly upstream of the DNA target site. For instance, the PAM sequence for Cas9 derived from *Streptococcus pyogenes* (SpCas9) is 5'-NGG-3'. To improve DSB target specificity, a nickase-mutant of SpCas9 has been developed by inactivating one of its two

catalytic domains (RuvC or HNH nuclease domain). The use of paired gRNAs (guide RNA), which are only able to cleave a single DNA strand, decreases the number of off-target DSBs by increasing the number of necessary complementary base pairs (Ran et al., 2013).

Unlike former methods of genome editing, CRISPR-based systems offer quickly available tools to change virtually any specific site in the genome as well as increasing therapeutic significance.

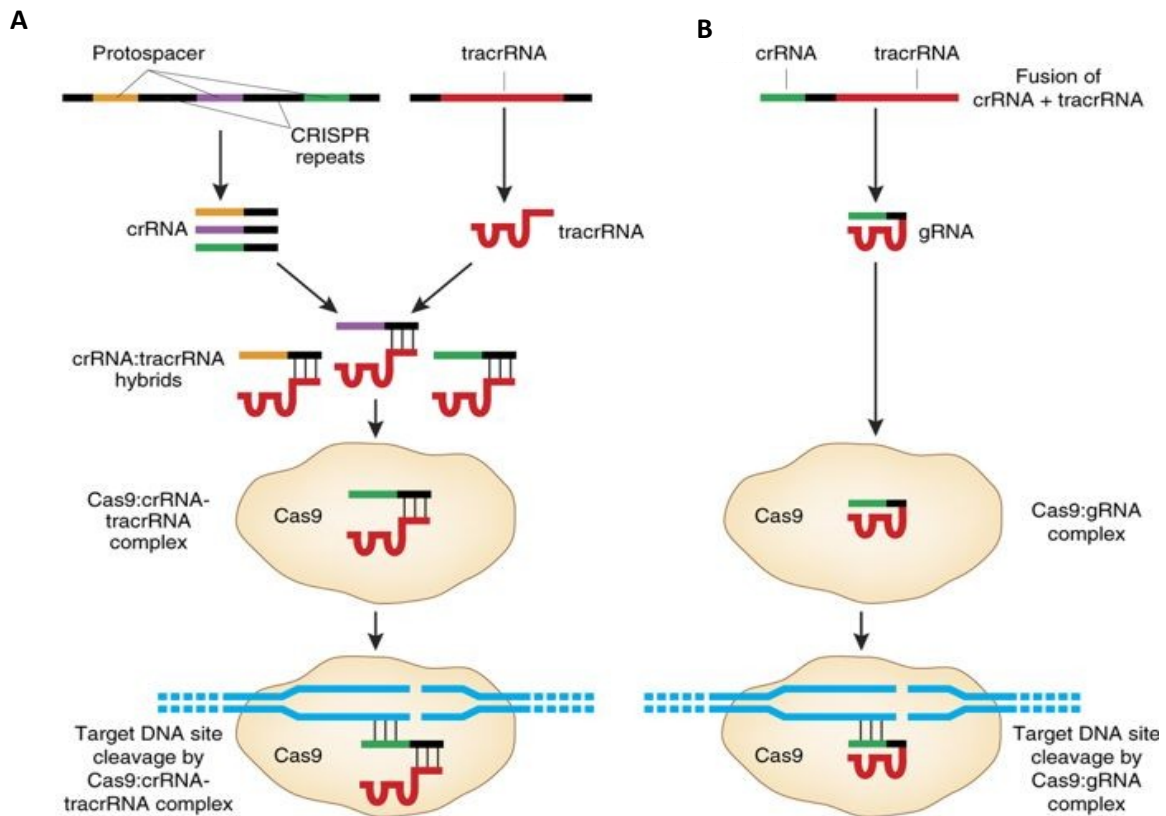


**Figure 5: Structure and working principle of biological and engineered CRISPR/Cas9 systems.** (A) In naturally occurring CRISPR systems, foreign DNA is incorporated as protospacers between CRISPR repeats. After transcription of the gene locus, crRNAs and tracrRNAs form crRNA-tracrRNA hybrids. Together with the Cas9 protein, they bind to complementary DNA sites and cleave the target locus. (B) Genetically engineered CRISPR/Cas9 systems most commonly use a crRNA-tracrRNA-complex, known as sgRNA. This sgRNA oligonucleotide binds to the complementary target sequence and induces the Cas9-mediated DSB. Graph adapted and modified from Sander & Joung, 2014.

## 2. Aim of the study

Since the identification of PDAC subtypes with different transcriptome profiles but similar genetic backgrounds, great effort has been put into defining the molecular mechanisms underlying PDAC heterogeneity. For lack of differing genetic driver mutations, I suggest that posttranslational epigenetic modifications could promote tumor heterogeneity (Regel, Hausmann, Benitz, Esposito & Kleeff, 2016).

This study aims at further characterizing the classical and basal pancreatic cancer subtypes in order to develop new treatment strategies. Human pancreatic cancer cell lines representing the classical or basal subtype will be used to identify subtype-specific differences in their transcriptome. Then, their epigenetic profiles and possible correlation to the molecular subtypes will be determined using advanced epigenetic methods like chromatin-immunoprecipitation and bisulfite methylation analysis.

The reversible nature of epigenetic modifications harbors great potential for pancreatic cancer treatment. It has been shown before that drug-induced inhibition as well as genetic knockout of epigenetic modifiers like *Ring1b* is able to greatly impair tumor formation in vivo and induce tumor cell reprogramming towards a less aggressive phenotype (Benitz et al., 2019). Nevertheless, the results of clinical studies with epigenetic drugs on patient survival fall short of the promising preclinical data (Pichlmeier & Regel, 2020). Therefore, the effects of histone acetylase and histone deacetylase inhibitor treatment were studied to investigate whether tumor cell reprogramming might depend on the epigenetic profile of the molecular subtype. Secondly, the effect of single-drug epigenetic treatments might be compromised by the highly dynamic nature of epigenetic changes. Hence, this study aimed at investigating whether a combinatory loss of epigenetic modifiers would initiate a cellular differentiation program in order to overcome therapy resistance. For this purpose, it was planned to generate a multiplex CRISPR/Cas9-mediated *HDAC2/DNMT3A/RING1B*-knockout cell line and subsequently perform basic cell assays.

### 3. Materials and Methods

#### 3.1. Specific chemicals and reagents

Table 1 Specific chemicals and reagents

Reagent	Manufacturer
2-Mercaptoethanol	Sigma-Aldrich, St. Louis, USA
Acrylamid / Bis solution, Rotiphorese®30 %	Carl Roth GmbH, Karlsruhe
Adenosine triphosphate 25 mM	Lucigen, Middleton, USA
Agarose SERVA for DNA Electrophoresis	SERVA, Heidelberg, Germany
Albumin Fraction V, Bovine serum albumin (BSA)	Carl Roth GmbH, Karlsruhe
Ammoniumperoxodisulfat (APS)	Carl Roth GmbH, Karlsruhe
Buffer Tango 10x	Fermentas, Waltham, USA
DABCO (1,4-Diazabicyclo[2.2.2]octane)	Sigma-Aldrich, St. Louis, USA
DAPI (4',6-diamidino-2-phenylindole dihydrochloride)	Sigma-Aldrich, St. Louis, USA
Deosynucleotide (dNTP) Mix 10 mM	Invitrogen, Carlsbad, USA
Dimethyl sulfoxid (DMSO)	Sigma-Aldrich, St. Louis, USA
Dithiothreitol (DTT) 0,1 M	Invitrogen, Carlsbad, USA
Donkey serum	Sigma-Aldrich, St. Louis, USA
Dulbecco's modified eagle's medium (DMEM) high glucose (4500 mg/l glucose)	Sigma-Aldrich, St. Louis, USA
Dulbecco's phosphate buffered saline (1X) (PBS)	Sigma-Aldrich, St. Louis, USA
Ethylenediaminetetraacetic acid disodium salt dihydrate (EDTA)	Sigma-Aldrich, St. Louis, USA
FastStart Essential DNA Green Master	Roche, Basel, Switzerland
Fetal bovine serum (FBS)	Sigma-Aldrich, St. Louis, USA
Fluorescence Mounting Medium with DAPI	Dako Agilent, Santa Clara, USA
Gemcitabine hydrochloride	Merck Millipore, Billerica, USA
GeneRuler 100 bp Plus DNA Ladder	Thermo Fisher Scientific, Waltham, USA
GoTaq® G2 Hot Start Master Mixes	Promega, Fitchburg, USA
Lipofectamine™ 2000 Transfection Reagent	Thermo Fisher Scientific, Waltham, USA
Magnesiumchloride 25 mM	Qiagen, Hilden

Milk powder, Blotting-Grade	Carl Roth GmbH, Karlsruhe
Nonident P-40 (NP-40) (IPEGAL® CA-630)	Sigma-Aldrich, St. Louis, USA
Orange Loading Dye 6x	Fermentas, Waltham, USA
PageRuler™ Plus prestained Protein Ladder (10 to 180 kDa)	Thermo Fisher Scientific, Waltham, USA
Penicillin/Streptomycin (P/S)	Sigma-Aldrich, St. Louis, USA
Pierce™ Phosphatase Inhibitor Tablets	Thermo Fisher Scientific, Waltham, USA
Pierce™ Protease Inhibitor Tablets	Thermo Fisher Scientific, Waltham, USA
PIPES (1,4-Piperazinediethanesulfonic acid)	Sigma-Aldrich, St. Louis, USA
Plasmid-safe ATP-dependent DNase	Lucigen, Middleton, USA
Plasmid-safe buffer 10x	Lucigen, Middleton, USA
Protein A agarose/salmon sperm DNA	Merck Millipore, Billerica, USA
Quick Load 1 kb DNA Ladder	New England Biolabs, Ipswich, USA
ReadyMix™ REDTaq® PCR Reaction Mix with MgCl <sub>2</sub>	Sigma-Aldrich, St. Louis, USA
RPMI Medium (Roswell park memorial institute medium) 1640 (1X)	Thermo Fisher Scientific, Waltham, USA
S-Adenosylmethionine	New England Biolabs, Ipswich, USA
Sodium bicarbonate (NaHCO <sub>3</sub> )	Sigma-Aldrich, St. Louis, USA
Sodium deoxycholate	Sigma-Aldrich, St. Louis, USA
Sodium dodecyl sulfate (SDS) Pellets	Carl Roth GmbH, Karlsruhe
SYBR™ Safe DNA Gel Stain	Thermo Fisher Scientific, Waltham, USA
T4 DNA ligase buffer 10x	Fermentas, Waltham, USA
TEMED (Tetramethylethylenediamine)	Carl Roth GmbH, Karlsruhe
TRIS PUFFERAN®	Carl Roth GmbH, Karlsruhe
Triton X-100	Sigma-Aldrich, St. Louis, USA
Trypsin-EDTA Solution (10X)	Sigma-Aldrich, St. Louis, USA
Tween® 20	Carl Roth GmbH, Karlsruhe

### 3.2. Kits

Table 2 Kits

Kit	Manufacturer
DNeasy Blood & Tissue Kit	QIAGEN, Hilden
Epitect Bisulfite Kit	QIAGEN, Hilden
Pierce™ BCA Protein Assay Kit	Thermo Fisher Scientific, Waltham, USA
Pierce™ ECL Western Blotting Substrate	Thermo Fisher Scientific, Waltham, USA
QIAquick PCR purification Kit	QIAGEN, Hilden
RevertAid First Strand cDNA Synthesis Kit	Thermo Fisher Scientific, Waltham, USA
RNeasy Plus Mini Kit	QIAGEN, Hilden
Plasmid Midi Kit	QIAGEN, Hilden

### 3.3. Antibodies

ChIP = Chromatin immunoprecipitation

ICW = In-cell western

IF = Immunofluorescence

WB = Western blot

#### 3.3.1. Primary antibodies

Table 3 Primary antibodies

Antibody	Host	Application / Dilution	Blocking solution	Manufacturer / Reference #
Anti-DNMT3A	Rabbit	WB 1:1000	5 % milk / TBS-T	Santa Cruz, Dallas, USA / sc-20703 (discontinued)
Anti-DNMT3A	Rabbit	WB 1:500	5 % milk / TBS-T	Santa Cruz, Dallas, USA / sc-365769
Anti-EpCAM	Mouse	IF 1:200	1 % BSA, 0.1 % Triton X-100 / PBS	Cell Signaling, Danvers, USA / #66020
Anti-Gapdh	Rabbit	WB 1:4000	5 % milk / TBS-T	Santa Cruz, Dallas, USA / sc-25778

Anti-H2AK119ub	Rabbit	ChIP 3 µg ICW 1:200	ChIP Dilution Buffer 1 % BSA, 0.1 % Triton X-100 / PBS	Cell Signaling, Danvers, USA / #8240
Anti-H3K27ac	Rabbit	ChIP 0.26 µg WB 1:1000	ChIP Dilution Buffer 5 % milk / TBS-T	Cell Signaling, Danvers, USA / #8173
Anti-H3K27me3	Mouse	ChIP 7 µg	ChIP Dilution Buffer	Abcam, Cambridge, UK / #6002
Anti-HDAC1	Mouse	WB 1:1000	5 % milk / TBS-T	Cell Signaling, Danvers, USA / #8173
Anti-HDAC2	Mouse	ICW 1:200 IF 1:100 WB 1:1000	1 % BSA, 0.1 % Triton X-100 / PBS 1 % BSA, 0.1 % Triton X-100 / PBS 5 % milk / TBS-T	Cell Signaling, Danvers, USA / #5113
Anti-Ring1B	Rabbit	WB 1:500	5 % BSA / TBS-T	Cell Signaling, Danvers, USA / #5694
Anti-Vimentin	Rabbit	IF 1:200	1 % BSA, 0.1 % Triton X-100 / PBS	Cell Signaling, Danvers, USA / #5741
Normal Rabbit IgG		ChIP 1 µg	ChIP Dilution Buffer	Cell Signaling, Danvers, USA / #2927

### 3.3.2. Secondary antibodies

Table 4 Secondary antibodies

Antibody	Host	Conjugate	Application / Dilution	Blocking solution	Manufacturer / Reference #
Anti-mouse IgG	Sheep	Horseradish peroxidase	WB 1:5000	1 % milk / TBS-T	GE Healthcare, Little Chalfont, UK NA931

Anti-rabbit IgG	Donkey	Horseradish peroxidase	WB	1:5000	1 % milk / TBS-T	GE Healthcare, Little Chalfont, UK NA934
Anti-mouse IgG	Goat	DyLight™ 680	ICW	1:1000	1 % BSA, 0.1 % Triton X-100 / PBS	Cell Signaling, Danvers, USA / #5470
Anti-mouse IgG	Donkey	FITC	IF	1:1000	1 % BSA, 0.1 % Triton X-100 / PBS	Jackson ImmunoResearch, Baltimore, USA / 715-095-151
Anti-rabbit IgG	Donkey	CY3r	ICW	1:1000	1 % BSA, 0.1 % Triton X-100 / PBS	Jackson ImmunoResearch, Baltimore, USA / 711-165-152

### 3.4. Enzymes

Table 5 Enzymes

Enzyme	Manufacturer
BbsI restriction enzyme	New England Biolabs, Ipswich, USA
CpG Methyltransferase (M. SssI)	New England Biolabs, Ipswich, USA
Eco31I restriction enzyme	Thermo Fisher Scientific, Waltham, USA
Hot Start Taq DNA polymerase	New England Biolabs, Ipswich, USA
Micrococcal Nuclease (MNase), 100 units/μl	Thermo Fisher Scientific, Waltham, USA
Proteinase K	Peqlab Biotechnologie GmbH, Erlangen
Quick ligase	New England Biolabs, Ipswich, USA
RNase A	Qiagen, Hilden
T7 DNA ligase	New England Biolabs, Ipswich, USA

### 3.5. Inhibitors

Table 6 Inhibitors

Inhibitors	Manufacturer
SAHA (Vorinostat)	Sigma-Aldrich, St. Louis, USA
5-Aza-2'-Deoxycytidine (Decitabine)	Cayman, Ann Arbor, USA
A485	Tocris, Bristol, UK

### 3.6. Oligonucleotides

All primers were designed for an annealing temperature of 55 °C and were ordered from Thermo Fisher Scientific (Waltham, USA) (25 nmol, desalted).

#### 3.6.1. Gene expression primer (for qRT-PCR)

Table 7 Gene expression primer

Primer	Sequence forward (5' → 3')	Sequence reverse (5' → 3')
<i>AIM2</i>	AGAGGTAAATAGCGCCTCACG	TTCTGTTACCTTCTGGACTACAAAC
<i>CREBBP</i>	GTACCATTCTCGCGATGCT	ATCAACGAAAGGTTCTGGGGT
<i>DNMT1</i>	GTGGAAGCCGGCAAAGC	TCCCACTCGAGCCTCCATA
<i>DNMT3A</i>	CTCGCGATTTCTCGAGTCCA	ATACCGGGAAGGTTACCCCA
<i>DNMT3B</i>	CTACCCGGGATGAACAGGATCT	AGTAGTCCTTCAGAGGGGCG
<i>EP300</i>	TGGCAGAAAGTTGGAGTTCTCTC	AAGAAACGCTCTCCCCTTGG
<i>EPCAM</i>	GCTGGAATTGTTGTGCTGGTTA	AAGATGTCTTCGTCCCACGC
<i>ERBB3</i>	TGAATGGCCTGAGTGTGACC	CGAATCCACTGCAGGAAGGA
<i>GATA6</i>	CCCCACAACACAACCTACAG	GCCCATCTTGACCCGAATACT
<i>GPM6B</i>	TCCCCGAAAAATATGTGGC	CGACTCTTAAACTTCAAACCGC
<i>HAT1</i>	GGAAATGGCGGGATTTGGTG	ATCCCCAAAGAGTTGATGGGT
<i>HDAC1</i>	GCCTTCTACACCACGGACC	TTGGACATGACCGGCTTGAAA

<i>HDAC2</i>	GAGGTGGCTACACAATCCGT	TCATTATATGGCAACTCATTGGGA
<i>HPRT</i>	TTGCTTTCCTTGGTCAGGCA	ATCCAACACTTCGTGGGGTC
<i>KRT5</i>	CGAGGAATGCAGACTCAGTG	GCTGCTGGAGTAGTAGCTTCC
<i>KRT6A</i>	CAGGACCTGGTGGAGGACTT	CTGGGACAGCTCTGCATCAT
<i>KRT81</i>	AGCAGAGGCTATGTGAAGGC	CTCCGCAGGTGGTGTTC AAT
<i>MYC</i>	TACAACACCCGAGCAAGGAC	AGCTAACGTTGAGGGGCATC
<i>PTHLH</i>	TCGAGGTTCAAAGGTTTGCCT	GTTTCAAGTGCGTGTGTCGT
<i>RING1A</i>	CGTTCACGACGTTGAATGGC	ACAGGGATACCCCATGGTCC
<i>RING1B</i>	ACAGGCCATGAACAGACTGC	TGCAGTGTGAACTGTCACCA
<i>S100A2</i>	ACAGATCCATGATGTGCAGTTCT	CCACTTTCTCCCCACAAAGC
<i>SMARCA4</i>	ACTACGAGCTCATCCGCAAG	GGAGTCTTCATAGATCAGGGAGC
<i>TBP</i>	ACTCCACTGTATCCCTCCCC	CAGCAAACCGCTTGGGATTA
<i>TP63</i>	CATTTGACCCTATTGCTTTTAGCCT	ATGAGCTGGGGTTTCTACGA

### 3.6.2. CHIP primer (for qRT-PCR)

Table 8 CHIP primer

Primer	Sequence forward (5' → 3')	Sequence reverse (5' → 3')
<i>EpCAM</i>	CCCCCGAAACGGGCATAATA	TTTGGAAACCCAAGTCCACC
<i>GATA6</i>	CTCCCCTCCACCCCTACTCG	GATAAGCGCTTCGAGGAGAGAA
<i>MYC</i>	CGTCCTCGGATTCTCTGCTC	CTTCGCTTACCAGAGTCGCT
<i>TP63</i>	CTCTCTCTGGGCAGGACTCA	TTCGCACAACCCACCAGAAA

### 3.6.3. Methylation-specific PCR (MSP) primer (for PCR)

MSP primers were designed with MethPrimer (Li, Dahiya, Rajvir, 2002.).

**Table 9 MSP primer**

Primer	Sequence forward (5' → 3')	Sequence reverse (5' → 3')
<i>EpCAM</i> <i>unmodified</i>	TAGGTTTTTTGTGGTTATTGAATTG	AAACAAACCCACTAATCCCTATCAT
<i>EpCAM</i> <i>methylated</i>	TAGGTTTTTTGCGGTTATCGAATC	GAACCCGCTAATCCCTATCGT
<i>TP63</i> <i>unmodified</i>	TTTAGGGATATTTAAAAGTTGGAGAGTG	TCAAATACTACAACCTCAAATCATA
<i>TP63</i> <i>methylated</i>	TTAGGGATATTTAAAAGTTGGAGAGC	TCGAAATACTACGACTCAAATCGTA

### 3.6.4. sgRNAs (single guide RNAs)

Single guide RNAs were designed with Zhang Lab's online CRISPR Design tool [crispr.mit.edu](http://crispr.mit.edu) (Ran et al., 2013) and CHOPCHOP (Labun et al., 2016 and Montague et al., 2014). An additional guanine was added at the 5' end where the sequence started with a different base.

**Table 10 sgRNAs**

Target gene	Overhang – additional guanine – sequence forward (5' → 3')	Overhang – sequence reverse (5' → 3')
<i>HDAC2</i>	CACC – G – TCAACTGGCGGTTTCAGTTGCTGG	AAAC – CCAGCAACTGAACCGCCAGTTGAC
<i>DNMT3A</i>	CACC – GGGAACAGCTTCCCCGCG	AAAC – CGCGGGGAAGCTGTTCCC
<i>RING1B</i>	CACC – GCATATGAGACGTGTAAACT	AAAC – AGTTTACACGTCTCATATGC

### 3.6.5. Sequencing primer

**Table 11 Sequencing primer**

Target gene	Sequence forward (5' → 3')	Sequence reverse (5' → 3')
<i>U6</i>	GAGGGCCTATTTCCCATGATTCC	-

### 3.7. Plasmids

Table 12 Plasmids

Plasmid	Manufacturer
Multiplex CRISPR/Cas9 Assembly System Kit	Addgene, Watertown, USA / Kit #1000000055
CRISPR/Cas9 KO (knockout) Control Plasmid	Santa Cruz, Dallas, USA / sc-418922

### 3.8. Cell lines

Table 13 Cell lines

Cell line	Characteristics
Capan-1	Human PDAC cell line, derived from liver metastasis
Capan-2	Human PDAC cell line
COLO 357	Human PDAC cell line, derived from metastatic lymph node
MIA PaCa-2	Human PDAC cell line
PANC-1	Human PDAC cell line
PaTu 8988s	Human PDAC cell line
PaTu 8988t	Human PDAC cell line

### 3.9. Consumption materials

Table 14 Consumption materials

Material	Manufacturer
96-well plate (qRT-PCR), white	STARLAB, Hamburg, Germany
Cell culture flasks (25 cm <sup>2</sup> , 75 cm <sup>2</sup> )	Sarstedt, Nürnberg, Germany
Cell culture plates (6-well, 24-well)	Greiner Bio-One, Kremsmünster, Austria
Cell culture plates, TC dish (100 mm <sup>2</sup> )	Sarstedt, Nürnberg, Germany
Chamber slide (8-well)	Thermo Fisher Scientific, Waltham, USA

Corning® 96-well Clear Bottom Black Polystyrene Microplates	Corning, New York, USA
Cryogenic tube	STARLAB, Hamburg, Germany
Neubauer chamber	Paul Marienfeld GmbH & Co. KG, Lauda-Königshofen
Nitrocellulose blotting membrane	GE Healthcare, Little Chalfont, UK
PCR reaction tube	Biozym, Oldendorf, Germany
Permanent Mounting Medium, VectaMount	Sigma-Aldrich, St. Louis, USA
Pipette filter tips (10 µl, 200 µl, 1000 µl)	Sarstedt, Nürnbrecht, Germany
Pipette tips (10 µl, 200 µl, 1000 µl)	Sarstedt, Nürnbrecht, Germany
Reaction tubes (0.5 ml, 1.5 ml, 2 ml)	Sarstedt, Nürnbrecht, Germany
Reaction tubes (15 ml, 50 ml)	Sarstedt, Nürnbrecht, Germany
Serological pipettes, sterile (5 ml, 10 ml, 25 ml)	Sarstedt, Nürnbrecht, Germany
Xtra-Clear Advanced Polyolefin Starseal	STARLAB, Hamburg, Germany

### 3.10. Equipment

**Table 15 Equipment**

<b>Equipment</b>	<b>Manufacturer</b>
AEJ200-4CM	Kern & Sohn, Stuttgart, Germany
Allegra 25R AJD05B010	Beckman Coulter, Brea, USA
Centrifuge 5417R	Eppendorf, Hamburg, Germany
Centrifuge 5418	Eppendorf, Hamburg, Germany
Centrifuge 5702R	Eppendorf, Hamburg, Germany
Compact Shaker KS-15 Control	Edmund Bühler GmbH, Bodelshausen, Germany
EW4200-2NM	Kern & Sohn, Stuttgart, Germany

FluoStar Omega	BMG Labtech, Ortenberg, Germany
Fusion FX	Vilber Lourmat GmbH, Eberhardzell, Germany
Heracell 240 CO2 Incubator	Marshall Scientific, Hampton, USA
Inkubator	BINDER GmbH, Tuttlingen, Germany
inoLab pH 720	WTW, Weilheim, Germany
IX50 Phase contrast inverted microscope	Olympus, Shinjuku, Japan
Leica DMI6000 B	Leica Microsystems GmbH, Wetzlar, Germany
LightCycler® 96	Roche, Basel, Switzerland
Mastercycler® pro vapo.protect	Eppendorf, Hamburg, Germany
Mini Plate Spinner Centrifuge-230EU	Corning, New York, USA
Mini PROTEAN® Tetra Cell	Bio-Rad, Herkules, USA
Mini Trans-Blot® Module	Bio-Rad, Herkules, USA
Pipetboy acu 2	Integra, Biebertal, Germany
PIPETMAN® classic	Gilson, Middleton, USA
PowerPac™ HC Power Supply	Bio-Rad, Herkules, USA
Sonoplus HD2070 with MS72 microtip	Bandelin, Berlin, Germany
SpectraMax® Plus 384 Microplate Reader	Molecular Devices, San José, USA
TS1 ThermoShaker	Biometra GmbH, Göttingen, Germany
Vortex Schüttler, 7-2020	neoLab Migge GmbH, Heidelberg, Germany

### 3.11. Computer applications

**Table 16 Computer applications**

Program	Producer
Axiovision SE64 Rel.4.9	Carl Zeiss AG, Oberkochen
CHOPCHOP	Zhang lab, Cambridge, UK

Citavi 6, V2	Swiss Academic Software GmbH, Wädenswil, Switzerland
FusionCaptAdvance (7.17.02a)	Vilber Lourmat GmbH, Eberhardzell, Germany
GraphPad Prism 5	GraphPad Software, Inc., La Jolla, USA
ImageJ	By Wayne Rasband, NIH, Bethesda, USA
Leica MM AF	Leica Microsystems GmbH, Wetzlar, Germany
Lightcycler <sup>®</sup> 96 software (version 1.1.0.1320)	Roche, Basel, Switzerland
MARS	BMG Labtech, Ortenberg, Germany
MethPrimer	Li Lab, Beijing, China
Microsoft Office	Microsoft, Redmond, USA
Softmax Pro 7.0	Molecular Devices, San José, USA

## 4. Methods

The manufacturers of all reagents and instruments are listed in the materials section (see chapter 3) and therefore not named again in the methods.

### 4.1. Cell biological methods

#### 4.1.1. Cell culture conditions

Table 17 Cell culture conditions

Cell line	Cell culture medium
Capan-1 Capan-2	DMEM high glucose (with L-glutamine)  1 % Penicillin/Streptomycin (P/S) (v/v)  20 % Fetal Bovine Serum (FBS) (v/v)
COLO 357 Panc-1	RPMI Medium 1640 (with L-glutamine)  1 % Penicillin/Streptomycin (P/S) (v/v)  10 % Fetal Bovine Serum (FBS) (v/v)
MIA PaCa-2 PaTu 8988s PaTu 8988t	DMEM high glucose (with L-glutamine)  1 % Penicillin/Streptomycin (P/S) (v/v)  10 % Fetal Bovine Serum (FBS) (v/v)

All cell culture experiments were performed under sterile conditions in a biological safety cabinet. Cell lines were cultivated with a specific cell culture medium listed above in an incubator at 37 °C and at a saturated atmosphere with 5 % CO<sub>2</sub>.

#### 4.1.2. Passaging of cells

Cells were passaged at 70 to 80 % confluence. After aspiration of the medium, cells were washed with PBS (1X) and incubated with trypsin (1X or 2X) in PBS for 10 to 20 minutes at 37 °C. When the cells were fully detached from the bottom of the flask, trypsin activity was stopped through the addition of cell culture medium containing FBS. The cell suspension was then centrifuged (5 min, 200 x g, room temperature (RT)) and resuspended in fresh cell culture medium. Cells were split in a ratio of 1:2 to 1:20 depending on cell growth and planned experiments.

#### 4.1.3. Cryopreservation of cells

<u>Freezing medium</u>	80 %	Fetal Bovine Serum (FBS) (v/v)
	20 %	Dimethyl sulfoxid (DMSO) (v/v)

To cryopreserve cells, they were first trypsinized and centrifuged (5 min, 1 200 revolutions per minute (rpm), RT). The cell pellet was resuspended in 1 ml of cell culture medium and transferred to a cryo tube. Finally, an equal volume of freezing medium was carefully added. Cells were stored at -150 °C.

#### 4.1.4. Revitalization of cells

Frozen cells were thawed quickly in a 37 °C water bath. Next, 5 ml of cell culture medium were added to the cell suspension. Cells were centrifuged (5 min, 1 200 rpm, RT) to remove any freezing medium and resuspended in fresh cell culture medium. Cells were grown in a 25 cm<sup>2</sup> cell culture flask for 24 hours before they were passaged and transferred to a new 75 cm<sup>2</sup> flask.

#### 4.1.5. Treatment of cells with inhibitors

Pancreatic cancer cell lines were treated with the epigenetic drugs Vorinostat, A485, and Decitabine at concentrations of 5 to 10 000 µM. **Vorinostat** was diluted with DMSO to a stock concentration of 5 mM and stored in 10 µl aliquots at – 80 °C for up to one month. **A485** was diluted with DMSO to a stock concentration of 10 mM and stored in 10 µl aliquots at -20 °C for up to one month. **Decitabine** was diluted with antibiotic-free cell culture medium (see Table 17) to a stock concentration of 10 mM and stored in 10 µl aliquots at -80 °C for up to one month.

To analyze drug response rates, 5 000 cells were seeded into wells of a 96-well plate and treated with Vorinostat or A485 on the following day. After 72 hours, an MTT (3-(4,5-Dimethylthiazol-2-yl)-2,5-diphenyltetrazolium bromide) cell assay was performed to determine the half maximal inhibitory concentration (IC<sub>50</sub>) (see 4.1.6). MIA PaCa-2 cells were treated with 5 µM Decitabine as a positive control for methylation assays (as described in 4.4.2.) Control cells were also treated with 1 ‰ of the soluble DMSO.

#### 4.1.6. MTT cell proliferation

MTT cell lysis buffer (1:25)

0.04 N HCl in isopropanol

The MTT assay is based on the reduction of the yellow 3-(4,5-Dimethylthiazol-2-yl)-2,5-diphenyltetrazolium bromide (MTT) reagent to purple formazan crystals by mitochondrial dehydrogenases to measure cellular metabolic activity. After cell lysis, the conversion rate is measured by a spectrophotometer. The level of absorbance is dependent on the number of viable cells per unit of time.

To measure cell proliferation, cells were seeded in a 96-well plate according to their growth rate to reach confluency on the day of the experiment. Cell number was determined after 0, 24, 48, 72, and 96 hours. At every time point, MTT reagent (0.5 µg/µl in PBS) was added to every single well and incubated for three hours at 37 °C. Then, the cell culture media was removed and the cells were lysed with 100 µl of MTT cell lysis buffer (30 min, RT, in the dark). Finally, MTT reduction was measured with the SpectraMax Plus 384 Microplate Reader (Molecular Devices) at 560 nm.

#### 4.1.7. MTT cell survival

Cell survival was measured 72 hours after inhibitor treatment of the cells (see 4.1.5). For this, MTT reagent (0.5 µg/µl in PBS) was added directly to the cell media in each well and incubated for three hours at 37 °C. After removal of the cell culture media, cells were lysed with 100 µl of MTT cell lysis buffer (30 min, RT, in the dark) (see 4.1.6) and MTT reduction was measured with the SpectraMax Plus 384 Microplate Reader (Molecular Devices) at 560 nm and 690 nm. Results were used to establish IC<sub>50</sub> values for the inhibitors Vorinostat, A485, and Decitabine.

#### 4.1.8. Gene editing with the CRISPR/Cas9 system

The CRISPR/Cas9 (Clustered Regularly Short Palindromic Repeats/CRISPR-associated protein 9) system was used to knock out the target genes *HDAC2*, *DNMT3A*, and *RING1B* in the pancreatic cancer cell line Panc-1.

Here, sgRNAs were designed with the online tools [crispr.mit.edu](http://crispr.mit.edu) (Ran et al., 2013) and CHOPCHOP (Labun et al., 2016, Montague et al., 2014) (see Table 10 sgRNAs). The ordered DNA oligonucleotides were diluted to a final concentration of 100 µM and subjected to T4 polynucleotide kinase-phosphorylation and double-strand annealing. In STEP 1 of the Golden Gate assembly, one sgRNA for each target gene was inserted into the corresponding plasmids from addgene's Multiplex CRISPR/Cas9 Assembly System Kit (pX330A-1x3, pX330S-2, pX330S-3) (Sakuma, Nishikawa, Kume,

Chayama & Yamamoto, 2014). BbsI-digestion, ligation, and additional exonuclease treatment to digest any residual non-circular DNA were performed according to the protocol provided by Ran et al., 2013. Successful annealing was checked by the presence of multiple bands on agarose gel electrophoresis due to plasmid topoisomers. The STEP 1 plasmids harboring one sgRNA each were transformed into DH5- $\alpha$  competent E.coli and isolated with the Qiagen Plasmid Midi Kit according to the manufacturer's instructions. STEP 2 of the Golden Gate assembly was performed in the same manner using the protocol by Sakuma et al., 2014 to assemble the single-oligonucleotides of each plasmid into one vector containing three sgRNAs (Figure 6). Finally, correct insertion of the HDAC2 oligonucleotide was verified by DNA sequencing using the U6fw primer (Table 11).

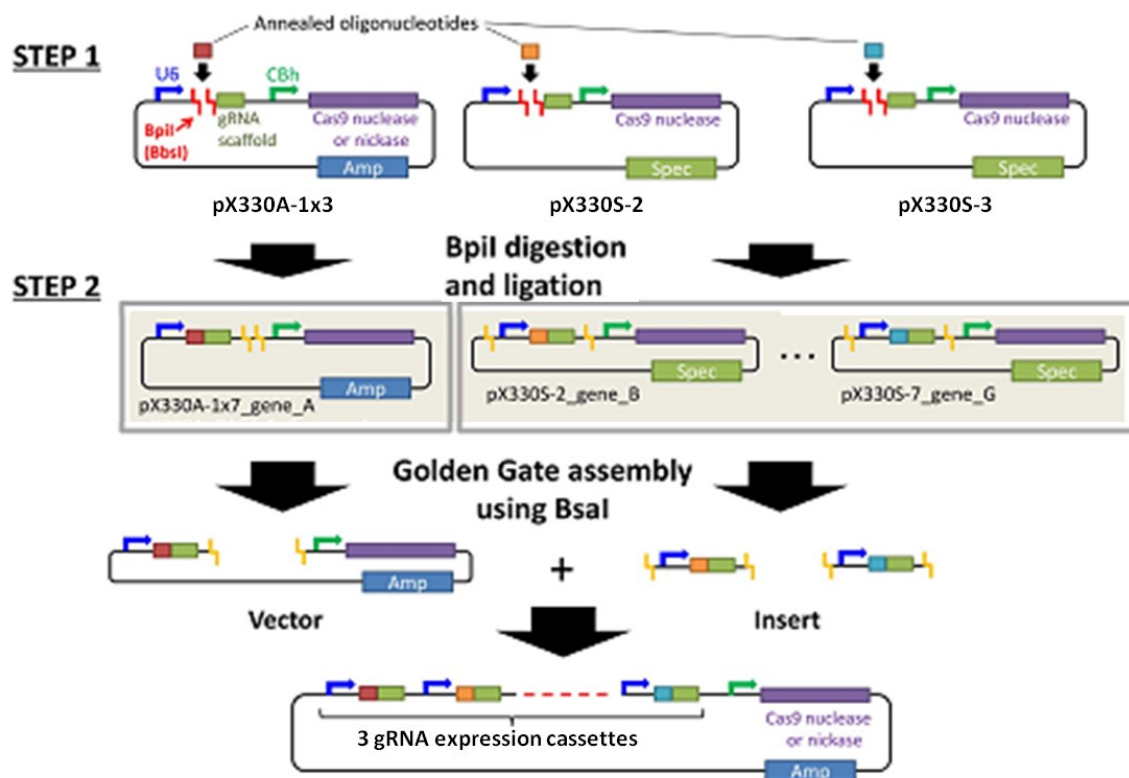


**Figure 6 Multiplex genome engineering.** (STEP 1) sgRNAs for each target sequence were annealed and inserted into BbsI-digested plasmids from the Multiplex CRISPR/Cas9 Assembly System Kit, producing three plasmids harboring a different sgRNA each. (STEP 2) The single-oligonucleotides from each plasmid were then assembled into one vector with multiple sgRNAs using BsaI-digestion and the Golden Gate assembly method. Graph adapted and modified from Sakuma et al., 2014.

For the transfection of the human pancreatic cancer cell line Panc-1,  $6 \times 10^5$  cells were seeded into wells of a 6-well plate one day prior to transfection. Cells were kept in an antibiotic-free cell culture medium for 24 hours. Lipofectamine 2000 was used according to the manufacturer's instructions. 4  $\mu$ g of plasmid DNA or 4  $\mu$ g of the CRISPR/Cas9 KO Control Plasmid and 8  $\mu$ l of Lipofectamine 2000 Reagent were diluted with RPMI cell culture medium to a total volume of 100  $\mu$ l each and incubated at room temperature (RT) for 5 min. Next, diluted DNA was added to the diluted Lipofectamine 2000

Reagent in a 1:1 ratio. Formation of DNA-lipofectamine complexes was enabled through incubation at RT for 15 min with frequent mixing on a vortex shaker. Finally, the solution was added dropwise to the cells. After 24 hours, transfection efficiency was checked in the fluorescence microscope using the GFP-tagged CRISPR/Cas9 KO Control Plasmid (green fluorescent protein). After 24 hours, single cells were seeded into the wells of a 96-well plate in complete cell culture medium and expanded for 4-6 weeks.

## **4.2. Molecular biological methods**

### **4.2.1. DNA isolation from cells**

The DNeasy Blood & Tissue Kit was used according to the manufacturer's protocol to isolate DNA from cultured tumor cell lines.

### **4.2.2. Determination of DNA concentration**

DNA concentration was determined with the SpectraMax Photometer at a wavelength of 260 nm. The sample purity was determined with the A<sub>260</sub>/A<sub>280</sub> absorption ratio and considered free of contaminants when showing values between 1.8 and 2.0.

### **4.2.3. RNA isolation from cells**

RNA was isolated from cultured cells using the QIAGEN RNeasy Plus Mini Kit according to the manufacturer's protocol and stored at - 80 °C. To prevent any contamination, the cells were washed with PBS before cell lysis.

### **4.2.4. Determination of RNA concentration**

RNA concentration was determined with the SpectraMax Photometer at a wavelength of 260 nm. An absorption ratio of A<sub>260</sub>/A<sub>280</sub> from 2.0 – 2.1 indicated protein, DNA, and contamination-free samples.

### **4.2.5. cDNA synthesis**

To transcribe RNA into cDNA (complementary DNA), 2 µg of RNA and random hexamer primers were used with the Thermo Fisher Scientific RevertAid First Strand cDNA Synthesis Kit according to the manufacturer's instructions. cDNA was diluted to a concentration of 20 ng/µl and stored at – 20 °C.

#### 4.2.6. Polymerase chain reaction (PCR)

The polymerase chain reaction is a molecular-biological method to amplify a specific genomic region from a DNA template. Before experimental use, all primers were tested in a PCR for their target specificity. A mixture of cDNA from all cell lines was used for primers for quantitative RT-PCR. For chromatin immunoprecipitation and methylation-specific primers, genomic DNA from all cell lines was used.

Pipetting scheme for 20 µl PCR reaction:

Reagent	Volume
DNA/cDNA	40 ng
Forward Primer (10 µM)	1 µl
Reverse Primer (10 µM)	1 µl
GoTaq® G2 Hot Start Master Mix (2X)	10 µl
ddH <sub>2</sub> O	to 20 µl
	20 µl

The PCR reaction was performed in an Eppendorf Mastercycler® PCR Cycler according to the following cycle conditions.

**Table 18 PCR program**

Step		Temperature [°C]	Time [sec]	Number of cycles
Initial denaturation		94	120	1
Amplification	Denaturing	94	30	40
	Annealing	55	30	
	Elongation	72	30	
Final elongation		72	600	1
Storage		4	∞	1

#### 4.2.7. Quantitative RT-PCR (qRT-PCR)

Quantitative reverse transcription PCR (qRT-PCR) was performed to quantify gene expression levels in pancreatic cancer cell lines.

The target cDNA is amplified through a conventional PCR reaction, whereby a fluorescence reporter probe, such as SYBR Green, intercalates into the double-stranded DNA and emits a fluorescence signal. The intensity of the fluorescence signals is measured in real-time at the end of each cycle and correlates with the amount of amplified DNA. Amplification is quantified using the so-called cycle threshold value ( $C_T$ ), which marks the number of cycles at which the fluorescent intensity of the sample first exceeds the background noise. The  $C_T$  values are normalized by subtracting the  $C_T$  value of an endogenous control gene, so-called housekeeping genes, to compare the level of transcript between the different samples. *TBP* (TATA-box binding protein) was used as a housekeeping gene in all qRT-PCR experiments.

Pipetting scheme for 20  $\mu$ l qRT-PCR reaction:

Reagent	Volume
cDNA (20 ng/ $\mu$ l)	2 $\mu$ l
Forward Primer (10 $\mu$ M)	1 $\mu$ l
Reverse Primer (10 $\mu$ M)	1 $\mu$ l
FastStart Essential DNA Green Master (2X)	10 $\mu$ l
ddH <sub>2</sub> O	6 $\mu$ l
	20 $\mu$ l

The samples were transferred into a qRT-PCR 96-well plate (STARLAB) as duplicates. The PCR reaction was performed in an Eppendorf LightCycler<sup>®</sup> 96 with the following conditions.

**Table 19 qRT-PCR program**

Step		Temperature [°C]	Time [sec]	Number of cycles
Initial denaturation		95	600	1
Amplification	Denaturing	95	15	45
	Annealing	55	15	
	Elongation	68	15	
Melting curve	Denaturation	95	10	1
	Hybridization	65	60	
	Melting	97	0.11 °C/sec	5 Acquisitions/sec
Storage		37	$\infty$	1

#### 4.2.8. Agarose gel electrophoresis

<u>TAE buffer (1x)</u>	40 mM	Tris(hydroxymethyl)aminomethane base
	1 mM	EDTA
	20 mM	Acetic acid

Agarose gel electrophoresis is performed to separate DNA fragments by length and to validate PCR products. For this, samples were loaded on a 1 % (w/v) agarose gel in 1x TAE containing 0.0001 % (v/v) SYBR® Safe DNA Gel stain. To compare the lengths of the separated DNA fragments, an appropriate DNA standard (GeneRuler 100 bp Plus DNA Ladder or Quick Load 1 kb DNA Ladder) was also applied to the gel. The DNA fragments were separated by applying 100 V for 30 - 40 minutes and visualized under ultraviolet (UV) light exposure in the Vilber Fusion FX device.

### 4.3. Biochemical methods

#### 4.3.1. Protein extraction

<u>Protein lysis buffer</u>	50 mM	Tris-HCl (pH 8.0)
	2 %	SDS (w/v)
	1X	Phosphatase-inhibitor
	1X	Protease-inhibitor

Cells were washed with PBS before adding an appropriate volume of protein lysis buffer to the cells (100 – 1 000 µl), depending on the cell number and culture dish. Adherent cells were mechanically removed from the cell culture dish with the top end of a plastic pipette tip. After a short incubation on ice, the cells were further disrupted using a sonicator (10 sec, 30 % amplitude). Through centrifugation (20 min, 20 000 x g, 4 °C), proteins (supernatant) were separated from the remaining cell debris (pellet).

#### 4.3.2. Determination of protein concentration

The Pierce™ BCA Protein Assay Kit, containing reagent A and B as well as BSA standards, was used to determine total protein concentrations. To do so, 10 µl of the isolated protein lysate were mixed with 200 µl of a reagent A / B mixture (ratio 1:50) in a 96-well plate and incubated at 37 °C for 30 minutes. The color of the solution will change to purple dependent on the protein concentration. Finally, the absorbance was measured with a spectrophotometer at 570 nm. The amount of total protein can be calculated using a standard row of BSA solutions with known concentrations (25 ng/µl, 125 ng/µl, 250 ng/µl, 500 ng/µl, 750 ng/µl, 1000 ng/µl, 1500 ng/µl, 2000 ng/µl) with the formula below:

$Y$  (protein concentration [ $\mu\text{g}/\mu\text{l}$ ]) =  $m$  (gradient) \*  $x$  (absorbance [nm]) +  $b$  (y axis intercept)

### 4.3.3. SDS polyacrylamide gel electrophoresis (SDS-PAGE)

<u>Running Buffer</u>	192 mM	Glycine
	25 mM	Tris-base
	0.1 %	SDS (v/v)
<u>SDS loading dye (5X)</u>	1M	Tris-base
	10 %	SDS (w/v)
	5 %	2-Mercaptoethanol (v/v)
	50 %	Glycerol (v/v)
	spatula tip	Bromphenol blue

SDS polyacrylamide gel electrophoresis is a method, which allows protein separation by molecular weight. SDS-PAGE gels contained a lower separating gel and an upper stacking gel. Gels were cast between two glass slides in a gel casting chamber. Specific combs were inserted to form loading pockets.

Equalized total protein samples (20 – 35  $\mu\text{g}$ ) were mixed with SDS loading dye (5X) and denatured at 95 °C for 5 minutes. Afterward, the samples and a protein ladder (PageRuler™ Plus prestained Protein Ladder) were loaded onto the stacking SDS-PAGE gel. Gel chambers were filled with running buffer and protein separation was carried out through the application of 30 mA until complete segregation of the proteins.

**Table 20 SDS-PAGE gel preparation**

Reagent	Separating gel (12.5 %)	Stacking gel (4 %)
ddH <sub>2</sub> O	3.2 ml	3.0 ml
Acrylamid / Bis solution 30 %	4.2 ml	750 $\mu\text{l}$
TRIS-HCl 1.5 M (pH 8.8)	2.6 ml	-
TRIS-HCl 0.5 M (pH 6.8)	-	1.3 ml
SDS 10 %	100 $\mu\text{l}$	50 $\mu\text{l}$
APS 10 %	50 $\mu\text{l}$	25 $\mu\text{l}$
TEMED	15 $\mu\text{l}$	10 $\mu\text{l}$

#### 4.3.4. Western blot

<u>Blotting Buffer</u>	192 mM	Glycine
	25 mM	Tris-base
	20 %	Methanol (v/v)
<u>TBS-T (1X)</u>	10 mM	Tris-HCl (pH 6.8)
	150 mM	NaCl
	0.05 %	Tween 20 (v/v)

After the separation of proteins by SDS-PAGE, proteins were blotted onto a nitrocellulose membrane. In a western blot tank filled with blotting buffer, the nitrocellulose membrane was placed on top of the separating gel and embedded with chromatography papers and sponges soaked in blotting buffer on both sides. The proteins were then transferred onto the membrane by applying 100 V for 60 to 90 minutes depending on the size of the proteins. To avoid unspecific antibody binding, the membrane was first blocked in either 5 % milk/TBS-T or 5 % BSA/TBS-T and incubated at RT for one to two hours with slight shaking. Then, the primary antibody was applied in blocking solution and incubated at 4 °C overnight. Unspecific antibody-binding was removed through washing with TBS-T (3x, 10 min, RT). Afterward, the membrane was incubated with a horseradish peroxidase (HRP)-linked secondary antibody against the primary antibody's host species in 1 % milk/TBS-T for one hour at RT. After three washing steps with TBS-T (10 min, RT each), the protein bands were visualized with ECL Western Blotting Substrate with the Fusion FX (Vilber Lourmat GmbH) imaging device.

#### 4.3.5. Immunofluorescence staining

<u>Blocking buffer</u>	5 %	donkey serum
	1 %	BSA
	0.1 %	Triton-X
		in PBS

15 000 cells were seeded into 8-well chamber slides and incubated for 24 hours prior to fixation with 4 % PFA (15 min, RT). Afterward, the slides were washed with PBS (3 x, 5 min, RT). Since the proteins of interest were histone modifications and therefore located in the nucleus, a cell permeabilization step was performed with 1 % BSA, 1 % Triton-X / PBS (20 min, 37 °C). After three washing steps with PBS (3 x 5 min, RT), the slides were blocked with blocking buffer containing 5 % donkey serum for two hours at RT to avoid unspecific antibody binding. After removing the blocking buffer, the primary antibody diluted in blocking buffer was added and incubated at 4 °C overnight. After three washing steps with PBS (3 x 5 min, RT), the fluorescent-labeled secondary antibody diluted in blocking buffer

was applied and incubated for one hour at room temperature. One more wash with PBS was performed before the cover slides were mounted using a fluorescence mounting medium with DAPI.

#### 4.3.6. In-cell western

<u>Blocking buffer</u>	5 %	donkey serum
	1 %	BSA
	0.1 %	Triton-X
<u>DABCO lysis buffer</u>	25 mg/ml	1,4-DiAzabicyclo[2.2.2]octane (pH 8.55) in PBS

CRISPR/Cas9 plasmid-transfected and expanded cells (generated in 4.1.8) were seeded into black 96-well plates with clear bottoms and were allowed to adhere overnight. Cells were fixed with 4 % PFA (15 min, RT) and subjected to three washing steps with PBS (5 min, RT each). To expose intranuclear proteins of interest, cell permeabilization was performed with 1 % BSA, 1 % Triton-X / PBS (20 min, 37 °C) followed by three washing steps with PBS (5 min, RT each). Then, the slides were blocked with blocking buffer containing 5 % donkey serum for two hours at RT to avoid unspecific antibody binding. After removing the blocking buffer, cells were incubated with the primary antibody diluted in blocking buffer at 4 °C overnight. After three washing steps with PBS (5 min, RT each), fluorochrome-conjugated secondary antibodies against the primary antibody's host were added and incubated for one hour at RT in the dark. Following another washing step with PBS (5 min, RT), DAPI staining (5 min at RT in the dark) concluded the staining process. To achieve a more even signal distribution within each well, DABCO lysis buffer was added to each well.

Fluorescent signals were measured using the FluoStar Omega spectrometer and analyzed with the MARS software with the following parameters:

**Table 21: In-cell western analysis parameters**

Primary antibody	Secondary antibody	Conjugate	Gain	Emission	Excitation
Anti-HDAC2	Anti-mouse IgG	FITC	2500	520	485
		DAPI	1200	460	355

The relative signal ratios of HDAC2 levels, measured by FITC (fluorescein-5-isothiocyanate) signal intensity, to total cell number, represented by DAPI signal intensity, were calculated.

## 4.4. Epigenetic methods

### 4.4.1. Chromatin immunoprecipitation (ChIP)

<u>Cell lysis buffer</u>	5 mM	PIPES (pH 8.0)
	85 mM	KCl
	0.5 %	NP-40 (v/v)
<u>MNase digestion buffer</u>	50 mM	Tris-HCl (pH 8.0)
	5 mM	CaCl <sub>2</sub>
<u>Nuclei lysis buffer</u>	1 %	SDS (w/v)
	10 mM	EDTA
	50 mM	Tris-HCl (pH 8.0)
<u>ChIP dilution buffer</u>	0.01 %	SDS (w/v)
	1.1 %	Triton X-100 (v/v)
	1.2 mM	EDTA
	16.7 mM	Tris-HCl (pH 8.0)
	167 mM	NaCl
<u>Low salt wash buffer</u>	0.1 %	SDS (w/v)
	1 %	Triton X-100 (v/v)
	2 mM	EDTA
	20 mM	Tris-HCl (pH 8.0)
	150 mM	NaCl
<u>High salt wash buffer</u>	0.1 %	SDS (w/v)
	1 %	Triton X-100 (v/v)
	2 mM	EDTA
	20 mM	Tris-HCl (pH 8.0)
	500 mM	NaCl
<u>Lithiumchloride wash buffer</u>	250 mM	LiCl
	1 %	NP-40 (v/v)
	1 %	Sodiumdeoxycholate (w/v)
	1 mM	EDTA
	10 mM	Tris-Hcl (ph 8.0)
<u>TE wash buffer</u>	10 mM	Tris-HCl (pH 8.0)
	1 mM	EDTA
<u>Elution buffer</u>	1 %	SDS (w/v)
	100 mM	NaHCO <sub>3</sub>

Chromatin immunoprecipitation investigates the interaction of proteins like transcription factors or histone modifications with specific DNA regions.

Cells were seeded into 10 cm cell culture plates in 10 ml cell culture medium to reach 90 % confluence at the start of the experiment. First, protein-DNA complexes need to be conserved

through crosslinking. For this, PFA was added directly to the medium to a final concentration of 1 % (v/v) and incubated for 10 min (RT) on a shaker. PFA was quenched through the addition of glycine (125 mM) and incubation for 5 min (RT). Before cell lysis, cells were placed on ice and washed with PBS twice to remove any reagents. Then, adherent cells were scraped from the cell culture dish with 1.5 ml of cell lysis buffer containing 1X protease inhibitor. The cell lysis buffer, which destroys only the outer cell membrane while leaving the nuclear envelope intact, enables the separation of cell nuclei through centrifugation (5 min, 300 x g, 4 °C). Next, the DNA is sheared into fragments of 300 – 600 bp by MNase digestion (75 U, 5 min, RT). The amount of enzyme and incubation times were empirically determined and validated with agarose gel electrophoresis in previous experiments (data not shown). After centrifugation (10 min, 300 x g, 4 °C), the cell nuclei were lysed with 1 ml nuclei lysis buffer with protease inhibitor (1X) and incubated on ice for 10 minutes. Samples were subjected to four cycles of sonication (10 sec, 10 % amplitude) to enhance chromatin fragmentation and bursting of the nucleic membranes. After centrifugation (10 min, 12 000 x g, 4 °C), the supernatant was resuspended in 2.8 ml of ChIP dilution buffer with protease inhibitor (1X). 1 % of the volume was saved as input control and the sample was divided into 1 ml aliquots for each antibody used. Samples were pre-cleared with 100 µl protein A agarose beads for one hour at 4 °C on a rotator. After removing the beads through centrifugation (1 min, 4 000 x g, 4 °C), ChIP-grade antibodies or an IgG control antibody were added and the samples were incubated at 4 °C on a rotator overnight. On the next day, the addition of protein A agarose beads, which bind to the F<sub>c</sub> fragment of the antibodies, allowed the isolation of antibody-protein complexes. To remove unspecific binding, antibody-protein-bead complexes were washed with a series of washing solutions (low salt, high salt, lithium chloride, and TE-wash buffers (2 washes)) and centrifuged after each washing step (1 min, 4 000 x g, 4 °C). Next, the protein-antibody complexes were eluted from the beads with 200 µl elution buffer and incubated at RT for 15 min. The input sample was also diluted with 200 µl elution buffer. Then, reverse-crosslinking was performed through the addition of NaCl (200 mM final concentration) followed by incubation at 65 °C overnight. After degradation of RNA (final concentration of 10 µg RNase A, 30 min, 37 °C) and proteins (final concentrations of 10 µg proteinase K, 10 mM EDTA, and 40 mM Tris-HCl, 60 min, 45 °C), the DNA was purified using the QIAquick PCR purification Kit according to the manufacturer's instructions. The DNA was eluted in 20 µl of ddH<sub>2</sub>O and the amount of precipitated DNA was quantified via qRT-PCR as the percentage of input.

#### 4.4.2. DNA methylation analysis

DNA methylation patterns were analyzed with the bisulfite conversion method, followed by a Methylation-specific PCR (MSP). Treatment of native DNA with sodium bisulfite results in deamination of unmethylated cytosine residues to uracil bases, whereas methylated cytosine residues remain unchanged. Using two sets of primer pairs for methylated and unmethylated products in an MSP reaction followed by agarose gel electrophoresis allows the differentiation between methylated and unmethylated genomic regions.

DNA was isolated with the DNeasy Blood & Tissue Kit and subjected to bisulfite conversion with the Epitect Bisulfite Kit according to the manufacturer's instructions. 2 µg of genomic DNA were utilized per bisulfite conversion reaction and eluted in 20 µl ddH<sub>2</sub>O. 2 µl of the converted DNA product were then amplified in two distinct PCR reactions with specific primers against methylated and unmethylated products. The PCR reactions were prepared as described in section 4.2.6 and run in an Eppendorf Mastercycler® PCR Cycler according to the following cycle conditions.

**Table 22: MSP PCR program**

Step		Temperature [°C]	Time [sec]	Number of cycles
Initial denaturation		94	120	1
Amplification	Denaturing	94	30	32 ( <i>EpCAM</i> ), 38 ( <i>GATA6</i> )
	Annealing	57	30	
	Elongation	72	30	
Final elongation		72	600	1
Storage		4	∞	1

As a positive control, DNA was methylated by the CpG methyltransferase M. SssI according to the manufacturer's instructions. The DNA was purified by standard ethanol precipitation and subjected to bisulfite conversion and PCR like the other samples.

Treatment of MiaPaca-2 cells with 5 µM 5-Aza-2'-deoxycytidine for 96 hours with fresh inhibitor every 48 hours served as a negative control. The DNA was purified using the DNeasy Blood & Tissue Kit and subjected to bisulfite conversion and PCR as described above.

## 5. Results

### 5.1. Characterizing pancreatic cancer cell lines representing the classical and basal subtype

Several studies have classified PDAC tissue specimens into two main molecular PDAC subtypes, a classical and basal-like subtype, based on their specific gene signature (Collisson et al., 2011, Moffitt et al., 2016, Bailey et al., 2016). To further characterize the gene expression profiles in the classical and basal subtype as well as the underlying molecular mechanisms, well-established pancreatic cancer cell lines representing low-grade and high-grade forms of pancreatic cancer, respectively were used in this study (Deer et al., 2010, Diaferia et al., 2016).

#### 5.1.1. Classical and basal PDAC cell lines show a subtype-specific expression profile

Seven established PDAC cell lines: Pa-Tu-S, Capan-1, Capan-2, Colo-357, Pa-Tu-T, Panc-1, and MiaPaca-2 were used as a pancreatic cancer tumor model. First, their assignment to the classical or basal PDAC subtype was determined. Brightfield images of all seven cell lines demonstrated their different morphology. While Pa-Tu-S, Capan-1, Capan-2, and Colo-357 demonstrated an epithelial-like morphology, Pa-Tu-T, Panc-1, and MiaPaca-2 exhibited spindle-like cells (Figure 7A, upper panel), which was already indicative of their affiliation to the classical or basal PDAC subtype, respectively. Moreover, immunofluorescence co-staining (see 4.3.5) of the epithelial cell adhesion molecule EpCAM, the mesenchymal marker Vimentin, and DAPI for nuclei staining showed high levels of EpCAM and an absent signal for Vimentin in the Pa-Tu-S, Capan-1, Capan-2, and Colo-357 cell lines (Figure 7A, lower panel). These four cell lines were therefore assigned to the classical PDAC subtype. In contrast, the remaining pancreatic cancer cell lines Pa-Tu-T, Panc-1, and MiaPaca-2 showed high levels of the mesenchymal marker Vimentin while lacking signals for EpCAM in the immunofluorescence co-staining (Figure 7A, lower panel). Hence, these three cell lines were assigned to the basal or mesenchymal PDAC subtype.

To further characterize the seven cell lines assigned to the two PDAC subtypes, gene expression analysis of epithelial and mesenchymal cell differentiation markers was performed. Target genes were selected from previously published gene signatures by Collisson et al. and Diaferia et al. (Collisson et al., 2011, Diaferia et al., 2016) and statistical significance between the classical and basal subtype was calculated by comparing the mean of relative gene expression of classical and basal cell lines in an unpaired Student's t-test. Relative gene expression analysis ( $\log_2$  fold change of  $\Delta Ct$  values, normalized to *TBP*) showed that cell lines representing the classical PDAC subtype (Pa-Tu-S, Capan-1, Capan-2, Colo-357) had significantly increased expression of epithelial differentiation

markers including *ELF3* (E74 like ETS transcription factor 3), *ERBB3* (Erb-B2 receptor tyrosine kinase 3), *GATA6*, *EpCAM*, *FGFBP1* (fibroblast growth factor binding protein 1), and *AGR2* (anterior gradient 2). However, the analyzed genes associated with mesenchymal differentiation like *S100A2* (S100 calcium binding protein A2) or *MYC* did not show significantly elevated gene expression levels in the previously confirmed basal cell lines (Pa-Tu-T, Panc-1, MiaPaca-2) compared to the classical cell lines (Pa-Tu-S, Capan-1, Capan-2, Colo-357) (Figure 7B). Furthermore, the heat map also illustrates the heterogeneity between individual PDAC cell lines classified to the same subtype. For example, *HNF1A* showed a high expression in two classical cell lines Pa-Tu-S and Colo-357, but low expression in Capan-1 and Capan-2, also classified as classical PDAC cell lines (Figure 7B).

Lastly, differences in cell proliferation rates within the molecular PDAC subtypes were determined with the help of MTT cell proliferation assays. Herefore, untreated cells were seeded in 96-well plates and cell growth was measured after 24, 48, 72, and 96 hours. The growth rate was normalized to the 0-hour mark and is shown in percent. Except for Colo-357, the classical and basal cell lines showed two separate cell growth clusters. While the classical cell lines Pa-Tu-S, Capan-1, and Capan-2 demonstrated a slow growth rate overall, the basal cell lines Pa-Tu-T, Panc-1, and MiaPaca-2 showed increased cell proliferation rates. An exception was measured for the classical cell line Colo-357, which revealed a similar growth pattern as the basal cell lines (Figure 7C).

Altogether, gene expression analysis defined four **classical (Pa-Tu-S, Capan-1, Capan-2, Colo-357)** and three **basal (Pa-Tu-T, Panc-1, MiaPaca-2)** molecular PDAC cell lines with distinct gene expression patterns. MTT cell proliferation assays showed two separate cell growth clusters with the exception of the Colo-357 cell line. The increased cell proliferation rates in the basal PDAC cell lines also correspond to clinical data, which showed significantly reduced survival times in patients with quasimesenchymal subtype tumors compared to patients with classical subtype tumors (Collisson et al., 2011).

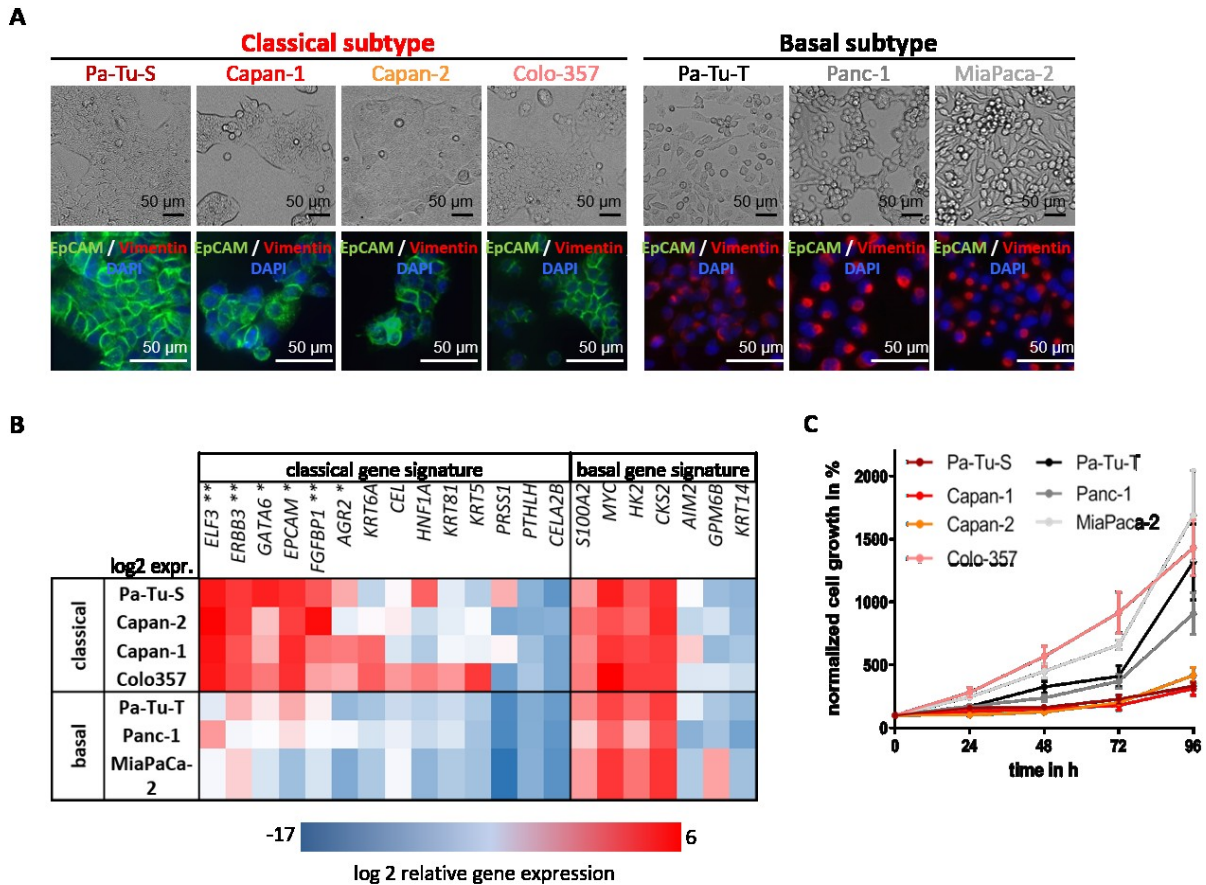


**Figure 7: Cell lines representing the classical PDAC subtype show high levels of epithelial cell differentiation markers compared to the basal subtype. (A)** Representative microscopic brightfield and immunofluorescence co-staining images of EpCAM (green), Vimentin (red), and DAPI (blue) of human pancreatic cancer cell lines representing the classical (Pa-Tu-S, Capan-1, Capan-2, Colo-357) and basal (Pa-Tu-T, Panc-1, MiaPaca-2) PDAC subtype. Scale bar 50 $\mu$ m. **(B)** Heat map illustrating relative gene expression profiles (log<sub>2</sub> fold change of  $\Delta$ Ct) of epithelial and mesenchymal classifier genes in classical and basal pancreatic cancer cell lines. mRNA expression values are represented as mean, Ct-values were normalized to housekeeping gene *TBP* (n=2-3). P-values were calculated by two-tailed, unpaired Student's t-test comparing the mean of relative gene expression of classical and basal cell lines, \*p < 0.05, \*\*p < 0.01. **(C)** Cell proliferation of classical (red tones) and basal (black tones) human PDAC cell lines using MTT assay, analyzed at 0, 24, 48, 72, and 96 hours (n = 3).

### 5.1.2. Important epithelial and mesenchymal differentiation markers are epigenetically regulated

For further analyses, I concentrated on *EpCAM* and *GATA6* as epithelial differentiation markers, as well as *TP63* and *MYC* as already established mesenchymal differentiation markers in PDAC (Collisson et al., 2011, Bailey et al., 2016, Somerville et al., 2018).

In order to characterize the subtype-specific expression patterns of *EpCAM*, *GATA6*, *TP63*, and *MYC*, log<sub>2</sub> gene expression analysis was performed by qPCR in all seven PDAC cell lines. All data were calculated as relative gene expression ( $\Delta$ Ct, normalized to *TBP*). Statistical significance between the classical and basal subtype was calculated by comparing the mean of relative gene expression of

classical and basal cell lines in an unpaired Student's t-test. Here, the expression of *EpCAM* was significantly increased in the four cell lines representing the classical subtype (Pa-Tu-S, Capan-1, Capan-2, and Colo-357) compared to the cell lines of the basal subtype (Pa-Tu-T, Panc-1, and MiaPaca-2). The expression of *GATA6* was also visibly enriched in the classical cell lines, although not statistically significant ( $p = 0.12$ ). The mesenchymal marker *TP63* showed a very high expression in the basal cell line MiaPaca-2 and a moderate expression level in the classical cell line Capan-1 and was therefore not subtype-specific in this study. The expression of the proto-oncogene *MYC* did not show any correlation to pancreatic cancer subtypes either (Figure 8A).

Importantly, data from the UCSC genome browser (<https://genome.ucsc.edu/>) showed that all four genes (*EpCAM*, *GATA6*, *TP63*, and *MYC*) exhibited various histone acetylation sites and CpG islands at their transcriptional start sites (Figure 8B).

Hence these results suggest that the subtype-specific expression profiles of cellular differentiation markers, such as *EpCAM* and *GATA6*, might be regulated through epigenetic modifications.

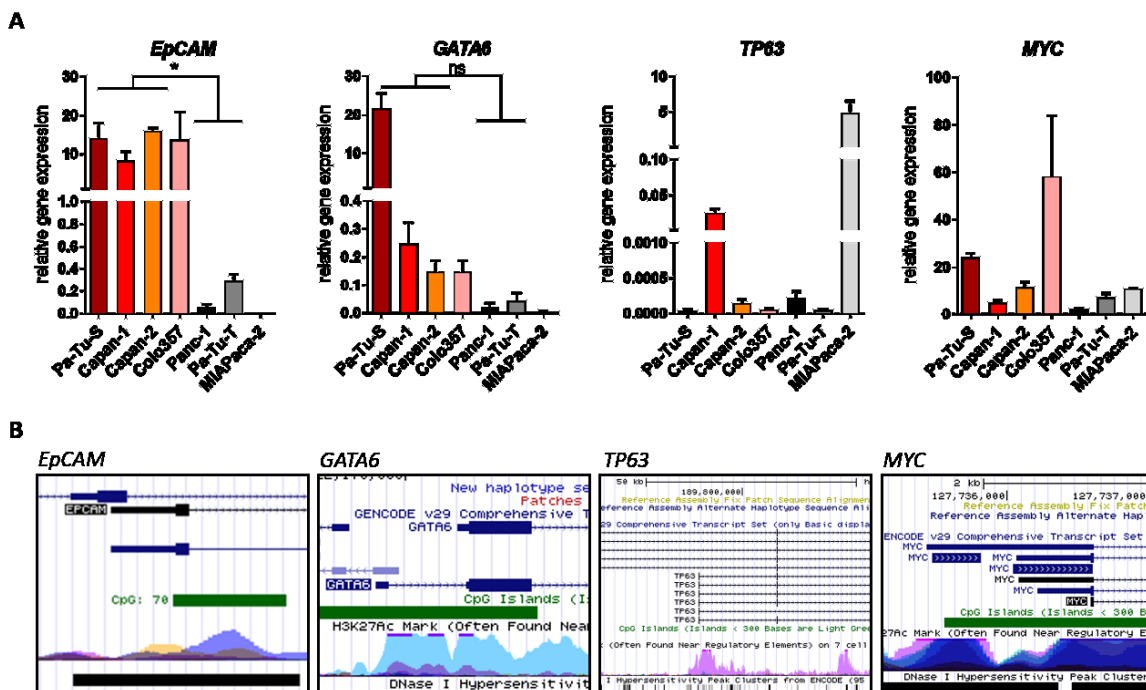


**Figure 8: Subtype-specific gene expression is regulated by histone modifications and DNA methylation. (A)** mRNA expression analysis of classical (*EpCAM*, *GATA6*) and mesenchymal (*MYC*, *TP63*) subtype-specific genes. Ct-values were normalized to housekeeping gene *TBP* ( $n = 2$ ). All data are represented as mean  $\pm$  standard error of the mean (SEM). P-values were calculated by two-tailed, unpaired Student's t-test comparing the mean of relative gene expression of classical and basal cell lines, \* $p < 0.05$ . ns = not significant **(B)** All four genes demonstrated histone acetylation sites and CpG islands at the transcriptional start site. Pictures were obtained from the UCSC Browser (<https://genome.ucsc.edu/>).

### 5.1.3. Epigenetic modifiers are differentially expressed in the two subtypes

Next, the relation between different epigenetic modifiers or their catalyzed modification and the two molecular PDAC subtypes was examined.

For this analysis, two cell lines from the classical (Pa-Tu-S, Capan-2) and two cell lines from the basal subtype (Pa-Tu-T, Panc-1) were used in immunoblot analysis. Figure 9A shows representative immunoblot images on the left panel as well as a quantification of protein levels normalized to GAPDH (glyceraldehydes-3-phosphate dehydrogenase) on the right panel. Statistical significance between classical and basal cell lines was calculated using the mean of normalized protein levels in both subtypes in an unpaired Student's t-test. Indeed, the western blot analysis showed that the acetylation of histone H3 on lysine 27 (H3K27ac) was significantly enriched in the classical subtype (Figure 9A, right panel). Protein levels of other epigenetic modifiers involved in histone deacetylation (HDAC1, HDAC2), histone ubiquitination (RING1B, H2AK119ub), or DNA methylation (DNMT3A) did not show a significant difference between the classical and basal subtype (Figure 9A).

To validate these results, relative gene expression analysis of important epigenetic modifying enzymes was performed in two classical (Pa-Tu-S, Capan-2) and two basal (Pa-Tu-T, Panc-1) PDAC cell lines. Figure 9B depicts the log<sub>2</sub> fold change of  $\Delta$ Ct values normalized to *TBP*. Statistical significance between the classical and basal subtype was calculated by comparing the mean of relative gene expression of classical and basal cell lines in an unpaired Student's t-test. The heat map illustrates that enzymes catalyzing histone deacetylation (*HDAC1*, *HDAC2*) and histone acetylation (*SMARCA4*, *HAT1*, *CREBBP*, *EP300*) were visibly elevated in the classical subtype. Furthermore, gene expression of *RING1A* and *RING1B*, which are members of the PRC1-complex and catalyze histone ubiquitination, was increased in the classical cell line Pa-Tu-S. In addition, levels of the DNA methyltransferase *DNMT3A* were significantly enriched in the classical PDAC cell lines compared to the basal cell lines (Figure 9B).

Overall, some epigenetic modifiers, which regulate histone acetylation and ubiquitination, seemed to be increased in the classical subtype. In addition, the de-novo DNA-methyltransferase *DNMT3A* was significantly overexpressed in the classical subtype compared to the basal subtype. However, there was a simultaneous enrichment of transcriptional activating and repressing epigenetic modifications within the same subtype. This suggests a complex interaction of activating and repressive epigenetic modifications at different transcriptional start sites to determine the subtype-specific gene expression profile.

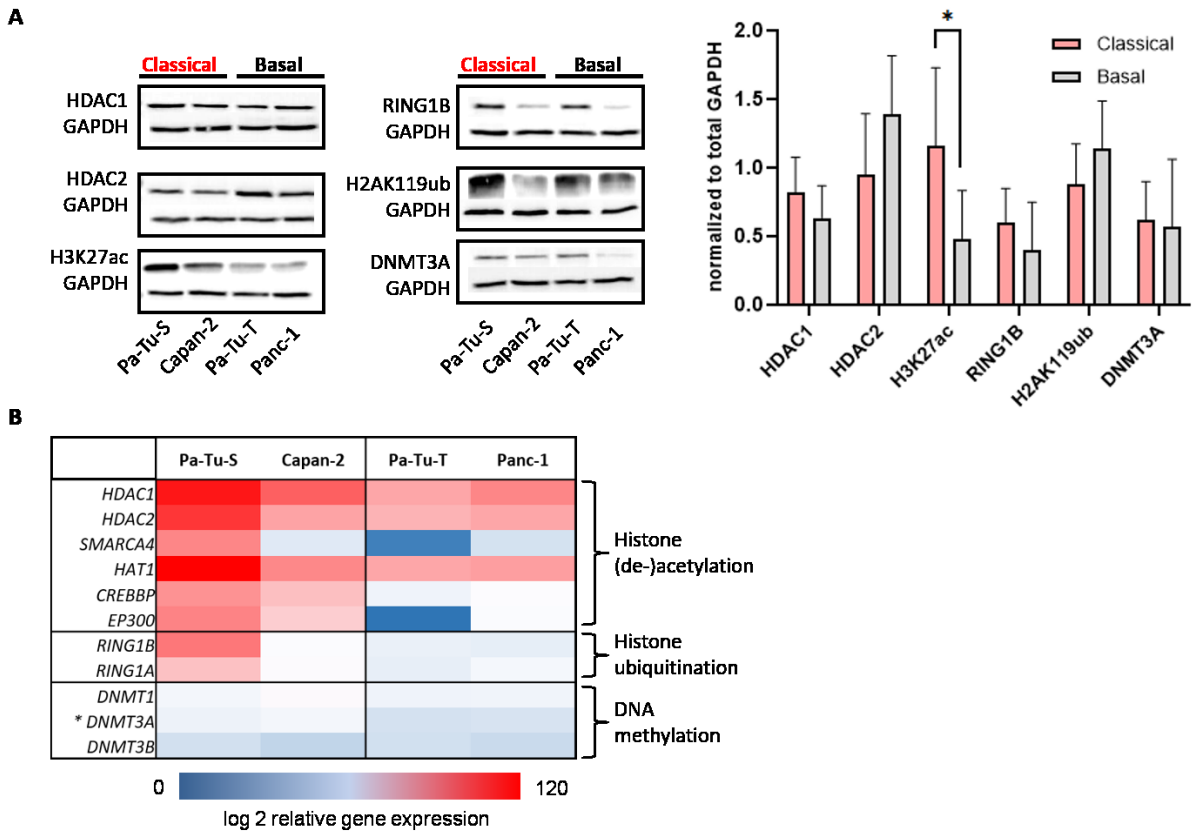


**Figure 9: Epigenetic modifiers show a subtype-specific expression pattern. (A)** Representative images and quantification of immunoblot analysis with indicated antibodies (normalized to GAPDH) in untreated pancreatic cancer cells (classical: Pa-Tu-S, Capan-2, basal: Pa-Tu-T, Panc-1). All data are represented as mean  $\pm$  SEM. P-values were calculated by two-tailed, unpaired Student's t-test comparing the mean of normalized protein levels of classical and basal cell lines, \* $p < 0.05$  ( $n = 3-6$ ). **(B)** Heat map illustrating gene expression levels of histone acetylation and deacetylation, histone ubiquitination, and DNA methylation. mRNA expression values are represented as mean, Ct-values were normalized to housekeeping gene *TBP* ( $n = 3$ ). P-values were calculated by two-tailed, unpaired Student's t-test comparing the mean of relative gene expression of classical and basal cell lines, \* $p < 0.05$ .

## 5.2. The transcription of subtype-specific markers is regulated through epigenetic modifications

So far, this study showed that important epithelial cell differentiation markers like EpCAM were significantly overexpressed in the classical subtype and that the classical and basal subtype displayed different overall levels of epigenetic modifications. Therefore, the correlation between the subtype-specific gene expression profile and the subtype-specific epigenetic modifications needed to be investigated next.

For this purpose, chromatin immunoprecipitation assays determined the abundance of specific histone modifications at promoter regions of target genes. In addition, bisulfite methylation analysis was able to identify the DNA-methylation status of promoter areas of target genes (see 4.4.1 and 4.4.2).

### **5.2.1. Transcription of *EpCAM* and *GATA6* is activated in the classical subtype and repressed in the basal subtype through histone modifications**

Chromatin immunoprecipitation (ChIP) against different histone marks at the promoter region of the epithelial differentiation genes *EpCAM* and *GATA6* and of the mesenchymal differentiation genes *MYC* and *TP63* was used in all seven cell lines to investigate whether the subtype-specific gene expression profile is directly regulated by histone modifications. Pull-down ChIP-DNA was quantified by quantitative PCR (qPCR) and normalized as the percentage of input. Immunoglobulin G (IgG) levels served as a negative control. Statistical significance was calculated using the mean histone modification levels of classical and basal PDAC cell lines in an unpaired Student's t-test.

In the classical cell lines, the promoter region of *EpCAM* was characterized by the presence of high levels of the activating histone acetylation H3K27ac and low levels of the repressive histone ubiquitination H2AK119ub. In contrast, H2AK119ub was significantly enriched at the *EpCAM* promoter in the basal cell lines while levels of the histone acetylation H3K27ac mark were decreased. ChIP assays of the promoter region of *GATA6* showed a similar enrichment of the activating histone acetylation H3K27ac in classical cell lines and elevated levels of the repressive histone ubiquitination H2AK119ub in the basal cell lines instead, although not statistically significant (Figure 10A). ChIP assays for the mesenchymal differentiation gene *MYC* showed that levels for the repressive histone ubiquitination H2AK119ub were slightly increased in the classical cell lines while levels of the activating histone acetylation H3K27ac were reduced in these cell lines. In the basal cell lines, the activating histone acetylation H3K27ac presented as the dominating histone modification. However, results were not as homogenous compared to the epithelial differentiation genes *EpCAM* and *GATA6*. The binding of chromatin acetylation and ubiquitination at the promoter site of *TP63* did not correlate with the transcriptional profile of the classical and basal subtypes (Figure 10B).

These results lead to the conclusion that the expression of the epithelial cell differentiation markers *EpCAM* and *GATA6* is epigenetically activated in the classical subtype through histone acetylation and silenced in the basal subtype through histone ubiquitination. The distribution of histone modifications at the promoter regions of the mesenchymal markers *MYC* and *TP63* showed only a limited correlation to the subtype-specific gene expression profile, suggesting additional regulatory factors.

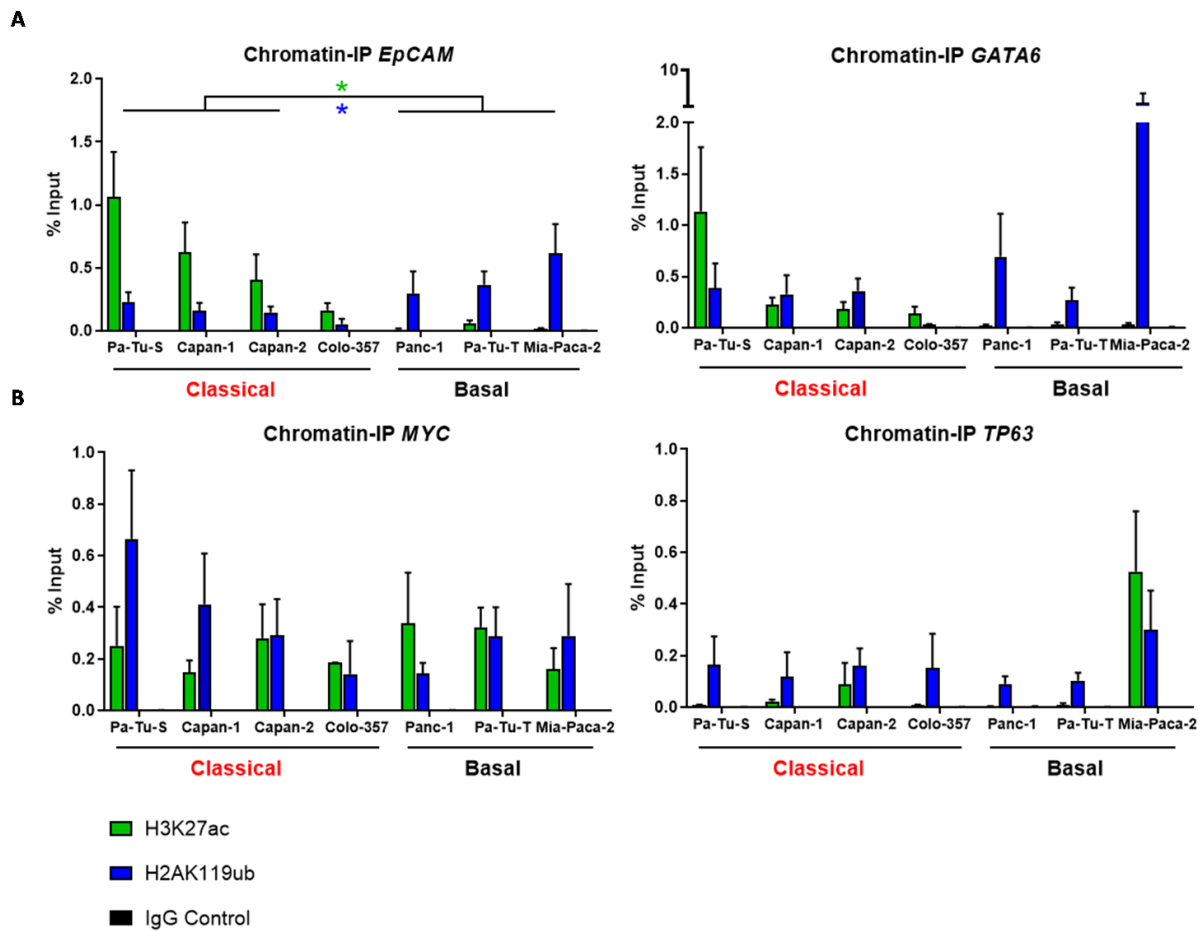


**Figure 10: Histone modifications are drivers for epigenetic regulation of differentiation genes.** Chromatin immunoprecipitation (ChIP) analysis of activating (H3K27ac) and repressive histone modifications (H2AK119ub) at the transcriptional start site of classical (A) and basal (B) target genes. ChIP DNA was quantified by quantitative PCR (qPCR) and normalized as the percentage of input. IgG levels served as a negative control. Data are represented as mean  $\pm$  SEM (n = 3-8). Statistical significance was calculated using the mean histone modification levels of classical and basal PDAC subtypes and analyzed by two-tailed, unpaired Student's t-test, \*p < 0.05.

### 5.2.2. *EpCAM* is epigenetically silenced through DNA methylation in the basal subtype

Important cellular differentiation genes presented CpG islands at their transcriptional start site suggesting the presence of DNA methylation as an additional regulatory factor (as indicated in Figure 8B). Although gene expression analysis only showed a significant difference in the expression of one DNA methyltransferase (*DNMT3A*) between the classical and basal subtype (Figure 9), the DNA methylation status at the promoter region of epithelial markers needed to be further analyzed. Therefore, genomic DNA of all seven PDAC cell lines was subjected to bisulfite conversion and the DNA methylation status was analyzed by Methylation-specific PCR (MSP) and DNA gel electrophoresis. M.SssI treatment of DNA from Pa-Tu-T cells served as a positive control. Treatment

of MIAPaca-2 cells with 10  $\mu$ M of the DNA hypomethylating agent 5-Aza-2'-Deoxycytidine served as a negative control.

The results showed that the promoter region of *EpCAM* was consistently unmethylated in the classical cell lines. The basal cell lines presented a heterogeneous methylation profile from unmethylated (Panc-1) over partially methylated (Pa-Tu-T) to fully methylated gene sites (MIAPaca-2) (Figure 11, upper panel). The methylation analysis of the transcriptional start site of *GATA6* showed an unmethylated gene locus in all cell lines regardless of their molecular subtype, except for Pa-Tu-S. The presence of bands for a methylated and unmethylated product in Pa-Tu-S cells suggested a heterozygous DNA methylation status in this cell line (Figure 11, lower panel).

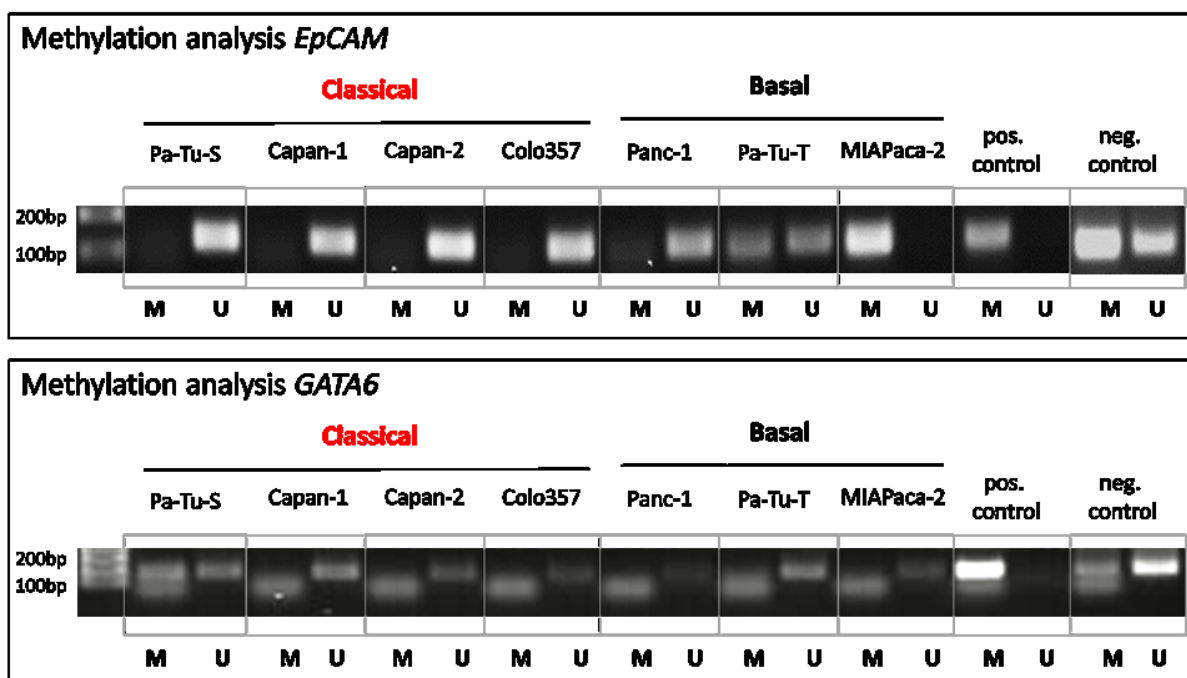


**Figure 11: Differentiation genes are epigenetically silenced through DNA methylation in the basal subtype.** Methylation-specific PCR and DNA gel electrophoresis after bisulfite treatment of native DNA. Specific primers against methylated and unmethylated products were used. M.SssI treatment of Pa-Tu-T cells served as a positive control, treatment of MIAPaca-2 cells with 10  $\mu$ M 5-Aza-2'-deoxycytidine served as a negative control. M = methylated product, U = unmethylated product.

Altogether, the subtype-specific transcription of the cellular differentiation gene *EpCAM* seems to be also regulated through DNA methylation, which suppresses its transcription in the basal subtype. The *GATA6* locus however, did not show a similar correlation between gene expression levels and DNA methylation status.

### **5.3. Cell survival response to single-drug histone acetylase or histone deacetylase inhibitor treatment is independent of the molecular subtype**

The previous finding in this study that the expression of epithelial differentiation markers is upregulated through histone acetylation in the classical subtype (Figure 10) suggests a differential response to chemical inhibition of histone acetylation or histone deacetylation agents between the two subtypes.

To analyze the therapeutic effects of epigenetic inhibitors on both subtypes, all seven cell lines were treated with increasing concentrations of the p300/CREBBP-inhibitor A485 or the class I and II HDAC-inhibitor Vorinostat for 72 hours, and cell survival was measured using an MTT assay (inhibitor treatment and MTT cell survival assays were performed together with Maria Escobar). Figure 12A shows that the overall response to the inhibitor treatment was very low and independent of the molecular subtypes. All PDAC cell lines barely responded to the treatment with the histone acetyltransferase-inhibitor A485. Only MIAPaCa-2 cells reached a 50 % survival rate at the maximum dosage of 10  $\mu$ M A485 (Figure 12A, left panel). Treatment with the histone deacetylase-inhibitor Vorinostat was able to inhibit cell survival to a greater extent, but only at very high doses above 1  $\mu$ M Vorinostat and also independent of the molecular subtype (Figure 12A, right panel).

To confirm the molecular effect of the epigenetic inhibitors, immunoblot analysis of all seven cell lines was performed after 24 hours of inhibitor treatment with the p300/CREBBP-inhibitor A485 or the class I and II HDAC-inhibitor Vorinostat (inhibitor treatment and immunoblot assays were performed together with Maria Escobar). Results were normalized to total GAPDH levels and statistical significance was calculated by one-way ANOVA. Representative immunoblot images of the classical cell line Pa-Tu-S and the basal cell line MiaPaca-2 are shown in Figure 12B (lower panels). All seven PDAC cell lines were included in the quantification of H3K27ac levels. The immunoblot data showed that the histone acetylation H3K27ac was significantly decreased in both subtypes after 1  $\mu$ M A485 HAT-inhibitor treatment (Figure 12B, left panel). In contrast, H3K27ac levels were significantly upregulated after 0.5  $\mu$ M Vorinostat HDAC-inhibitor treatment in the basal cell lines only (Figure 12B, right panel). The already high H3K27ac levels in the classical cell lines slightly increased after Vorinostat treatment without reaching statistical significance.

To summarize, inhibitor treatment of pancreatic cancer cells with a HAT-inhibitor or HDAC-inhibitor had significant effects on histone acetylation levels. However, targeting histone acetylation did not have a substantial effect on cell survival in the classical or in the basal subtype. Presumably, the effect of the two epigenetic drugs may have been diminished through compensatory mechanisms, e.g. an upregulation or downregulation of other epigenetic modifiers. Targeting several epigenetic modifiers in combination could overcome this limitation to provoke a therapeutic response.

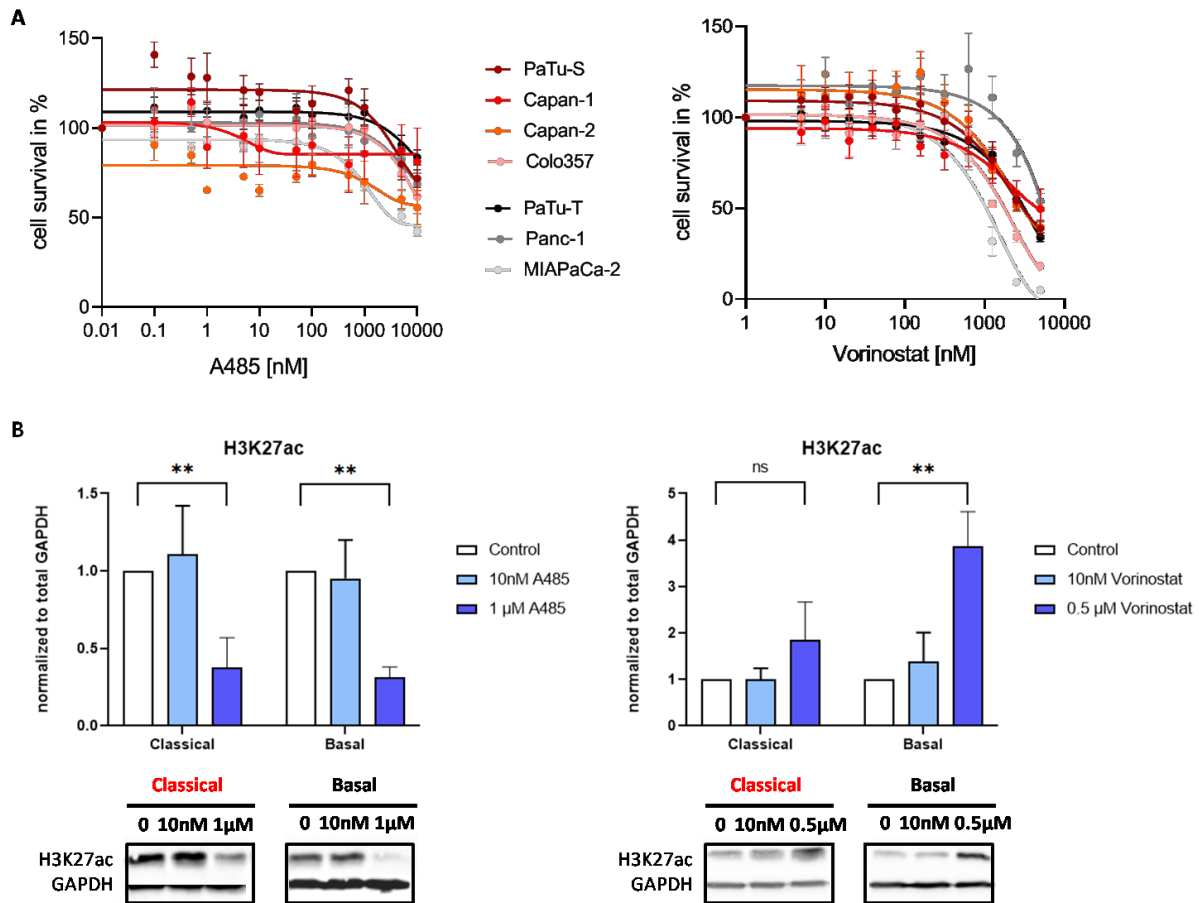


**Figure 12: Cell survival response to single-drug histone acetylase or histone deacetylase inhibitor treatment is independent of the molecular subtype.** (A) MTT cell survival assay of cells treated with increasing concentrations of the p300/CREBBP inhibitor A485 ( $n = 5$ ) or the class I and II HDAC inhibitor Vorinostat ( $n = 7$ ) after 72 hours. (B) Quantification of H3K27ac immunoblot analysis (normalized to GAPDH) of classical (Pa-Tu-S, Capan-1, Capan-2, Colo-357) and basal (Pa-Tu-T, Panc-1, MIAPaca-2) PDAC cell lines. Representative images for classical and basal cell lines are data from Pa-Tu-S and MIA-Paca-2, respectively. Cells were treated with indicated concentrations of A485 or Vorinostat for 24 hours ( $n = 3$ ). All data are represented as mean  $\pm$  SEM. For (B) P-values were calculated by one-way ANOVA, \* $p < 0.05$ , \*\* $p < 0.01$ , ns = not significant. Inhibitor treatment, cell survival assays and western blot assays were performed together with Maria Escobar.

#### 5.4. Genetic reprogramming of pancreatic cancer cells through knockout of a combination of epigenetic modifiers

So far, the results of this study demonstrate that epithelial differentiation markers are differentially expressed between the classical and basal subtype (Figure 8) and that epigenetic modifications play a significant role in the regulation of these specific gene expression profiles (Figure 10). However, single-drug treatment with epigenetic inhibitors did not have a significant effect on overall cell survival (Figure 12). In order to improve tumor cell reprogramming efficiency, I aimed at generating a triple knockout cell line lacking a combination of epigenetic modifiers.

#### 5.4.1. Generating a multiplex CRISPR-Cas9 plasmid

The effect of a combinatory loss of epigenetic modifiers could be analyzed using a triple-knockout pancreatic cancer cell line depleting HDAC2, DNMT3A, and RING1B simultaneously. For this purpose a multiplex knockout plasmid was constructed using the CRISPR/Cas9 vector system from Addgene's Multiplex CRISPR/Cas9 Assembly System Kit (Sakuma et al., 2014) (Figure 13A, see also 4.1.8).

For each gene locus of *HDAC2*, *DNMT3A*, and *RING1B*, multiple gRNAs were designed with Zhang Lab's online CRISPR Design tool *crispr.mit.edu* (Ran et al., 2013) and CHOPCHOP (Labun et al., 2016 and Montague et al., 2014) to test their target specificity. Figure 13B depicts the final gRNA sequences for each target gene. The 3'-nucleotide PAM-sequence (green box) needed to be directly downstream of the sgRNA-sequence. To improve transcription efficiency by the U6 RNA polymerase III, an additional guanine base was added at the 5'-end where the sequence originally started with a different base (blue). The four nucleotide CACC overhang (orange) was complementary to the overhang produced by BbsI restriction of the CRISPR/Cas9 vector. Gel electrophoresis and DNA sequencing of the plasmid were used to check for correct restriction and ligation. After BbsI enzyme restriction, the presence of one single band exhibited successful cutting into a linear plasmid. Correct incorporation of the sgRNA sequences and the generation of a circular plasmid produced multiple DNA bands at the 10 kbp marker due to the presence of plasmid topoisomers (Figure 13C).

Exemplary DNA-sequencing of the plasmid after the STEP 1 ligation (see 4.1.8) showed correct insertion of the *DNMT3A* sgRNA sequence (Figure 13D).

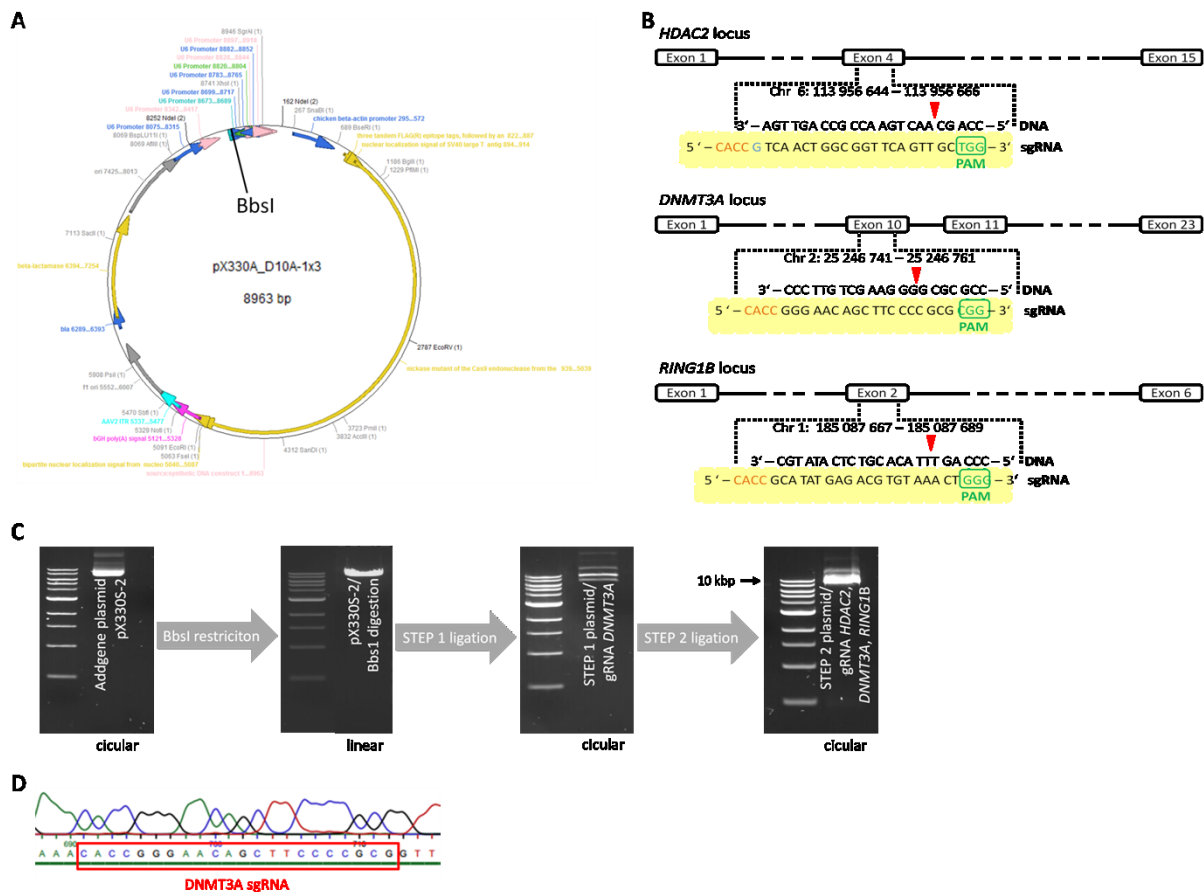


**Figure 13: CRISPR-Cas9 multiplex knockout – Plasmid construction.** (A) CRISPR/Cas9 vector with BbsI restriction site and U6 promoter from Takashi Yamamoto (Addgene kit # 1000000055) (B) gRNA design for the three target genes (*HDAC2*, *DNMT3A*, *RING1B*). gRNA sequences were designed with Zhang Lab’s online CRISPR Design tool *crispr.mit.edu* (Ran et al., 2013) and CHOPCHOP (Labun et al., 2016 and Montague et al., 2014). An additional guanine was added at the 5’ end where the sequence started with a different base (blue). The 5’-NGG-3’ PAM-sequence is marked in green. 5’-CACC-3’ overhang for DNA ligation is marked in orange. Red arrowheads indicate the location of the DNA double-strand break. (C) Plasmid gel electrophoresis after BbsI restriction, STEP 1 and STEP 2 ligation, respectively. (D) DNA sequencing result after STEP 1 insertion of *DNMT3A* gRNA. The red box shows the sgRNA-sequence.

### 5.4.2. Establishing a multiplex knockout cell line

After designing and Step1-cloning of multiple gRNAs for each gene locus, the target specificity of each gRNA was tested by Step1-plasmid transfection of Panc-1 cells and western blot analysis of the mixed cell population. Figure 14A shows the immunoblot data of some of the tested gRNAs as well as the final gRNA for each target gene (red box). None of the gRNAs against *HDAC2* produced a visible reduction of *HDAC2* levels in this mixed population. Nevertheless, gRNA4 was chosen to continue with further experiments. Notably, the protein levels of *DNMT3A* and *RING1B* were slightly reduced in the mixed cell population using gRNA11 for targeting *DNMT3A* and gRNA9 for targeting *RING1B*, respectively (Figure 14A, red box). The overall transfection efficiency was measured by simultaneous

transfection of Panc-1 cells with a GFP-tagged control-plasmid and averaged at about 60 % (data not shown).

After assembling the multiplex gRNA plasmid in Step2-cloning, Panc-1 cells were transfected with the multiplex plasmid containing all three selected gRNAs. Single-cell clones were seeded and cultivated in 96-well plates. In cell western blot experiments were used to check the transfection efficiency of the *HDAC2* gRNA again (Figure 14B). Furthermore, normal western blot analysis was conducted to screen for a complete *HDAC2* knockout (Figure 14C). Unfortunately, the in-cell western blot revealed a very heterogeneous pattern of the fluorescence signals, which were normalized to the total number of cells. No obvious *HDAC2* knockout was identified in the tested 58 single-cell clones. Some clones even showed higher HDAC2 levels than untransfected Panc-1 cells, which were used as a positive control (Figure 14B). Moreover, promising single-cell clones with changes in cell morphology were also screened by western blot analysis. Again, none of the screened clones showed a complete knockout for HDAC2. Levels for H3K27ac were also unchanged in comparison to the positive control (Figure 14C).

Although correct insertion of the gRNAs in the plasmid was confirmed through gel electrophoresis (Figure 13C), no successful triple-knockout pancreatic cancer cell line lacking the epigenetic modifiers *HDAC2*, *DNMT3A*, and *RING1B* could be generated. A combinatory loss of all three epigenetic modifiers most likely impedes vital cellular functions to such an extent that cell survival is no longer possible. Since the plasmid did not have a selection marker, it is possible that all surviving single-cell clones were not successfully transfected in the first place and all successfully transfected clones died before enough cells or proteins could be harvested for the screening. In order to rule out limited gRNA efficiency of the *HDAC2* gRNA, the single-cell clones should also be screened for DNMT3A and RING1B levels.

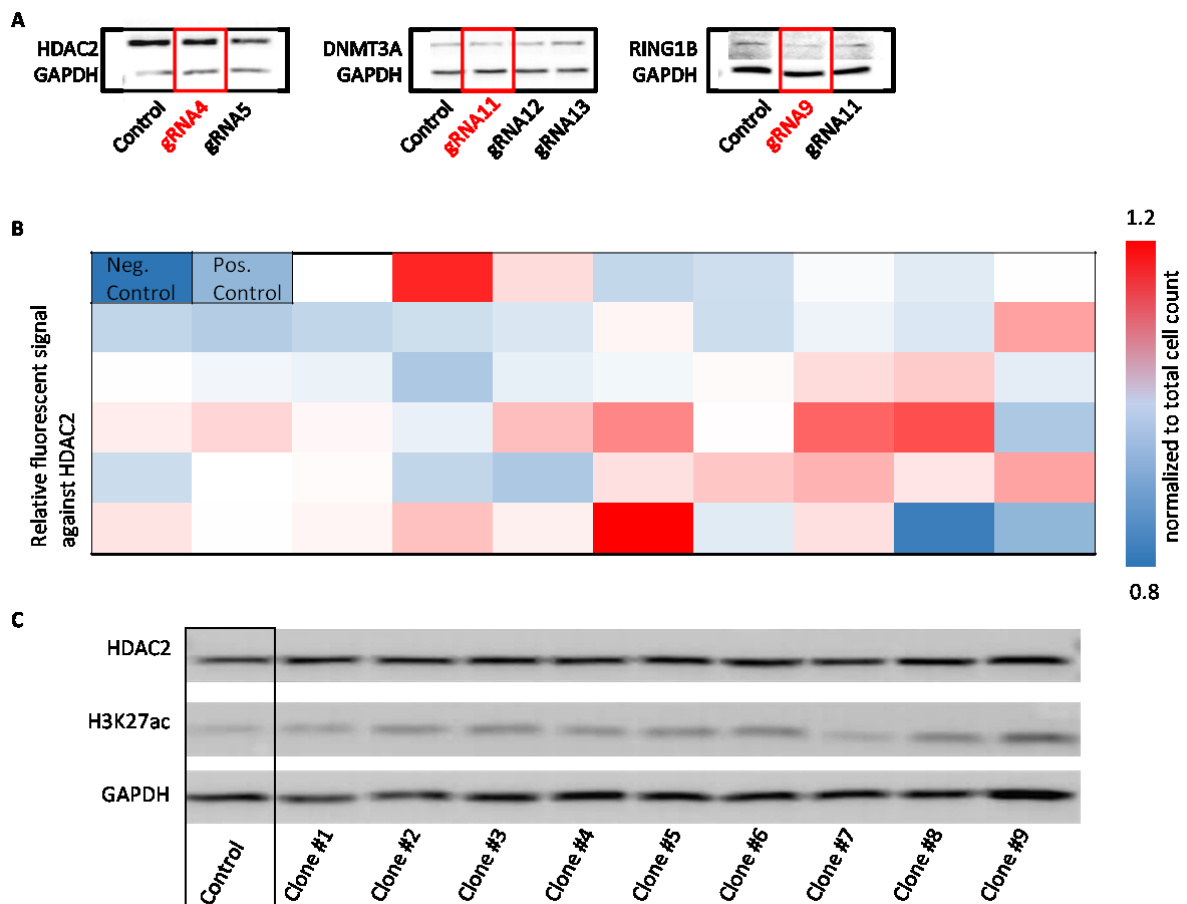


**Figure 14: CRISPR-Cas9 multiplex knockout – Transfection efficiency and single-cell clones. (A)** Representative images of immunoblot analysis of transfected Panc-1 cells with different gRNAs. Antibody signals of HDAC2, DNMT3A, RING1B, and GAPDH. Red boxes mark gRNAs used in further analysis. Untreated Panc-1 cells served as control. **(B)** In-cell western analysis of transfected single-cell clones with an HDAC2 antibody. Panc-1 cells were transfected with a multiplex CRISPR/Cas9 plasmid against *HDAC2*, *DNMT3A*, and *RING1B*. Fluorescence signal (FITC-staining) was measured with Softmax Pro 7.0 and normalized to the total number of cells. Mean of 2-3 experiments is shown in the heatmap. Empty well served as a negative control, untreated Panc-1 cells served as a positive control. **(C)** Representative images of transfected Panc-1 single-cell clones with antibodies against HDAC2, H3K27ac, and GAPDH as the loading control. Panc-1 cells were subject to transfection with multiplex gRNA plasmid against *HDAC2*, *DNMT3A*, and *RING1B*. Untreated Panc-1 cells served as control.

## 6. Discussion

The need for more efficient therapeutic strategies is highlighted by the discrepancy between pancreatic cancer incidence and mortality. While it accounts for only 2.5 % of newly diagnosed cancers per year, it is responsible for about 4.5 % of cancer deaths per year worldwide (Bray et al., 2018). Therapeutic options remain limited, especially for locally advanced tumors, which represent the majority of pancreatic cancer cases due to the lack of early symptoms.

Large-scale genome sequencing data revealed a fairly homogenous mutational profile with a number of main driving mutations including *KRAS*, *CDKN2A*, *SMAD3*, and *TP53* (Jones et al., 2008). However, the whole genome-sequencing results also identified several passenger mutations which contribute to tumor heterogeneity in PDAC (Bailey et al., 2016). In order to improve therapeutic outcomes, several groups have defined distinct molecular PDAC subtypes with clinical significance, based on transcriptome data (Collisson et al., 2011, Moffitt et al., 2016, Bailey et al., 2016). Particularly, overall survival and response to Gemcitabine treatment correlated with subtype allocation (Collisson et al., 2011). These results highlight the importance of uncovering the molecular mechanisms defining PDAC subtypes in order to discover new druggable targets and to put clinically effective patient stratification systems in place. In addition, large-scale genome sequencing data revealed that epigenetic modifying enzymes are among the frequently altered genes (Bailey et al., 2016). The lack of adequate mutational differences between molecular PDAC subtypes has led to the hypothesis that epigenetic modifications including histone modifications and DNA methylation could have a significant impact on therapy response and clinical outcome (Regel, Mayerle and Mahajan, 2020). The reversible nature of epigenetic modifications makes them an attractive target for new epigenetic reprogramming therapies. For instance, depletion of the epigenetic remodeler *Ring1b* impaired tumor formation and was able to sustain a differentiation program in pancreatic acinar cells to prevent cancer development in vivo (Benitz et al., 2019).

To further understand the complex mechanisms of PDAC heterogeneity, this study aimed at investigating whether PDAC subtypes and their defined signature genes show differences in their epigenetic profiles. Moreover, inhibitor treatment and genetic knockout experiments tested the effects of epigenetic remodeling approaches in vitro.

## 6.1. Transcriptional profiles define PDAC subtypes

Various gene expression studies on PDAC patient samples showed overlapping results defining a classical and basal/quasimesenchymal pancreatic cancer subtype (Collisson et al., 2011, Moffitt et al., 2016, Bailey et al., 2016). In this study, seven well-established low-grade and high-grade PDAC cell lines were assigned to the classical (Pa-Tu-S, Capan-1, Capan-2, Colo-357) or basal molecular PDAC subtype (Pa-Tu-T, Panc-1, MiaPaca-2) based on their gene expression profiles. The gene expression results confirmed the existence of several markers, which are specific for the classical subtype, such as *ELF3*, *ERBB3*, *GATA6*, *EpCAM*, *FGFBP1*, and *AGR2* in the classical cell lines (Pa-Tu-S, Capan-1, Capan-2, Colo-357) (see Figure 7B), which is in accordance with previously published data (Collisson et al., 2011, Chan-Seng-Yue et al., 2020). Mesenchymal markers were selected based on gene expression profiles of basal subtypes in other solid tumor entities, such as lung adenocarcinoma (Yang et al., 2020) or bladder cancer (Damrauer et al., 2014). However, none of the gene signatures previously associated with mesenchymal cells such as *KRT14A* showed elevated expression levels in the basal pancreatic cancer cell lines (see Figure 7B) (Collisson et al., 2011). These results are comparable with studies showing that the basal or squamous-like subtype is above all characterized by a loss of epithelial differentiation markers such as *EpCAM*, *GATA6*, *CDKN2A*, *SMAD4*, and *KDM6A* (Chan-Seng-Yue et al., 2020, Andricovich et al., 2018). The only consistently mutated genes, which were found to be specific to the basal subtype, proved to be point mutations of *KRAS* and *TP63* as well as amplifications of the protooncogene *MYC* (Lenkiewicz et al., 2020). Nevertheless, the expression of the mesenchymal markers *TP63* and *MYC* did not show a significant correlation to the classical or basal PDAC subtypes in this study. While levels of *TP63* were considerably increased in the basal cell line MiaPaca-2, they also showed moderately increased expression levels in the classical cell line Capan-1. The highest expression levels for the proto-oncogene *MYC* were found in the classical PDAC cell line Colo-357 with no significant correlation to molecular PDAC subtypes either (see Figure 8A). Hence, the identification of basal classifier genes in human pancreatic cancer remains a continuous problem. Interestingly, results also showed significant differences in protein levels between cell lines of the same subtype throughout the entire project. For instance, gene expression levels of the epithelial differentiation marker *GATA6* were highly increased in only one of the four classical PDAC cell lines (Pa-Tu-S), while its expression was only slightly elevated in the other three classical PDAC cell lines compared to the basal cell lines (see Figure 8A). Therefore, statistical analysis did not show a significant difference in the mean expression levels between the classical and basal PDAC cell lines. To conclude, although the pancreatic cancer cell lines used in this study were assigned to the classical or basal subtype based on their overall gene expression profiles, their transcriptomic profiles were at times highly heterogenic. This needs to be considered when translating in vitro findings to in vivo experiments.

## 6.2. The role of epigenetic modifications in molecular subtypes

To further characterize the molecular mechanisms behind transcriptional PDAC subtypes, epigenomics have been increasingly investigated. Epigenetic modifiers are not only significantly changed and involved in nearly all major aspects of cancer biology, but are also among the most frequently mutated passenger genes in PDAC (Lomberk et al., 2018, Bailey et al., 2016). Furthermore, Benitz et al. were able to show that *Ring1b*-mediated epigenetic silencing of transcriptional regulatory genes for acinar cells represents a leading event in pancreatic tumorigenesis followed by additional repressive histone modifications to stabilize the tumor phenotype (Benitz et al., 2019). In this study, the correlation between changes in the epigenome and molecular subtype affiliation in PDAC cells was investigated. Particular interest laid on how epigenetic modifications regulate subtype-specific gene expression profiles.

In line with several published studies, it was found that important epigenetic modifiers, such as histone deacetylases (*HDAC1*, *HDAC2*), histone acetyl transferases and readers (*SMARCA4*, *HAT1*, *CREBBP*, *EP300*), histone ubiquitin ligases (*RING1A*, *RING1B*), and a DNA methyltransferase (*DNMT3A*) were differentially expressed between the classical and basal subtype (see Figure 9B) (Lomberk et al., 2018, Patil et al., 2020). The validation of these results with immunoblot analysis also showed statistically significant enrichment of the acetylation of histone H3 on lysine 27 (H3K27ac) in the classical cell lines compared to the basal cell lines (see Figure 9A). However, the collective gene expression data showed that activating histone acetylation marks as well as repressive histone modifications, like histone deacetylation and histone ubiquitination marks, were upregulated in the classical subtype at the same time (see Figure 9B). The simultaneous enrichment of transcriptional activating and repressing epigenetic modifications within the same subtype suggests a complex interaction of activating and repressing epigenetic modifications at different transcriptional start sites in order to define the subtype-specific transcriptomic profiles. Therefore, the specific epigenetic profile of each target gene needs to be analyzed in the classical and basal subtype. To investigate the immediate effects of histone remodeling patterns at the transcriptional start site of important epithelial and mesenchymal differentiation genes, chromatin immunoprecipitation against the histone acetylation H3K27ac and the histone ubiquitination H2AK119ub was conducted. The activating histone acetylation mark H3K27ac was greatly enriched at the promoter site of the epithelial differentiation genes *EpCAM* and *GATA6* in the classical cell lines, indicating active transcription of these genes. In contrast, basal cell lines depicted high levels of the repressive histone ubiquitination mark H2AK119ub at the transcriptional start site of *EpCAM* and *GATA6* while levels of the activating histone acetylation mark H3K27ac were decreased (see Figure 10A). Chromatin immunoprecipitation for H3K27ac and H2AK119ub at the promoter region of the protooncogene *MYC*, which is described as a mesenchymal differentiation gene, showed inverse results indicating

active transcription in the basal cell lines and transcriptional repression in the classical cell lines (see Figure 10B). These results confirmed the correlation between histone modifications and molecular subtypes shown in transcriptomic analyses of microdissected tumor samples (Lomberk et al., 2018). Importantly, some transcription factors, such as *GATA6*, act as super-enhancers and exert additional regulatory functions on downstream transcription factors after their epigenetic activation in the classical subtype. Thereby, their activating influence on target pathways such as pancreatic development, metabolic pathways, and RAS-signaling is amplified (Lomberk et al., 2018). In the basal subtype, only MET was identified as a super-enhancer regulating cell proliferation and EMT (Lomberk et al., 2018). In accordance with current findings that the expression of *GATA6* is repressed in the more aggressive basal subtype, epigenetic repression of *GATA6* in the classical subtype through EZH2-dependent histone trimethylation of H3K27me3 and subsequent histone ubiquitination of H2AK119ub through the PRC1 components RING1A and RING1B has been shown to lead to PDAC progression (Patil et al., 2020).

Besides posttranslational histone modifications, the DNA methylation pattern is also known to be frequently altered in PDAC compared to normal pancreatic tissue (Zhang, Lu, Zhou & Zheng, 2008). Furthermore, the DNA methylation status of pancreas development genes like *FAM150A* (ALK and LTK ligand 1), *HNF1A*, or *RASSF10* (Ras association domain family member 10) negatively correlates with patient survival (Thompson, Rubbi, Dawson, Donahue & Pellegrini, 2015). Large-scale analyses of DNA methylation patterns in pancreatic cancer using the TCGA dataset revealed three distinct methylation clusters correlating to histological tumor grade and tumor staging (Mishra and Guda, 2017). Thus, this study aimed at investigating if the molecular subtypes proposed by Collisson et al. are characterized by specific DNA methylation patterns on the *EpCAM* and *GATA6* gene promoter. Therefore, bisulfite DNA methylation analysis was conducted at the transcriptional start site of the epithelial differentiation genes *EpCAM* and *GATA6* in four classical (Pa-Tu-S, Capan-1, Capan-2, Colo-357) and three basal (Pa-Tu-T, Panc-1, MiaPaca-2) pancreatic cancer cell lines. In correlation with the subtype-specific expression profile, the *EpCAM* gene locus was consistently unmethylated in the classical cell lines indicating transcriptional activation (see Figure 11 upper panel). The *GATA6* locus was also mostly unmethylated in the classical cell lines, with the exception of the Pa-Tu-S cell line, which presented a heterozygous DNA methylation status (see Figure 11 lower panel). The basal cell lines showed a heterogeneous methylation profile for both gene loci without consistent correlation to the *EpCAM* or *GATA6* gene expression levels (see Figure 11 both panels). These results lead to the conclusion that the lack of DNA methylation at the *EpCAM* gene locus in the classical cell lines correlates with activated transcription of the epithelial differentiation marker in the classical subtype. However, the overall heterogeneous results with unmethylated, partially methylated, and fully methylated promoter sites within the same subtype argue against a strong influence of DNA

methylation on the subtype-specific transcriptomic profiles of *EpCAM* and *GATA6*. Most likely, other epigenetic regulations, such as histone modifications play a more crucial part in regulating the subtype-specific expression of these differentiation genes. There is also increasing evidence that DNA methylation may not only occur at CpG islands around the promoter region but also intragenically and distal of the transcriptional start site. Distal DNA methylation has been reported to have an activating effect on transcription, contrary to 'traditional' DNA methylation at the promoter region (Mishra & Guda, 2017). Importantly, DNA hypermethylation around the transcriptional start site of genes with tumor suppressor activity like *FAM150A*, *HNF6*, or *RASSF10* correlated with shorter survival times in pancreatic cancer patients while more broadly distributed DNA hypermethylation at distant DNA sites correlated with longer survival times (Thompson et al., 2015). Thus, the positioning of DNA methylation sites needs to be considered when determining the methylation status.

Altogether, these results showed that the transcription of important cellular differentiation genes is epigenetically regulated through histone modifications in the classical and basal subtype. In this study, the DNA methylation status only played a minor role in defining the subtype-specific gene expression profiles. Hence, complex functions and interactions of different epigenetic regulators still need further research.

### **6.3. Therapeutic targeting of epigenetic modifiers**

Several research groups have studied the therapeutic effects of targeting epigenetic modifications in pancreatic cancer. For example, chemical *Ring1b* inhibition through PRT4165 decreased ADM formation, which is an early degeneration event in vitro and in vivo, and promoted a shift towards a more differentiated tumor phenotype of PDAC tumor cells (Benitz et al., 2019). Furthermore, uncovering a tumor-specific epigenetic profile could reveal new druggable target genes in PDAC. For instance, Nicolle et al. identified the hypomethylated cholesterol transporter gene *NPC1L1* (NPC1 like intracellular cholesterol transporter 1) as a therapeutic target for Ezetimib showing reduced viability of PDAC cell lines as well as reduced growth of spheroids and organoids from patient-derived xenografts in vitro and in vivo after Ezetimib treatment (Nicolle et al., 2017). However, the results of clinical studies using epigenetic drugs often fall short of the promising preclinical data (Pichlmeier & Regel, 2020). Therefore, this study investigates whether the response to epigenetic drugs depends on the molecular subtype and thus, patients could potentially benefit from further stratification.

Single-drug treatment of classical and basal pancreatic cancer cell lines with the histone acetylase-inhibitor A485, as well as the histone deacetylase-inhibitor Vorinostat, did not only show very little response even at high dosing, it was also in part independent of the molecular subtype. In order to

verify the effect of the epigenetic inhibitors on a molecular level, H3K27ac histone acetylation levels were determined 24 hours after inhibitor treatment. Indeed, the acetylation levels significantly decreased in both subtypes after treatment with the HAT-inhibitor A485. After 24 hours of treatment with the HDAC-inhibitor Vorinostat, H3K27ac-levels significantly increased in the basal cell lines only. In the classical cell lines, the already high H3K27ac acetylation levels could not be further enriched through Vorinostat treatment. In conclusion, although long-term treatment with histone acetylation inhibitors or histone deacetylation inhibitors had a significant effect on H3K27ac histone acetylation levels in classical and basal PDAC cell lines, the effects on overall cell survival were only marginal at very high dose rates. A possible reason for the limited therapeutic effects and a major restriction of HDAC-inhibitors is their pleiotropic properties. They exert inhibitory functions on multiple HDAC isoforms each regulating the expression of a variety of different cancer hallmark genes. Thus, off-target effects are frequent and can diminish the desired outcome (Citron & Fabris, 2020). Furthermore, inhibiting the complete enzymatic activity of epigenetic remodelers without the possibility to rescue their physiological function poses a great problem. Finally, the role of epigenetic readers and other regulators like microRNAs must be taken into consideration when discussing the efficiency and safety of epigenetic drugs (Azizi et al., 2014).

Nevertheless, the combination therapy of different epigenetic remodelers has shown promising effects in preclinical trials. For example, combination therapy of the DNMT-inhibitor 5-Azacytidine with the class I HDAC-inhibitor Givinostat sensitized high-grade serous ovarian cancer to immune checkpoint inhibitors in vivo (Stone et al., 2017). There has also been evidence that the combinatory inhibition of EHMT2 (Euchromatic Histone Lysine Methyltransferase 2), which catalyzes the methylation of lysine 9 at histone 3 (H3K9me), and DNMT showed synergistic effects in a breast cancer cell line (Park et al., 2016). Altogether, these results demonstrate how closely different epigenetic modifications interact with each other. In order to maximize therapeutic response, the effects of combinatory therapies of epigenetic modifiers need to be further investigated.

#### **6.4. Unsuccessful triple-knockout of epigenetic modifiers in pancreatic cancer cells**

CRISPR/Cas9-mediated knockout of epigenetic remodelers that are overexpressed in pancreatic cancer has been proven to induce epigenetic remodeling. For instance, a complete knockout of the epigenetic remodeler Ring1b in an aggressive murine pancreatic cancer cell line induced tumor cell reprogramming processes towards a more epithelial tumor phenotype (Benitz et al., 2019). Interestingly, levels of Dnmt3a were significantly increased in these Ring1b knockout cells (Deubler, 2016). This could represent a compensatory mechanism in cancer cells to ensure transcriptional repression of differentiation genes and further demonstrates the flexible character of epigenetic

regulations. In line with previous results of this study showing that single-drug treatment with epigenetic inhibitors does not have a significant effect on cell survival, the effect of a combinatory loss of multiple epigenetic modifiers targeting histone acetylation, histone ubiquitination, and DNA methylation at the same time was studied.

In order to interfere in the complex and flexible epigenetic profiles of PDAC cells, I successfully constructed a golden-gate CRISPR/Cas9 plasmid with sgRNAs against *HDAC2*, *RING1B*, and *DNMT3A* to induce a genetic knockout of multiple genes. The sgRNA sequences were designed with the help of Zhang Lab's online CRISPR Design tool *crispr.mit.edu* (Ran et al., 2013) and CHOPCHOP (Labun et al., 2016 and Montague et al., 2014). A four nucleotide overhang (CACC) at the 5' end was added to complement the overhang produced by BbsI restriction of the CRISPR/Cas9 vector. Furthermore, an additional guanine base was added at the 5' end where the sequence originally started with a different base to improve transfection efficiency by the U6 RNA polymerase III (see Figure 13B). In STEP 1 of the cloning process, one sgRNA for each target gene was inserted into the corresponding CRISPR/Cas9 vector from the Addgene's Multiplex CRISPR/Cas9 Assembly System Kit by BbsI restriction and T7 ligation (Ran et al., 2013, Sakuma et al., 2014). In STEP 2 of the multiplex genome engineering process, the gRNAs from each individual plasmid were then assembled into a common vector using BsaI-digestion and Quick ligase ligation (Sakuma et al., 2014). Correct annealing was verified by the presence of plasmid topoisomer-bands on gel electrophoresis as well as by DNA sequencing (see Figure 13C-D). Lastly, Panc-1 cells were transfected with the multiplex plasmid containing all three selected gRNAs using the lipofection method. After transfection, single-cell clones were seeded and cultivated to check for complete gene knockout. However, due to the lack of a fluorescent marker or an antibiotic resistance gene in the plasmid, no positive selection for successfully transfected clones could be carried out. Unfortunately, western blot analysis, as well as in-cell western experiments, showed that none of the cultured single-cell clones were successful knockout cell lines for HDAC2. The single-cell clones remain to be screened for DNMT3A and RING1B levels to rule out limited gRNA efficiency of the *HDAC2* gRNA. However, it is quite possible that early cell death within the first few days after the multiplex knockout of all successfully transfected clones occurred. Currently, there are no studies available on the survivability of a combinatory knockout of different epigenetic modifiers in pancreatic cancer cells. Hence, it is possible that the loss of three major epigenetic regulators involved in a variety of oncogenic pathways is not compatible with cell survival. Furthermore, simultaneous knockout of multiple epigenetic modifying enzymes may deprive cells of their natural compensatory mechanisms through up- or downregulation of other epigenetic regulators. To overcome these limitations, consecutive knockout of different epigenetic modifiers could be performed. Moreover, a selection gene needs to be included in the plasmid to monitor and ensure sufficient transfection efficiency.

## 7. Summary and outlook

Large-scale gene expression analyses have demonstrated that pancreatic ductal adenocarcinoma can be classified into different molecular subtypes with clinical significance (Collisson et al., 2011, Moffitt et al., 2016, Bailey et al., 2016). So far, great effort has been put into unveiling the factors responsible for tumor heterogeneity in pancreatic cancer. Since epigenetic modifiers are, besides the four driver gene mutations *KRAS*, *p16*, *p53*, and *SMAD4*, among the most frequently mutated genes in PDAC, this study aimed at investigating the role of epigenetic changes in the two molecular PDAC cancer subtypes, represented by a classical and basal phenotype, as well as their therapeutic potential in pancreatic cancer cell lines (Bailey et al., 2016).

The data showed that subtype-specific gene expression of cellular differentiation marker genes, such as *EpCAM* and *GATA6*, is epigenetically regulated. Chromatin-immunoprecipitation results demonstrated that the expression of these epithelial differentiation marker genes is activated through histone acetylation marks in the classical subtype. In contrast, their expression is repressed in the basal or quasimesenchymal subtype through increased levels of histone ubiquitination as well as a loss of histone acetylation marks. DNA methylation seemed to only play a minor part in regulating subtype-specific gene expression profiles of *EpCAM* and *GATA6*.

Despite subtype-specific histone acetylation levels, single-drug treatment with chemical inhibitors targeting histone acetylation and deacetylation marks only showed limited effects in vitro. Classical and basal PDAC cell lines were almost completely resistant to HAT inhibitor treatment with A485. Only one of the basal cell lines, MIAPaca-2, reached a 50 % survival rate at the maximum dosage of 10  $\mu$ M A485 (see Figure 12A, left panel). High doses of the HDAC inhibitor Vorinostat were able to inhibit cell survival to a greater extent, but the response was independent of the transcriptomic subtypes. It is possible that a compensatory upregulation of other epigenetic modifications limits the therapeutic effects. Hence, a multiplex CRISPR/Cas9 knockout plasmid targeting a combination of epigenetic modifiers (*HDAC2*, *DNMT3A*, *RING1B*) was constructed to induce simultaneous genetic knockout of all three target genes. However, transfection of a basal pancreatic cancer cell line with this plasmid did not yield a successful knockout cell line. Most likely, the combinatory knockout impaired critical cellular functions to such an extent that cell death occurred. To overcome the limitations of a multiplex CRISPR/Cas9 knockout strategy, a successive knockout of one target gene after the other might be a more successful strategy to analyze the effect of a combinatory loss of different epigenetic modifiers. Furthermore, a selection marker should be included in the plasmids to ensure successful transfection. The generated knockout cell line can then be used for transcriptome analysis by RNA sequencing as well as for basic cell assays and drug sensitivity tests.

In order to translate preclinical data with epigenetic inhibitors into successful clinical trials, further studies are needed to determine subtype-specific changes after epigenetic targeting. For instance, unpublished data within the working group showed that HAT inhibitor treatment of cell lines with a classical PDAC subtype strongly downregulated the expression of *GATA6* and decreased Gemcitabine drug sensitivity indicating a poorer outcome. These results emphasize the importance of establishing patient stratification systems in order to maximize the success of current treatment strategies.

Overall, this thesis showed that the transcriptomic profiles defining molecular PDAC subtypes are in part regulated through epigenetic modifications. Although the targeting of single epigenetic modifiers showed some success in tumor cell reprogramming, the therapeutic targeting with epigenetic drugs remains limited. Thus, the precise effects of combination therapies with multiple epigenetic inhibitors need further investigation.

## 8. References

- Abreu Velez, Ana Maria, Howard, Michael S. (2015): Tumor-suppressor Genes, Cell Cycle Regulatory Checkpoints, and the Skin. In: *North American journal of medical sciences* 7 (5), S. 176–188. DOI: 10.4103/1947-2714.157476.
- Adamska, Aleksandra, Domenichini, Alice, Falasca, Marco (2017): Pancreatic Ductal Adenocarcinoma: Current and Evolving Therapies. In: *International journal of molecular sciences* 18 (7). DOI: 10.3390/ijms18071338.
- Andricovich, Jaclyn, Perkail, Stephanie, Kai, Yan, Casasanta, Nicole, Peng, Weiqun, Tzatsos, Alexandros (2018): Loss of KDM6A Activates Super-Enhancers to Induce Gender-Specific Squamous-like Pancreatic Cancer and Confers Sensitivity to BET Inhibitors. In: *Cancer cell* 33 (3), 512–526.e8. DOI: 10.1016/j.ccell.2018.02.003.
- Aylon, Yael, Oren, Moshe (2011): New plays in the p53 theater. In: *Current opinion in genetics & development* 21 (1), S. 86–92. DOI: 10.1016/j.gde.2010.10.002.
- Azizi, Masoumeh, Teimoori-Toolabi, Ladan, Arzanani, Mohsen Karimi, Azadmanesh, Kayhan, Fard-Esfahani, Pezhman, Zeinali, Sirous (2014): MicroRNA-148b and microRNA-152 reactivate tumor suppressor genes through suppression of DNA methyltransferase-1 gene in pancreatic cancer cell lines. In: *Cancer Biology & Therapy* 15 (4), S. 419–427. DOI: 10.4161/cbt.27630.
- Bailey, Peter, Chang, David K., Nones, Katia, Johns, Amber L., Patch, Ann-Marie, Gingras, Marie-Claude et al. (2016): Genomic analyses identify molecular subtypes of pancreatic cancer. In: *Nature* 531 (7592), S. 47–52. DOI: 10.1038/nature16965.
- Bardeesy, Nabeel, DePinho, Ronald A. (2002): Pancreatic cancer biology and genetics. In: *Nature reviews. Cancer* 2 (12), S. 897–909. DOI: 10.1038/nrc949.
- Becker, Andrew E., Hernandez, Yasmin G., Frucht, Harold, Lucas, Aimee L. (2014): Pancreatic ductal adenocarcinoma: risk factors, screening, and early detection. In: *World journal of gastroenterology* 20 (32), S. 11182–11198. DOI: 10.3748/wjg.v20.i32.11182.
- Bednar, J., Horowitz, R. A., Grigoryev, S. A., Carruthers, L. M., Hansen, J. C., Koster, A. J., Woodcock, C. L. (1998): Nucleosomes, linker DNA, and linker histone form a unique structural motif that directs the higher-order folding and compaction of chromatin. In: *Proceedings of the National Academy of Sciences of the United States of America* 95 (24), S. 14173–14178. DOI: 10.1073/pnas.95.24.14173.
- Benitez, Cecil M., Goodyer, William R., Kim, Seung K. (2012): Deconstructing pancreas developmental biology. In: *Cold Spring Harbor perspectives in biology* 4 (6). DOI: 10.1101/cshperspect.a012401.
- Benitz, Simone, Straub, Tobias, Mahajan, Ujjwal Mukund, Mutter, Jurik, Czerniak, Stefan, Unruh, Tatjana et al. (2019): Ring1b-dependent epigenetic remodelling is an essential prerequisite for pancreatic carcinogenesis. In: *Gut*. DOI: 10.1136/gutjnl-2018-317208.
- Bernstein, Bradley E., Meissner, Alexander, Lander, Eric S. (2007): The mammalian epigenome. In: *Cell* 128 (4), S. 669–681. DOI: 10.1016/j.cell.2007.01.033.
- Bird, Adrian (2002): DNA methylation patterns and epigenetic memory. In: *Genes & development* 16 (1), S. 6–21. DOI: 10.1101/gad.947102.
- Bird, Adrian (2007): Perceptions of epigenetics. In: *Nature* 447 (7143), S. 396–398. DOI: 10.1038/nature05913.

- Brand, Randall E., Lerch, Markus M., Rubinstein, Wendy S., Neoptolemos, John P., Whitcomb, David C., Hruban, Ralph H. et al. (2007): Advances in counselling and surveillance of patients at risk for pancreatic cancer. In: *Gut* 56 (10), S. 1460–1469. DOI: 10.1136/gut.2006.108456.
- Bray, Freddie, Ferlay, Jacques, Soerjomataram, Isabelle, Siegel, Rebecca L., Torre, Lindsey A., Jemal, Ahmedin (2018): Global cancer statistics 2018: GLOBOCAN estimates of incidence and mortality worldwide for 36 cancers in 185 countries. In: *CA: a cancer journal for clinicians* 68 (6), S. 394–424. DOI: 10.3322/caac.21492.
- Bynigeri, Ratnakar R., Jakkampudi, Aparna, Jangala, Ramaiah, Subramanyam, Chivukula, Sasikala, Mitnala, Rao, G. Venkat et al. (2017): Pancreatic stellate cell: Pandora's box for pancreatic disease biology. In: *World journal of gastroenterology* 23 (3), S. 382–405. DOI: 10.3748/wjg.v23.i3.382.
- Cancer Genome Atlas Research Network. Electronic address, a.a.d.h.e. and N. Cancer Genome Atlas Research (2017): Integrated Genomic Characterization of Pancreatic Ductal Adenocarcinoma. In: *Cancer cell* 32 (2), 185–203.e13. DOI: 10.1016/j.ccell.2017.07.007.
- Chan, Emily, Arlinghaus, Lori R., Cardin, Dana B., Goff, Laura, Berlin, Jordan D., Parikh, Alexander et al. (2016): Phase I trial of Vorinostat added to chemoradiation with capecitabine in pancreatic cancer. In: *Radiotherapy and oncology : journal of the European Society for Therapeutic Radiology and Oncology* 119 (2), S. 312–318. DOI: 10.1016/j.radonc.2016.04.013.
- Chandrasegaram, M. D., Goldstein, D., Simes, J., Gebiski, V., Kench, J. G., Gill, A. J. et al. (2015): Meta-analysis of radical resection rates and margin assessment in pancreatic cancer. In: *The British journal of surgery* 102 (12), S. 1459–1472. DOI: 10.1002/bjs.9892.
- Chan-Seng-Yue, Michelle, Kim, Jaeseung C., Wilson, Gavin W., Ng, Karen, Figueroa, Eugenia Flores, O'Kane, Grainne M. et al. (2020): Transcription phenotypes of pancreatic cancer are driven by genomic events during tumor evolution. In: *Nature genetics* 52 (2), S. 231–240. DOI: 10.1038/s41588-019-0566-9.
- Chen, Jihong, GhAzawi, Feras M., Li, Qiao (2010): Interplay of bromodomain and histone acetylation in the regulation of p300-dependent genes. In: *Epigenetics* 5 (6), S. 509–515. DOI: 10.4161/epi.5.6.12224.
- Chen, Shi, Chen, Jiangzhi, Zhan, Qian, Zhu, Yi, Chen, Hao, Deng, Xiaying et al. (2014): H2AK119Ub1 and H3K27Me3 in molecular staging for survival prediction of patients with pancreatic ductal adenocarcinoma. In: *Oncotarget* 5 (21), S. 10421–10433.
- Chuang, Shu-Chun, Gallo, Valentina, Michaud, Dominique, Overvad, Kim, Tjønneland, Anne, Clavel-Chapelon, Françoise et al. (2011): Exposure to environmental tobacco smoke in childhood and incidence of cancer in adulthood in never smokers in the European Prospective Investigation into Cancer and Nutrition. In: *Cancer causes & control : CCC* 22 (3), S. 487–494. DOI: 10.1007/s10552-010-9723-2.
- Citron, Francesca, Fabris, Linda (2020): Targeting Epigenetic Dependencies in Solid Tumors: Evolutionary Landscape Beyond Germ Layers Origin. In: *Cancers* 12 (3), S. 682. DOI: 10.3390/cancers12030682.
- Clayton, Alison L., Hazzalin, Catherine A., Mahadevan, Louis C. (2006): Enhanced histone acetylation and transcription: a dynamic perspective. In: *Molecular cell* 23 (3), S. 289–296. DOI: 10.1016/j.molcel.2006.06.017.
- Collado, Manuel, Blasco, Maria A., Serrano, Manuel (2007): Cellular senescence in cancer and aging. In: *Cell* 130 (2), S. 223–233. DOI: 10.1016/j.cell.2007.07.003.

- Collisson, Eric A., Sadanandam, Anguraj, Olson, Peter, Gibb, William J., Truitt, Morgan, Gu, Shenda et al. (2011): Subtypes of pancreatic ductal adenocarcinoma and their differing responses to therapy. In: *Nature medicine* 17 (4), S. 500–503. DOI: 10.1038/nm.2344.
- Conroy, Thierry, Hammel, Pascal, Hebbar, Mohamed, Ben Abdelghani, Meher, Wei, Alice C., Raoul, Jean-Luc et al. (2018): FOLFIRINOX or Gemcitabine as Adjuvant Therapy for Pancreatic Cancer. In: *The New England journal of medicine* 379 (25), S. 2395–2406. DOI: 10.1056/NEJMoa1809775.
- Croce, Carlo M. (2008): Oncogenes and cancer. In: *The New England journal of medicine* 358 (5), S. 502–511. DOI: 10.1056/NEJMra072367.
- D'Addario, Claudio, Di Francesco, Andrea, Pucci, Mariangela, Finazzi Agrò, Alessandro, Maccarrone, Mauro (2013): Epigenetic mechanisms and endocannabinoid signalling. In: *The FEBS journal* 280 (9), S. 1905–1917. DOI: 10.1111/febs.12125.
- Damrauer, Jeffrey S., Hoadley, Katherine A., Chism, David D., Fan, Cheng, Tiganelli, Christopher J., Wobker, Sara E. et al. (2014): Intrinsic subtypes of high-grade bladder cancer reflect the hallmarks of breast cancer biology. In: *Proceedings of the National Academy of Sciences of the United States of America* 111 (8), S. 3110–3115. DOI: 10.1073/pnas.1318376111.
- Decourcelle, Amélie, Leprince, Dominique, Dehennaut, Vanessa (2019): Regulation of Polycomb Repression by O-GlcNAcylation: Linking Nutrition to Epigenetic Reprogramming in Embryonic Development and Cancer. In: *Frontiers in endocrinology* 10, S. 117. DOI: 10.3389/fendo.2019.00117.
- Deer, Emily L., González-Hernández, Jessica, Coursen, Jill D., Shea, Jill E., Ngatia, Josephat, Scaife, Courtney L. et al. (2010): Phenotype and genotype of pancreatic cancer cell lines. In: *Pancreas* 39 (4), S. 425–435. DOI: 10.1097/MPA.0b013e3181c15963.
- Deubler, Sabrina (2016): The role of the epigenetic remodeller RING1b in pancreatic carcinogenesis. Unpublished master's thesis, Fakultät für Chemie, Technische Universität München, Munich, Germany.
- Diaferia, Giuseppe R., Balestrieri, Chiara, Prosperini, Elena, Nicoli, Paola, Spaggiari, Paola, Zerbi, Alessandro, Natoli, Gioacchino (2016): Dissection of transcriptional and cis-regulatory control of differentiation in human pancreatic cancer. In: *The EMBO journal* 35 (6), S. 595–617. DOI: 10.15252/emj.201592404.
- Duell, Eric J. (2012): Epidemiology and potential mechanisms of tobacco smoking and heavy alcohol consumption in pancreatic cancer. In: *Molecular carcinogenesis* 51 (1), S. 40–52. DOI: 10.1002/mc.20786.
- Eser, S., Schnieke, A., Schneider, G., Saur, D. (2014): Oncogenic KRAS signalling in pancreatic cancer. In: *British journal of cancer* 111 (5), S. 817–822. DOI: 10.1038/bjc.2014.215.
- European Study Group on Cystic Tumours of the Pancreas (2018): European evidence-based guidelines on pancreatic cystic neoplasms. In: *Gut* 67 (5), S. 789–804. DOI: 10.1136/gutjnl-2018-316027.
- Farmer, Hannah, McCabe, Nuala, Lord, Christopher J., Tutt, Andrew N. J., Johnson, Damian A., Richardson, Tobias B. et al. (2005): Targeting the DNA repair defect in BRCA mutant cells as a therapeutic strategy. In: *Nature* 434 (7035), S. 917–921. DOI: 10.1038/nature03445.
- Ferlay J, Ervik M, Lam F, Colombet M, Mery L, Piñeros M, Znaor A, Soerjomataram I, Bray F (2020). Global Cancer Observatory: Cancer Today. Lyon, France: International Agency for Research on Cancer. Available from: <https://gco.iarc.fr/today>, accessed [16 February 2022].

- Flavahan, William A., Gaskell, Elizabeth, Bernstein, Bradley E. (2017): Epigenetic plasticity and the hallmarks of cancer. In: *Science (New York, N.Y.)* 357 (6348). DOI: 10.1126/science.aal2380.
- Fu, Chih-Yuan, Yeh, Chun-Nan, Hsu, Jun-Te, Jan, Yi-Yin, Hwang, Tsann-Long (2007): Timing of mortality in severe acute pancreatitis: experience from 643 patients. In: *World journal of gastroenterology* 13 (13), S. 1966–1969. DOI: 10.3748/wjg.v13.i13.1966.
- Fuks, Francois, Hurd, Paul J., Wolf, Daniel, Nan, Xincheng, Bird, Adrian P., Kouzarides, Tony (2003): The methyl-CpG-binding protein MeCP2 links DNA methylation to histone methylation. In: *The Journal of biological chemistry* 278 (6), S. 4035–4040. DOI: 10.1074/jbc.M210256200.
- Giardiello, F. M., Brensinger, J. D., Tersmette, A. C., Goodman, S. N., Petersen, G. M., Booker, S. V. et al. (2000): Very high risk of cancer in familial Peutz-Jeghers syndrome. In: *Gastroenterology* 119 (6), S. 1447–1453. DOI: 10.1053/gast.2000.20228.
- Golan, Talia, Hammel, Pascal, Reni, Michele, van Cutsem, Eric, Macarulla, Teresa, Hall, Michael J. et al. (2019): Maintenance Olaparib for Germline BRCA-Mutated Metastatic Pancreatic Cancer. In: *The New England journal of medicine* 381 (4), S. 317–327. DOI: 10.1056/NEJMoa1903387.
- Goodspeed, Andrew, Heiser, Laura M., Gray, Joe W., Costello, James C. (2016): Tumor-Derived Cell Lines as Molecular Models of Cancer Pharmacogenomics. In: *Molecular cancer research : MCR* 14 (1), S. 3–13. DOI: 10.1158/1541-7786.MCR-15-0189.
- Guerra, Carmen, Schuhmacher, Alberto J., Cañamero, Marta, Grippo, Paul J., Verdaguer, Lena, Pérez-Gallego, Lucía et al. (2007): Chronic pancreatitis is essential for induction of pancreatic ductal adenocarcinoma by K-Ras oncogenes in adult mice. In: *Cancer cell* 11 (3), S. 291–302. DOI: 10.1016/j.ccr.2007.01.012.
- Halangk, W., Lerch, M. M., Brandt-Nedele, B., Roth, W., Ruthenbueger, M., Reinheckel, T. et al. (2000): Role of cathepsin B in intracellular trypsinogen activation and the onset of acute pancreatitis. In: *The Journal of clinical investigation* 106 (6), S. 773–781. DOI: 10.1172/JCI9411.
- Hald, Jacob, Hjorth, J. Peter, German, Michael S., Madsen, Ole D., Serup, Palle, Jensen, Jan (2003): Activated Notch1 prevents differentiation of pancreatic acinar cells and attenuate endocrine development. In: *Developmental biology* 260 (2), S. 426–437. DOI: 10.1016/s0012-1606(03)00326-9.
- Hayflick, L., Moorhead, P. S. (1961): The serial cultivation of human diploid cell strains. In: *Experimental cell research* 25, S. 585–621. DOI: 10.1016/0014-4827(61)90192-6.
- Hebrok, Matthias (2003): Hedgehog signaling in pancreas development. In: *Mechanisms of development* 120 (1), S. 45–57.
- Henry, Brandon Michael, Skinningsrud, Bendik, Saganiak, Karolina, Pękala, Przemysław A., Walocha, Jerzy A., Tomaszewski, Krzysztof A. (2019): Development of the human pancreas and its vasculature - An integrated review covering anatomical, embryological, histological, and molecular aspects. In: *Annals of anatomy = Anatomischer Anzeiger : official organ of the Anatomische Gesellschaft* 221, S. 115–124. DOI: 10.1016/j.aanat.2018.09.008.
- Hezel, Aram F., Kimmelman, Alec C., Stanger, Ben Z., Bardeesy, Nabeel, DePinho, Ronald A. (2006): Genetics and biology of pancreatic ductal adenocarcinoma. In: *Genes Dev.* 20 (10), S. 1218–1249. DOI: 10.1101/gad.1415606.
- Hildegard M. Schuller (2002): Mechanisms of smoking-related lung and pancreatic adenocarcinoma development. In: *Nat Rev Cancer* 2 (6), S. 455–463. DOI: 10.1038/nrc824.

- Hingorani, Sunil R., Petricoin, Emanuel F., Maitra, Anirban, Rajapakse, Vinodh, King, Catrina, Jacobetz, Michael A. et al. (2003): Preinvasive and invasive ductal pancreatic cancer and its early detection in the mouse. In: *Cancer cell* 4 (6), S. 437–450.
- Hruban, Ralph H., Maitra, Anirban, Goggins, Michael (2008): Update on pancreatic intraepithelial neoplasia. In: *International journal of clinical and experimental pathology* 1 (4), S. 306–316.
- Hsu, Patrick D., Lander, Eric S., Zhang, Feng (2014): Development and applications of CRISPR-Cas9 for genome engineering. In: *Cell* 157 (6), S. 1262–1278. DOI: 10.1016/j.cell.2014.05.010.
- Hyun, Kwangbeom, Jeon, Jongcheol, Park, Kihyun, Kim, Jaehoon (2017): Writing, erasing and reading histone lysine methylations. In: *Experimental & molecular medicine* 49 (4), e324. DOI: 10.1038/emm.2017.11.
- Jennings, Rachel E., Berry, Andrew A., Strutt, James P., Gerrard, David T., Hanley, Neil A. (2015): Human pancreas development. In: *Development (Cambridge, England)* 142 (18), S. 3126–3137. DOI: 10.1242/dev.120063.
- Jensen, Jan Nygaard, Cameron, Erin, Garay, Maria Veronica R., Starkey, Thomas W., Gianani, Roberto, Jensen, Jan (2005): Recapitulation of elements of embryonic development in adult mouse pancreatic regeneration. In: *Gastroenterology* 128 (3), S. 728–741. DOI: 10.1053/j.gastro.2004.12.008.
- Jinek, Martin, Chylinski, Krzysztof, Fonfara, Ines, Hauer, Michael, Doudna, Jennifer A., Charpentier, Emmanuelle (2012): A programmable dual-RNA-guided DNA endonuclease in adaptive bacterial immunity. In: *Science (New York, N.Y.)* 337 (6096), S. 816–821. DOI: 10.1126/science.1225829.
- Johnson, C. D., Besselink, M. G., Carter, R. (2014): Acute pancreatitis. In: *BMJ (Clinical research ed.)* 349, g4859. DOI: 10.1136/bmj.g4859.
- Jones, Siân, Zhang, Xiaosong, Parsons, D. Williams, Lin, Jimmy Cheng-Ho, Leary, Rebecca J., Angenendt, Philipp et al. (2008): Core signaling pathways in human pancreatic cancers revealed by global genomic analyses. In: *Science* 321 (5897), S. 1801–1806. DOI: 10.1126/science.1164368.
- Josling, Gabrielle A., Selvarajah, Shamista A., Petter, Michaela, Duffy, Michael F. (2012): The Role of Bromodomain Proteins in Regulating Gene Expression. In: *Genes* 3 (2), S. 320–343. DOI: 10.3390/genes3020320.
- JS, Damrauer, KA, Hoadley, DD, Chism, C, Fan, CJ, Tiganelli, SE, Wobker et al. (2014): Intrinsic Subtypes of High-Grade Bladder Cancer Reflect the Hallmarks of Breast Cancer Biology. In: *Proceedings of the National Academy of Sciences of the United States of America* 111 (8). DOI: 10.1073/pnas.1318376111.
- Jubierre, Luz, Jiménez, Carlos, Rovira, Eric, Soriano, Aroa, Sábado, Constantino, Gros, Luis et al. (2018): Targeting of epigenetic regulators in neuroblastoma. In: *Experimental & molecular medicine* 50 (4), S. 51. DOI: 10.1038/s12276-018-0077-2.
- Kawaguchi, Yoshiya, Cooper, Bonnie, Gannon, Maureen, Ray, Michael, MacDonald, Raymond J., Wright, Christopher V. E. (2002): The role of the transcriptional regulator Ptf1a in converting intestinal to pancreatic progenitors. In: *Nature genetics* 32 (1), S. 128–134. DOI: 10.1038/ng959.
- Kim, Joo Y., Hong, Seung-Mo (2018): Precursor Lesions of Pancreatic Cancer. In: *Oncology research and treatment* 41 (10), S. 603–610. DOI: 10.1159/000493554.

- Kleeff, Jorg, Korc, Murray, Apte, Minoti, La Vecchia, Carlo, Johnson, Colin D., Biankin, Andrew V. et al. (2016): Pancreatic cancer. In: Nature reviews. Disease primers 2, S. 16022. DOI: 10.1038/nrdp.2016.22.
- Knudson, A. G. (1971): Mutation and cancer: statistical study of retinoblastoma. In: Proceedings of the National Academy of Sciences of the United States of America 68 (4), S. 820–823. DOI: 10.1073/pnas.68.4.820.
- Kunovsky, Lumir, Tesarikova, Pavla, Kala, Zdenek, Kroupa, Radek, Kysela, Petr, Dolina, Jiri, Trna, Jan (2018): The Use of Biomarkers in Early Diagnostics of Pancreatic Cancer. In: Canadian journal of gastroenterology & hepatology 2018, S. 5389820. DOI: 10.1155/2018/5389820.
- Labun, Kornel, Montague, Tessa G., Gagnon, James A., Thyme, Summer B., Valen, Eivind (2016): CHOPCHOP v2: a web tool for the next generation of CRISPR genome engineering. In: Nucleic acids research 44 (W1), W272-6. DOI: 10.1093/nar/gkw398.
- Lambert, Aurélien, Schwarz, Lilian, Borbath, Ivan, Henry, Aline, van Laethem, Jean-Luc, Malka, David et al. (2019): An update on treatment options for pancreatic adenocarcinoma. In: Therapeutic advances in medical oncology 11, 1758835919875568. DOI: 10.1177/1758835919875568.
- Lane, D. P. (1992): Cancer. p53, guardian of the genome. In: Nature 358 (6381), S. 15–16. DOI: 10.1038/358015a0.
- Lankisch, Paul Georg, Apte, Minoti, Banks, Peter A. (2015): Acute pancreatitis. In: Lancet (London, England) 386 (9988), S. 85–96. DOI: 10.1016/S0140-6736(14)60649-8.
- Larsson, Susanna C., Orsini, Nicola, Wolk, Alicja (2007): Body mass index and pancreatic cancer risk: A meta-analysis of prospective studies. In: International journal of cancer 120 (9), S. 1993–1998. DOI: 10.1002/ijc.22535.
- Le, Dung T., Durham, Jennifer N., Smith, Kellie N., Wang, Hao, Bartlett, Bjarne R., Aulakh, Laveet K. et al. (2017): Mismatch repair deficiency predicts response of solid tumors to PD-1 blockade. In: Science (New York, N.Y.) 357 (6349), S. 409–413. DOI: 10.1126/science.aan6733.
- Leitlinienprogramm Onkologie (Deutsche Krebsgesellschaft, Deutsche Krebshilfe, AWMF): S3-Leitlinie Exokrines Pankreaskarzinom, Kurzversion 2.0, 2021 , AWMF Registernummer: 032-010OL <https://www.leitlinienprogramm-onkologie.de/leitlinien/pankreaskarzinom/>, (Zugriff am: 11.03.2022)
- Lenkiewicz, Elizabeth, Malasi, Smriti, Hogenson, Tara L., Flores, Luis F., Barham, Whitney, Phillips, William J. et al. (2020): Genomic and Epigenomic Landscaping Defines New Therapeutic Targets for Adenosquamous Carcinoma of the Pancreas. In: Cancer research 80 (20), S. 4324–4334. DOI: 10.1158/0008-5472.CAN-20-0078.
- Levine, Arnold J., Oren, Moshe (2009): The first 30 years of p53: growing ever more complex. In: Nature reviews. Cancer 9 (10), S. 749–758. DOI: 10.1038/nrc2723.
- Li, Long-Cheng, Dahiya, Rajvir (2002): MethPrimer: designing primers for methylation PCRs. In: Bioinformatics (Oxford, England) 18 (11), S. 1427–1431.
- Liu, F. (2001): SMAD4/DPC4 and pancreatic cancer survival. Commentary re: M. Tascilar et al., The SMAD4 protein and prognosis of pancreatic ductal adenocarcinoma. Clin. Cancer Res., 7: 4115-4121, 2001. In: Clinical cancer research : an official journal of the American Association for Cancer Research 7 (12), S. 3853–3856.
- Löhr, Matthias, Klöppel, Günter, Maisonneuve, Patrick, Lowenfels, Albert B., Lüttges, Jutta (2005): Frequency of K-ras mutations in pancreatic intraductal neoplasias associated with

- pancreatic ductal adenocarcinoma and chronic pancreatitis: a meta-analysis. In: *Neoplasia* (New York, N.Y.) 7 (1), S. 17–23. DOI: 10.1593/neo.04445.
- Lomberk, Gwen, Blum, Yuna, Nicolle, Rémy, Nair, Asha, Gaonkar, Krutika Satish, Marisa, Laetitia et al. (2018): Distinct epigenetic landscapes underlie the pathobiology of pancreatic cancer subtypes. In: *Nature communications* 9 (1), S. 1978. DOI: 10.1038/s41467-018-04383-6.
- Lomberk, Gwen A., Iovanna, Juan, Urrutia, Raul (2016): The promise of epigenomic therapeutics in pancreatic cancer. In: *Epigenomics* 8 (6), S. 831–842. DOI: 10.2217/epi-2015-0016.
- Longnecker, Daniel S. (2014): *The Pancreapedia: Exocrine Pancreas Knowledge Base. Anatomy and Histology of the Pancreas.*
- Lowenfels, A. B., Maisonneuve, P., Cavallini, G., Ammann, R. W., Lankisch, P. G., Andersen, J. R. et al. (1993): Pancreatitis and the risk of pancreatic cancer. International Pancreatitis Study Group. In: *The New England journal of medicine* 328 (20), S. 1433–1437. DOI: 10.1056/NEJM199305203282001.
- Lowenfels, A. B., Maisonneuve, P., Dimagno, E. P., Elitsur, Y., Gates, L. K., Perrault, J., Whitcomb, D. C. (1997): Hereditary pancreatitis and the risk of pancreatic cancer. International Hereditary Pancreatitis Study Group. In: *Journal of the National Cancer Institute* 89 (6), S. 442–446. DOI: 10.1093/jnci/89.6.442.
- Lynch, Shannon M., Vrieling, Alina, Lubin, Jay H., Kraft, Peter, Mendelsohn, Julie B., Hartge, Patricia et al. (2009): Cigarette smoking and pancreatic cancer: a pooled analysis from the pancreatic cancer cohort consortium. In: *American journal of epidemiology* 170 (4), S. 403–413. DOI: 10.1093/aje/kwp134.
- Lynch, Thomas J., Bell, Daphne W., Sordella, Raffaella, Gurubhagavatula, Sarada, Okimoto, Ross A., Brannigan, Brian W. et al. (2004): Activating mutations in the epidermal growth factor receptor underlying responsiveness of non-small-cell lung cancer to gefitinib. In: *The New England journal of medicine* 350 (21), S. 2129–2139. DOI: 10.1056/NEJMoa040938.
- Maisonneuve, P., Lowenfels, A. B., Müllhaupt, B., Cavallini, G., Lankisch, P. G., Andersen, J. R. et al. (2005): Cigarette smoking accelerates progression of alcoholic chronic pancreatitis. In: *Gut* 54 (4), S. 510–514. DOI: 10.1136/gut.2004.039263.
- Maisonneuve, Patrick, Lowenfels, Albert B. (2010): Epidemiology of pancreatic cancer: an update. In: *Digestive diseases (Basel, Switzerland)* 28 (4-5), S. 645–656. DOI: 10.1159/000320068.
- Martínez-Romero, Carles, Rooman, Ilse, Skoudy, Anouchka, Guerra, Carmen, Molero, Xavier, González, Ana et al. (2009): The epigenetic regulators Bmi1 and Ring1B are differentially regulated in pancreatitis and pancreatic ductal adenocarcinoma. In: *The Journal of pathology* 219 (2), S. 205–213. DOI: 10.1002/path.2585.
- Massagué, J., Blain, S. W., Lo, R. S. (2000): TGFbeta signaling in growth control, cancer, and heritable disorders. In: *Cell* 103 (2), S. 295–309. DOI: 10.1016/s0092-8674(00)00121-5.
- Masui, Toshihiko, Long, Qiaoming, Beres, Thomas M., Magnuson, Mark A., MacDonald, Raymond J. (2007): Early pancreatic development requires the vertebrate Suppressor of Hairless (RBPJ) in the PTF1 bHLH complex. In: *Genes & development* 21 (20), S. 2629–2643. DOI: 10.1101/gad.1575207.
- Midha, Shallu, Chawla, Saurabh, Garg, Pramod Kumar (2016): Modifiable and non-modifiable risk factors for pancreatic cancer: A review. In: *Cancer letters* 381 (1), S. 269–277. DOI: 10.1016/j.canlet.2016.07.022.

- Miller, Jeffrey C., Tan, Siyuan, Qiao, Guijuan, Barlow, Kyle A., Wang, Jianbin, Xia, Danny F. et al. (2011): A TALE nuclease architecture for efficient genome editing. In: *Nature biotechnology* 29 (2), S. 143–148. DOI: 10.1038/nbt.1755.
- Millward, Michael, Price, Timothy, Townsend, Amanda, Sweeney, Christopher, Spencer, Andrew, Sukumaran, Shawgi et al. (2012): Phase 1 clinical trial of the novel proteasome inhibitor marizomib with the histone deacetylase inhibitor Vorinostat in patients with melanoma, pancreatic and lung cancer based on in vitro assessments of the combination. In: *Investigational new drugs* 30 (6), S. 2303–2317. DOI: 10.1007/s10637-011-9766-6.
- Mishra, Nitish Kumar, Guda, Chittibabu (2017): Genome-wide DNA methylation analysis reveals molecular subtypes of pancreatic cancer. In: *Oncotarget* 8 (17), S. 28990–29012. DOI: 10.18632/oncotarget.15993.
- Moffitt, Richard A., Marayati, Raoud, Flate, Elizabeth L., Volmar, Keith E., Loeza, S. Gabriela Herrera, Hoadley, Katherine A. et al. (2015): Virtual microdissection identifies distinct tumor- and stroma-specific subtypes of pancreatic ductal adenocarcinoma. In: *Nature genetics* 47 (10), S. 1168–1178. DOI: 10.1038/ng.3398.
- Mojica, Francisco J. M., Díez-Villaseñor, César, García-Martínez, Jesús, Soria, Elena (2005): Intervening sequences of regularly spaced prokaryotic repeats derive from foreign genetic elements. In: *Journal of molecular evolution* 60 (2), S. 174–182. DOI: 10.1007/s00239-004-0046-3.
- Montague, Tessa G., Cruz, José M., Gagnon, James A., Church, George M., Valen, Eivind (2014): CHOPCHOP: a CRISPR/Cas9 and TALEN web tool for genome editing. In: *Nucleic acids research* 42 (Web Server issue), W401-7. DOI: 10.1093/nar/gku410.
- Murtaugh, L. Charles (2007): Pancreas and beta-cell development: from the actual to the possible. In: *Development (Cambridge, England)* 134 (3), S. 427–438. DOI: 10.1242/dev.02770.
- Nan, X., Ng, H. H., Johnson, C. A., Laherty, C. D., Turner, B. M., Eisenman, R. N., Bird, A. (1998): Transcriptional repression by the methyl-CpG-binding protein MeCP2 involves a histone deacetylase complex. In: *Nature* 393 (6683), S. 386–389. DOI: 10.1038/30764.
- Neoptolemos, John P., Kleeff, Jörg, Michl, Patrick, Costello, Eithne, Greenhalf, William, Palmer, Daniel H. (2018): Therapeutic developments in pancreatic cancer: current and future perspectives. In: *Nature reviews. Gastroenterology & hepatology* 15 (6), S. 333–348. DOI: 10.1038/s41575-018-0005-x.
- Neoptolemos, John P.; Palmer, Daniel H.; Ghaneh, Paula; Psarelli, Eftychia E.; Valle, Juan W.; Halloran, Christopher M. et al. (2017): Comparison of adjuvant gemcitabine and capecitabine with gemcitabine monotherapy in patients with resected pancreatic cancer (ESPAC-4): a multicentre, open-label, randomised, phase 3 trial. In: *The Lancet* 389 (10073), S. 1011–1024. DOI: 10.1016/S0140-6736(16)32409-6.
- Neoptolemos, John P., Stocken, Deborah D., Bassi, Claudio, Ghaneh, Paula, Cunningham, David, Goldstein, David et al. (2010): Adjuvant chemotherapy with fluorouracil plus folinic acid vs Gemcitabine following pancreatic cancer resection: a randomized controlled trial. In: *JAMA* 304 (10), S. 1073–1081. DOI: 10.1001/jama.2010.1275.
- Nicolle, Rémy, Blum, Yuna, Marisa, Laetitia, Loncle, Celine, Gayet, Odile, Moutardier, Vincent et al. (2017): Pancreatic Adenocarcinoma Therapeutic Targets Revealed by Tumor-Stroma Cross-Talk Analyses in Patient-Derived Xenografts. In: *Cell reports* 21 (9), S. 2458–2470. DOI: 10.1016/j.celrep.2017.11.003.

- Ohtani, Naoko, Yamakoshi, Kimi, Takahashi, Akiko, Hara, Eiji (2004): The p16INK4a-RB pathway: molecular link between cellular senescence and tumor suppression. In: *The journal of medical investigation* : JMI 51 (3-4), S. 146–153.
- Olivier, Magali, Hollstein, Monica, Hainaut, Pierre (2010): TP53 mutations in human cancers: origins, consequences, and clinical use. In: *Cold Spring Harbor perspectives in biology* 2 (1), a001008. DOI: 10.1101/cshperspect.a001008.
- Oren, Moshe, Rotter, Varda (2010): Mutant p53 gain-of-function in cancer. In: *Cold Spring Harbor perspectives in biology* 2 (2), a001107. DOI: 10.1101/cshperspect.a001107.
- Oshima, Minoru, Okano, Keiichi, Muraki, Shinobu, Haba, Reiji, Maeba, Takashi, Suzuki, Yasuyuki, Yachida, Shinichi (2013): Immunohistochemically detected expression of 3 major genes (CDKN2A/p16, TP53, and SMAD4/DPC4) strongly predicts survival in patients with resectable pancreatic cancer. In: *Annals of surgery* 258 (2), S. 336–346. DOI: 10.1097/SLA.0b013e3182827a65.
- Ougolkov, Andrei V., Bilim, Vladimir N., Billadeau, Daniel D. (2008): Regulation of pancreatic tumor cell proliferation and chemoresistance by the histone methyltransferase enhancer of zeste homologue 2. In: *Clinical cancer research : an official journal of the American Association for Cancer Research* 14 (21), S. 6790–6796. DOI: 10.1158/1078-0432.CCR-08-1013.
- Pan, Fong Cheng, Wright, Chris (2011): Pancreas organogenesis: from bud to plexus to gland. In: *Developmental dynamics : an official publication of the American Association of Anatomists* 240 (3), S. 530–565. DOI: 10.1002/dvdy.22584.
- Pandol, Stephen J. (2010): *The Exocrine Pancreas*. San Rafael (CA).
- Park, Sang Eun, Yi, Hye Jin, Suh, Nayoung, Park, Yun-Yong, Koh, Jae-Young, Jeong, Seong-Yun et al. (2016): Inhibition of EHMT2/G9a epigenetically increases the transcription of Beclin-1 via an increase in ROS and activation of NF-κB. In: *Oncotarget* 7 (26), S. 39796–39808. DOI: 10.18632/oncotarget.9290.
- Patil, Shilpa, Steuber, Benjamin, Kopp, Waltraut, Kari, Vijayalakshmi, Urbach, Laura, Wang, Xin et al. (2020): EZH2 Regulates Pancreatic Cancer Subtype Identity and Tumor Progression via Transcriptional Repression of GATA6. In: *Cancer research* 80 (21), S. 4620–4632. DOI: 10.1158/0008-5472.CAN-20-0672.
- Pichlmeier S., Regel I. (2020) Epigenetic Targeting. In: Michalski C., Rosendahl J., Michl P., Kleeff J. (eds) *Translational Pancreatic Cancer Research. Molecular and Translational Medicine*. Humana, Cham. [https://doi.org/10.1007/978-3-030-49476-6\\_12](https://doi.org/10.1007/978-3-030-49476-6_12)
- Pishvaian, Michael J., Bender, Robert J., Halverson, David, Rahib, Lola, Hendifar, Andrew E., Mikhail, Sameh et al. (2018): Molecular Profiling of Patients with Pancreatic Cancer: Initial Results from the Know Your Tumor Initiative. In: *Clinical cancer research : an official journal of the American Association for Cancer Research* 24 (20), S. 5018–5027. DOI: 10.1158/1078-0432.CCR-18-0531.
- Prévo, Pierre-Paul, Simion, Alexandru, Grimont, Adrien, Colletti, Marta, Khalaileh, Abed, van den Steen, Géraldine et al. (2012): Role of the ductal transcription factors HNF6 and Sox9 in pancreatic acinar-to-ductal metaplasia. In: *Gut* 61 (12), S. 1723–1732. DOI: 10.1136/gutjnl-2011-300266.
- Rahib, Lola, Smith, Benjamin D., Aizenberg, Rhonda, Rosenzweig, Allison B., Fleshman, Julie M., Matrisian, Lynn M. (2014): Projecting cancer incidence and deaths to 2030: the unexpected burden of thyroid, liver, and pancreas cancers in the United States. In: *Cancer research* 74 (11), S. 2913–2921. DOI: 10.1158/0008-5472.CAN-14-0155.

- Ramsey, Mitchell L., Conwell, Darwin L., Hart, Phil A.: Complications of Chronic Pancreatitis. In: *Dig Dis Sci* 62 (7), S. 1745–1750. DOI: 10.1007/s10620-017-4518-x.
- Ran, F. Ann, Hsu, Patrick D., Wright, Jason, Agarwala, Vineeta, Scott, David A., Zhang, Feng (2013b): Genome engineering using the CRISPR-Cas9 system. In: *Nature protocols* 8 (11), S. 2281–2308. DOI: 10.1038/nprot.2013.143.
- Rawla, Prashanth, Sunkara, Tagore, Gaduputi, Vinaya (2019): Epidemiology of Pancreatic Cancer: Global Trends, Etiology and Risk Factors. In: *World Journal of Oncology* 10 (1), S. 10–27. DOI: 10.14740/wjon1166.
- Rebours, Vinciane, Gaujoux, Sébastien, d'Assignies, Gaspard, Sauvanet, Alain, Ruzniewski, Philippe, Lévy, Philippe et al. (2015): Obesity and Fatty Pancreatic Infiltration Are Risk Factors for Pancreatic Precancerous Lesions (PanIN). In: *Clinical cancer research : an official journal of the American Association for Cancer Research* 21 (15), S. 3522–3528. DOI: 10.1158/1078-0432.CCR-14-2385.
- Regel, Ivonne, Hausmann, Simone, Benitz, Simone, Esposito, Irene, Kleeff, Jörg (2016): Pathobiology of pancreatic cancer: implications on therapy. In: *Expert review of anticancer therapy* 16 (2), S. 219–227. DOI: 10.1586/14737140.2016.1129276.
- Regel, Ivonne, Mayerle, Julia, Mahajan, Ujjwal Mukund (2020): Current Strategies and Future Perspectives for Precision Medicine in Pancreatic Cancer. In: *Cancers* 12 (4). DOI: 10.3390/cancers12041024.
- Reichert, Maximilian, Rustgi, Anil K. (2011): Pancreatic ductal cells in development, regeneration, and neoplasia. In: *The Journal of clinical investigation* 121 (12), S. 4572–4578. DOI: 10.1172/JCI57131.
- Rivlin, Noa, Brosh, Ran, Oren, Moshe, Rotter, Varda (2011): Mutations in the p53 Tumor Suppressor Gene: Important Milestones at the Various Steps of Tumorigenesis. In: *Genes & cancer* 2 (4), S. 466–474. DOI: 10.1177/1947601911408889.
- Rizzo, R. J., Szucs, R. A., Turner, M. A. (1995): Congenital abnormalities of the pancreas and biliary tree in adults. In: *Radiographics : a review publication of the Radiological Society of North America, Inc* 15 (1), 49–68, quiz 147–8. DOI: 10.1148/radiographics.15.1.7899613.
- Rozenblum, E., Schutte, M., Goggins, M., Hahn, S. A., Panzer, S., Zahurak, M. et al. (1997): Tumor-suppressive pathways in pancreatic carcinoma. In: *Cancer research* 57 (9), S. 1731–1734.
- Sakuma, Tetsushi, Nishikawa, Ayami, Kume, Satoshi, Chayama, Kazuaki, Yamamoto, Takashi (2014): Multiplex genome engineering in human cells using all-in-one CRISPR/Cas9 vector system. In: *Scientific reports* 4, S. 5400. DOI: 10.1038/srep05400.
- Samanta, Debangshu, Datta, Pran K. (2012): Alterations in the Smad pathway in human cancers. In: *Frontiers in bioscience (Landmark edition)* 17, S. 1281–1293.
- Sander, Jeffrey D., Joung, J. Keith (2014): CRISPR-Cas systems for editing, regulating and targeting genomes. In: *Nature biotechnology* 32 (4), S. 347–355. DOI: 10.1038/nbt.2842.
- Sato, Norihiro, Fukushima, Noriyoshi, Hruban, Ralph H., Goggins, Michael (2008): CpG island methylation profile of pancreatic intraepithelial neoplasia. In: *Modern pathology : an official journal of the United States and Canadian Academy of Pathology, Inc* 21 (3), S. 238–244. DOI: 10.1038/modpathol.3800991.
- Scheffzek, K., Ahmadian, M. R., Kabsch, W., Wiesmüller, L., Lautwein, A., Schmitz, F., Wittinghofer, A. (1997): The Ras-RasGAP complex: structural basis for GTPase activation and its loss in

- oncogenic Ras mutants. In: *Science (New York, N.Y.)* 277 (5324), S. 333–338. DOI: 10.1126/science.277.5324.333.
- Scherer, W. F., Syverton, J. T., Gey, G. O. (1953): Studies on the propagation in vitro of poliomyelitis viruses. IV. Viral multiplication in a stable strain of human malignant epithelial cells (strain HeLa) derived from an epidermoid carcinoma of the cervix. In: *The Journal of experimental medicine* 97 (5), S. 695–710. DOI: 10.1084/jem.97.5.695.
- Schneider, Günter, Krämer, Oliver H., Schmid, Roland M., Saur, Dieter (2011): Acetylation as a transcriptional control mechanism-HDACs and HATs in pancreatic ductal adenocarcinoma. In: *Journal of gastrointestinal cancer* 42 (2), S. 85–92. DOI: 10.1007/s12029-011-9257-1.
- Schutte, M., Hruban, R. H., Geradts, J., Maynard, R., Hilgers, W., Rabindran, S. K. et al. (1997): Abrogation of the Rb/p16 tumor-suppressive pathway in virtually all pancreatic carcinomas. In: *Cancer research* 57 (15), S. 3126–3130.
- Seymour, Philip A., Freude, Kristine K., Tran, Man N., Mayes, Erin E., Jensen, Jan, Kist, Ralf et al. (2007): SOX9 is required for maintenance of the pancreatic progenitor cell pool. In: *Proceedings of the National Academy of Sciences of the United States of America* 104 (6), S. 1865–1870. DOI: 10.1073/pnas.0609217104.
- Siân Jones, Xiaosong Zhang, D. Williams Parsons, Jimmy Cheng-Ho Lin, Rebecca J. Leary, Philipp Angenendt et al. (2008): Core Signaling Pathways in Human Pancreatic Cancers Revealed by Global Genomic Analyses. In: *Science* 321 (5897), S. 1801–1806. DOI: 10.1126/science.1164368.
- Slamon, D. J., Leyland-Jones, B., Shak, S., Fuchs, H., Paton, V., Bajamonde, A. et al. (2001): Use of chemotherapy plus a monoclonal antibody against HER2 for metastatic breast cancer that overexpresses HER2. In: *The New England journal of medicine* 344 (11), S. 783–792. DOI: 10.1056/NEJM200103153441101.
- Somerville, Tim D. D., Xu, Yali, Miyabayashi, Koji, Tiriach, Hervé, Cleary, Cristian R., Maia-Silva, Diogo et al. (2018): TP63-Mediated Enhancer Reprogramming Drives the Squamous Subtype of Pancreatic Ductal Adenocarcinoma. In: *Cell reports* 25 (7), 1741-1755.e7. DOI: 10.1016/j.celrep.2018.10.051.
- Sonoyama, Takayuki, Sakai, Akiko, Mita, Yuichiro, Yasuda, Yukiko, Kawamoto, Hirofumi, Yagi, Takahito et al. (2011): TP53 codon 72 polymorphism is associated with pancreatic cancer risk in males, smokers and drinkers. In: *Molecular medicine reports* 4 (3), S. 489–495. DOI: 10.3892/mmr.2011.449.
- Sorek, Rotem, Kunin, Victor, Hugenholtz, Philip (2008): CRISPR--a widespread system that provides acquired resistance against phages in bacteria and archaea. In: *Nature reviews. Microbiology* 6 (3), S. 181–186. DOI: 10.1038/nrmicro1793.
- Stanger, Ben Z., Hebrok, Matthias (2013): Control of cell identity in pancreas development and regeneration. In: *Gastroenterology* 144 (6), S. 1170–1179. DOI: 10.1053/j.gastro.2013.01.074.
- Stathis, Anastasios, Moore, Malcolm J. (2010): Advanced pancreatic carcinoma: current treatment and future challenges. In: *Nature reviews. Clinical oncology* 7 (3), S. 163–172. DOI: 10.1038/nrclinonc.2009.236.
- Stone, Meredith L., Chiappinelli, Katherine B., Li, Huili, Murphy, Lauren M., Travers, Meghan E., Topper, Michael J. et al. (2017): Epigenetic therapy activates type I interferon signaling in murine ovarian cancer to reduce immunosuppression and tumor burden. In: *Proceedings of*

the National Academy of Sciences of the United States of America 114 (51), E10981-E10990. DOI: 10.1073/pnas.1712514114.

- Suker, Mustafa, Beumer, Berend R., Sadot, Eran, Marthey, Lysiane, Faris, Jason E., Mellon, Eric A. et al. (2016): FOLFIRINOX for locally advanced pancreatic cancer: a systematic review and patient-level meta-analysis. In: *The Lancet Oncology* 17 (6), S. 801–810. DOI: 10.1016/S1470-2045(16)00172-8.
- Sung, Hyuna, Ferlay, Jacques, Siegel, Rebecca L., Laversanne, Mathieu, Soerjomataram, Isabelle, Jemal, Ahmedin, Bray, Freddie (2021): Global Cancer Statistics 2020: GLOBOCAN Estimates of Incidence and Mortality Worldwide for 36 Cancers in 185 Countries. In: *CA: a cancer journal for clinicians* 71 (3), S. 209–249. DOI: 10.3322/caac.21660.
- Tempero, Margaret A. (2019): NCCN Guidelines Updates: Pancreatic Cancer. In: *Journal of the National Comprehensive Cancer Network : JNCCN* 17 (5.5), S. 603–605. DOI: 10.6004/jnccn.2019.5007.
- Tenner, Scott, Baillie, John, DeWitt, John, Vege, Santhi Swaroop (2013): American College of Gastroenterology guideline: management of acute pancreatitis. In: *The American journal of gastroenterology* 108 (9), 1400-15, 1416. DOI: 10.1038/ajg.2013.218.
- Thompson, Michael J., Rubbi, Liudmilla, Dawson, David W., Donahue, Timothy R., Pellegrini, Matteo (2015): Pancreatic cancer patient survival correlates with DNA methylation of pancreas development genes. In: *PloS one* 10 (6), e0128814. DOI: 10.1371/journal.pone.0128814.
- Träger, Max M., Dhayat, Sameer A. (2017): Epigenetics of epithelial-to-mesenchymal transition in pancreatic carcinoma. In: *International journal of cancer* 141 (1), S. 24–32. DOI: 10.1002/ijc.30626.
- Tramacere, Irene, Scotti, Lorenza, Jenab, Mazda, Bagnardi, Vincenzo, Bellocco, Rino, Rota, Matteo et al. (2010): Alcohol drinking and pancreatic cancer risk: a meta-analysis of the dose-risk relation. In: *International journal of cancer* 126 (6), S. 1474–1486. DOI: 10.1002/ijc.24936.
- Uomo, G., Rabitti, P. G. (2000): Chronic pancreatitis: relation to acute pancreatitis and pancreatic cancer. In: *Annali italiani di chirurgia* 71 (1), S. 17–21.
- Varley, Katherine E., Gertz, Jason, Bowling, Kevin M., Parker, Stephanie L., Reddy, Timothy E., Pauli-Behn, Florencia et al. (2013): Dynamic DNA methylation across diverse human cell lines and tissues. In: *Genome research* 23 (3), S. 555–567. DOI: 10.1101/gr.147942.112.
- Vasen, H. F., Gruis, N. A., Frants, R. R., van der Velden, P. A., Hille, E. T., Bergman, W. (2000): Risk of developing pancreatic cancer in families with familial atypical multiple mole melanoma associated with a specific 19 deletion of p16 (p16-Leiden). In: *International journal of cancer* 87 (6), S. 809–811.
- Villasenor, Alethia, Chong, Diana C., Henkemeyer, Mark, Cleaver, Ondine (2010): Epithelial dynamics of pancreatic branching morphogenesis. In: *Development (Cambridge, England)* 137 (24), S. 4295–4305. DOI: 10.1242/dev.052993.
- Weinstein, John N. (2012): Drug discovery: Cell lines battle cancer. In: *Nature* 483 (7391), S. 544–545. DOI: 10.1038/483544a.
- Whitcomb, D. C., Gorry, M. C., Preston, R. A., Furey, W., Sossenheimer, M. J., Ulrich, C. D. et al. (1996): Hereditary pancreatitis is caused by a mutation in the cationic trypsinogen gene. In: *Nature genetics* 14 (2), S. 141–145. DOI: 10.1038/ng1096-141.
- Yang, Bin, Zhang, Wei, Zhang, Mengmeng, Wang, Xuhong, Peng, Shengzu, Zhang, Rongsheng (2020): KRT6A Promotes EMT and Cancer Stem Cell Transformation in Lung Adenocarcinoma. In:

Technology in cancer research & treatment 19, 1533033820921248. DOI: 10.1177/1533033820921248.

Yonezawa, Suguru, Higashi, Michiyo, Yamada, Norishige, Goto, Masamichi (2008): Precursor lesions of pancreatic cancer. In: Gut and liver 2 (3), S. 137–154. DOI: 10.5009/gnl.2008.2.3.137.

Zhang, Mang-Li, Lu, Sen, Zhou, Lin, Zheng, Shu-Sen (2008): Correlation between ECT2 gene expression and methylation change of ECT2 promoter region in pancreatic cancer. In: Hepatobiliary & pancreatic diseases international : HBPD INT 7 (5), S. 533–538.

## 9. Appendix

### 9.1. List of tables

Table 1: Specific chemicals and reagents .....	21
Table 2: Kits .....	23
Table 3: Primary antibodies .....	23
Table 4: Secondary antibodies .....	24
Table 5: Enzymes .....	25
Table 6: Inhibitors .....	26
Table 7: Gene expression primer .....	26
Table 8: ChIP primer .....	27
Table 9: MSP primer .....	28
Table 10: sgRNAs .....	28
Table 11: Sequencing primer .....	28
Table 12: Plasmids .....	29
Table 13: Cell lines .....	29
Table 14: Consumption materials .....	29
Table 15: Equipment .....	30
Table 16: Computer applications .....	31
Table 17: Cell culture conditions .....	33
Table 18: PCR program .....	38
Table 19: qRT-PCR program .....	39
Table 20: SDS-PAGE gel preparation .....	41
Table 21: In-cell western analysis parameters .....	43
Table 22: MSP PCR program .....	46

## 9.2. List of figures

Figure 1 Cancer incidence and mortality. ....	1
Figure 2: Acinar-to-ductal metaplasia mediates PDAC development. ....	5
Figure 3: Epigenetic mechanisms. ....	12
Figure 4: Overview of active and repressive histone modifications. ....	15
Figure 5: Structure and working principle of biological and engineered CRISPR/Cas9 systems. ....	19
Figure 6 Multiplex genome engineering. ....	36
Figure 7: Cell lines representing the classical PDAC subtype show high levels of epithelial cell differentiation markers compared to the basal subtype. ....	49
Figure 8: Subtype-specific gene expression is regulated by histone modifications and DNA methylation. ....	50
Figure 9: Epigenetic modifiers show a subtype-specific expression pattern. ....	52
Figure 10: Histone modifications are drivers for epigenetic regulation of differentiation genes. ....	54
Figure 11: Differentiation genes are epigenetically silenced through DNA methylation in the basal subtype. ....	55
Figure 12: Cell survival response to single-drug histone acetylase or histone deacetylase inhibitor treatment is independent of the molecular subtype. ....	57
Figure 13: CRISPR-Cas9 multiplex knockout – Plasmid construction. ....	59
Figure 14: CRISPR-Cas9 multiplex knockout – Transfection efficiency and single-cell clones. ....	61

## Acknowledgements

First of all, I would like to thank **Dr. Ivonne Regel** for initiating and supervising my dissertation project. You truly sparked my interest in epigenetics and always encouraged me to improve and acquire new skills. I feel very blessed to have been able to benefit from your tremendous knowledge and experience in this field of study. Your commitment in the lab is extraordinary and I am very grateful that you always had an open ear for my questions and concerns.

My sincere thank also goes to **Prof. Dr. Julia Mayerle** for supervising my thesis. Your insightful feedback on my presentations in our lab meetings and your experience helped me improve my project and grow my presentation skills.

I would like to thank **Prof. Dr. Roland Kappler** for being my second advisor and for your valuable input and feedback.

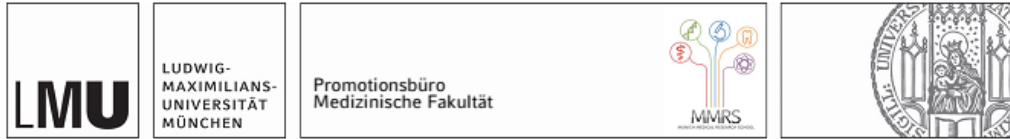
I am very grateful for all of my colleagues who have accompanied me during my time in the lab. I have enjoyed spending time with you in and outside of the lab. My special thank goes to **Dr. Simone Benitz** for teaching me her chromatin-IP protocol, to **Anna Kirmayr** for introducing me to the cell culture work, to **Lisa Fahr** for moving the epigenetic projects forward, to **Jurik Mutter** for supporting me in my everyday struggles, to **Dr. Ujjwal Mukund Mahajan** for your generous technical support and to **Yonggan Xue** and **Xi Li** for your friendship and pleasant company. I also want to thank **Maria Escobar** for helping me get settled in the lab and for your continued work on our project as well as **Simon Gahr** for always hunting down my antibodies in time.

I am very thankful for my dear friend **David Arppe**, who proofread my thesis very attentively and helped me standardize my writing.

I would also like to thank **Dr. Ulrike Szeimies** and **her parents** for introducing me to the field of medicine, for always fostering my scientific interests and for your continued professional and emotional support on my academic journey.

Finally, my deepest gratitude goes towards my **parents** and my sister **Alicia** for always having my back and supporting me in every way possible. You have encouraged me in times of trouble, motivated me to do my best, listened to my concerns and always believed in my success. I truly could not have done it without your unconditional support!

# Affidavit



## Eidesstattliche Versicherung

**Pichlmeier, Svenja**

Name, Vorname

Ich erkläre hiermit an Eides statt,

dass ich die vorliegende Dissertation mit dem Titel

**Epigenetic reprogramming of pancreatic cancer cells as a new therapeutic option**

selbständig verfasst, mich außer der angegebenen keiner weiteren Hilfsmittel bedient und alle Erkenntnisse, die aus dem Schrifttum ganz oder annähernd übernommen sind, als solche kenntlich gemacht und nach ihrer Herkunft unter Bezeichnung der Fundstelle einzeln nachgewiesen habe.

Ich erkläre des Weiteren, dass die hier vorgelegte Dissertation nicht in gleicher oder in ähnlicher Form bei einer anderen Stelle zur Erlangung eines akademischen Grades eingereicht wurde.

**München, 13.01.2023**

Ort, Datum

**Svenja Pichlmeier**

Unterschrift Doktorandin bzw. Doktorand